Dissecting the Multifaceted Antibody Response to Influenza A Virus and Severe Acute Respiratory Syndrome Coronavirus 2

Lauren Gentles

A dissertation

submitted in partial fulfillment of the

requirements for the degree of

Doctor of Philosophy

University of Washington

2022

Reading Committee:

Jesse Bloom, Chair

Adam Geballe

Justin Taylor

Program Authorized to Offer Degree:

Microbiology

University of Washington

Abstract

Dissecting the Multifaceted Antibody Response to Influenza A Virus and Severe Acute Respiratory Syndrome Coronavirus 2

Lauren Gentles

Chair of the Supervisory Committee:

Jesse Bloom

Department of Microbiology

Antibodies are the first line of defense against invading respiratory pathogens, and their effectiveness at preventing infection and disease depends heavily on what antigens are targeted. For both influenza A virus and severe acute respiratory coronavirus 2 (SARS-CoV-2), antibodies directed at the receptor-binding surface proteins, hemagglutinin (HA) and spike, respectively, are known to neutralize virus infection and are associated with protection [1–5]. Antibodies targeting non-neutralizing epitopes on many different viral proteins also play important roles in reducing the length and severity of disease and tend to target more conserved regions than most neutralizing antibodies [1,5–11]. Here, I present my work aimed at understanding the development and interaction of neutralizing and non-neutralizing antibodies with two respiratory viruses, influenza A virus and SARS-CoV-2.

First, I test the durability of antibody binding to the stem domain of HA after the accumulation of mutations naturally over 17 years in both the H1 and H3 lineages. To accomplish this, I created chimeric HA proteins combining the head domain of an avian influenza virus to which humans have not been exposed with the HA stem domain of seasonal influenza strains spanning 17 years of sequence evolution [12–16]. This allowed me to measure serum antibody binding specifically to the HA stem domain. I measured the binding of human sera collected concurrent to when the first seasonal stem strain I tested was circulating and compared that to the binding of the same sera to the stem from a seasonal strain circulating 17 years later. Based on these measurements for a number of human serum samples, we find that HA stem antibody binding wanes at a similar rate for both H1 and H3 HAs despite a faster rate of sequence evolution in the H3 lineage.

In a separate set of experiments, I describe a new assay for measuring the potency of antibodies targeting the influenza A virus receptor-cleaving protein neuraminidase (NA). Our method allows for the testing of anti-NA antibodies in a format similar to traditional neutralization assays for antibodies targeting (HA). Briefly, we paired a modified HA that can perform membrane fusion but cannot bind to cellular receptors and NA containing the mutation G147R which confers the receptor-binding function to NA [17,18]. This creates a virus that is dependent on NA for attachment to cells and can thus be neutralized by anti-NA antibodies. We found that this method works best for antibodies targeting sites near the catalytic active site of NA. We were able to select for an escape mutation with one such monoclonal antibody demonstrating the utility of our methods for mapping anti-NA antibody epitopes.

Finally, I address the pressing issue of antibody durability in the context of the ongoing SARS-CoV-2 pandemic by measuring neutralizing and non-neutralizing antibody responses in children for up to 52 weeks following infection. In collaboration with Seattle Children’s hospital, we

performed pseudoneutralization [3,19,20] and the Abbott Laboratories SARS-CoV-2 IgG assay on samples collected from 32 children at approximately 4- and 24- weeks post-symptom onset. For both neutralizing anti-spike antibody titers and anti-nucleocapsid (N) antibodies, we observed a high degree of variability from participant to participant. Overall, neutralization titers changed very little over the observation period, while anti-N levels decrease substantially. When compared to a separate, previously characterized, adult cohort [3], we find age-related differences in the antibody responses. Specifically, children tend to have lower neutralizing antibody titers than adults early following infection that become similar to adults in the following six months. Strikingly, anti-nucleocapsid antibodies are much lower in children than adults and wane faster in children over time.

TABLE OF CONTENTS

Page

LIST OF FIGURES

LIST OF TABLES

ACKNOWLEDGEMENTS

The support, guidance, and patience I have received during my thesis work has propelled me through this wonderful learning experience. I am incredibly grateful for have been surrounded by nurturing colleagues and under the thoughtful mentorship of Jesse Bloom. Working at Fred Hutchinson Cancer Research Center has been a dream environment thanks to the warm and welcoming scientific atmosphere, the ever-abundant supply of free food at seminars, and cozy study/naptime nooks. Most of all, I will miss the Fred Hutch community where there is no shortage of people who care and want to see you succeed.

Under Jesse's guidance, my scientific path has proven adventuresome as I have had the opportunity to take on projects and join collaborations spanning many aspects of influenza A virus and SARS-CoV-2 virology. Scientifically, Jesse's encouragement has led me to think more deeply about research problems and try novel experimental approaches. I am grateful for the many exciting research ideas that I've had the privilege to work on in the lab. Jesse has enabled me to take scientific risks in pursuing creative projects, and even when some did not work out, I learned so much in the process. As a mentor, Jesse has always been supportive and understanding. When experiments don't quite go as planned, Jesse is always quick to talk through any issues and point me towards resources and people who can help with technical issues. For example, I had no coding experience prior to joining the lab, and Jesse presented me with opportunities to jump into computational projects where I could begin to develop this skill. With a lot of patience and encouragement, I have learned far more than I thought achievable. Lastly, the lab environment that Jesse has helped create has kept my graduate experience fun and eventful. For instance, I appreciated the length and effort that Jesse and other lab members have gone to in order to surprise people on their birthday with special treats and woefully bad singing. Whether through fake meetings or surprise presentations, this birthday tradition has never failed to make us feel special. Life events continue to happen during graduate school, and eventful moments like when I got married were commemorated by the time-honored tradition of receiving a wedding duck from Jesse – a celebratory token I will treasure forever.

The transformation that Andrea Loes brought to the lab after becoming our lab manager is simply astounding. Her constant efforts to improve the lab has made it wonderful place to work. Beyond this, Andrea has supported me through tough times in grad school always providing sound advice and reassurance when I've needed it most. It has been a pleasure to work with her scientifically as well. Andrea has always been willing to listen to new ideas, troubleshoot problems, and provide valuable scientific critique regardless of the many tasks she juggles managing the lab. I am very grateful for her friendship during my time in the lab.

Of course, my experience in the Bloom lab would not be whole without the many labmates who have supported me along the way. I am especially indebted to Kate Crawford who patiently worked with me several projects and helped me join and eventually teach the Fred Hutch Girls Who Code club. Both Kate and Sarah Hilton were never too busy to stop and help me debug code or talk about science, and without their support I would not have been able to tackle the daunting challenge of learning to code. I want thank Allie Greaney for her encouragement always quick to complement and ask about how work and life are going. I will always look up to Juhye Lee who set the bar for excellence in grad school and helped me learn the ropes as a new student. Our shared experience snowshoeing for the first time at a conference in Colorado was also a highlight of grad school. A special thank you is also due to Rachel Eguia, David Bacsik, Tyler Starr, Tal Einav, Mike Doud, Shirleen Soh, and Alistair Russell for all providing support, mentoring, and comradery during my graduate experience. All the members that have come and gone during my time in the Bloom lab have helped me to create many special memories.

Upon starting graduate school, I was absolutely terrified of the daunting challenges completing a PhD program entails, and I was nervous that I wouldn't make it through my first year. I could not have picked a better first rotation than the lab of Adam Geballe. I am thankful for the welcoming environment of the Geballe lab where Adam was never too busy to sit and just talk about science or take the time to introduce me to the Fred Hutch community. I learned a lot about molecular virology during my rotation and gained confidence in my ability to succeed in grad school. My last rotation in Julie Overbaugh's lab was equally

impactful on my graduate career. I want to thank Julie for providing thoughtful guidance not only during my rotation but throughout my time in grad school. Prior to my rotation in Julie's lab, I was interested in virus-antibody interactions but had only ever focused on the virus side of these interactions. I learned so much about antibody structure, function, and affinity maturation during my time in the Overbaugh lab which has impacted how I think about every aspect of my thesis work.

The Microbiology Department has been instrumental in nurturing my graduate education. I would like to thank the other graduate students in my cohort especially Julia Dreifus and Sam Durfey who have been there to celebrate the good time and face the difficult challenges of grad school. Not to mention our adventures backpacking together in the beautiful Pacific Northwest forests. Phil Burke has also always been a smiling face providing kind words and encouragement. Working next door to each other at the Fred Hutch, Phil has always been just around the corner when I need to talk to someone who is going through the same milestones of grad school.

Many thanks are owed to Seattle Children's Hospital and especially to Jan Englund and Leanne Kehoe. Jan and Leanne and many others did all of the heavy lifting to make the study of pediatric antibody responses possible. Their guidance on this project was essential for its success. I am grateful for their patience during my first foray into clinical virology which included an abundance of emails from me at odd hours. This work has turned out to be a truly rewarding and insightful experience.

Grad school would not have even been in the cards for me if it were not for all of my former mentors who were invested and dedicated to my scientific education. I am grateful for my undergraduate mentors Young Min Kwon and Byungwhi Kong who introduced me to molecular biology and let me get my first taste of working in a lab. My first chance to become immersed in virology was in the lab of Chioma Okeoma at the University of Iowa's Research Experience for Undergraduates program. I am deeply indebted to Chioma for allowing me to take on an exciting ambitious project that spurred my love of viruses and for her example as an incredible woman scientist. Nearly all of the nitty-gritty molecular virology that I know today and

have used throughout grad school has come from working with Chris Brooke at the NIH in the lab of Jon Yewdell. I am incredibly thankful for my time in the Yewdell lab which was truly an amazing experience that introduced me to a whole world of influenza biology and set me up for success in grad school.

Grad school, at times, is a test of endurance. A test that I would not have passed without my funny, caring, and loving husband, Jonathan. Waking up to freshly brewed coffee every morning and our daily walks to Magnuson Park have propelled me through even the most trying times, especially over the past few years since the pandemic began. Of course, he has been there to share the many, many joys of grad school and life in Washington as well. The interest he has taken in my research has always made me feel valued and appreciated, at times spurring me to see problems from a different perspective. I am lucky to have had him by my side through this wonderful journey.

Without the emphasis on science and academics from my family, I likely would have never explored research in biomedical sciences. I owe much of my love of science to my mom who, as a community college professor, always let me interact with her teaching lab as a child. From peering at pond scum under a microscope to examining a wide range of preserved animal specimens, this unusual experience introduced me to the world of life science. I am also indebted to my dad for the late nights spent helping put together science fair posters, days helping me study, and weekends driving me to school events. My success throughout grad school would not be possible without the lifelong support I have received from both my parents. In addition to the support network my parents have provided, the near weekly calls with my sister, Emily, have been invaluable to surviving grad school. Her funny wit and never-ending tails of exciting adventures have provided an uplifting and welcome relief to the sometimes-dreary Seattle days. Our shared experiences going through grad school have also provided me with an understanding shoulder to lean on, and I am always looking forward to when she will visit me next.

Chapter 1.

INTRODUCTION

1.1 A robust antibody response is elicited following influenza infection or vaccination

1.1.1 Influenza A viruses hemagglutinin evolves to evade antibody immunity.

The burden of disease caused by influenza virus infection continues to pose a significant threat to global public health [21]. Seasonal circulation remains prevalent despite the fact that infection and vaccination by influenza A virus elicits a robust antibody response primarily targeting the immunodominant hemagglutinin (HA) receptor-binding protein imbedded in the host-derived viral envelope [22–25]. Only antibodies targeting HA are known to be neutralizing, meaning that they prevent the virus from infecting susceptible cells. As such, they have long been used as a correlate of protection, and thus, HA is the current target for seasonal influenza vaccines. HA, however, is highly mutationally tolerant, particularly within the known the antigenic sites of the membrane-distal head domain that make up the majority of neutralizing antibody epitopes [26,27]. This feature of the HA protein allows for rapid selection of mutations at sites of antibody binding resulting in immune escape [28–31]. This process is known as antigenic drift and is the primary reason why influenza continues to cause yearly epidemics and also why seasonal vaccines need to be evaluated yearly and frequently reformulated.

1.1.2 Targeting the hemagglutinin stem domain to elicit a more durable neutralizing antibody response

During viral maturation, HA is proteolytically cleaved in to two subunits, HA_1 and HA_2 [32]. The HA_1 subunit primarily encodes the head domain of HA with the stem domain mostly encoded by HA_2 and the C-terminal domain of HA_1. Because the membrane-proximal stem domain of HA is relatively more conserved than the head domain, it has become a coveted target for vaccine strategies aimed at eliciting more durable immune responses [33]. Influenza strains are broken down into two groups of antigenically similar strains which are further subdivided into subtypes within each group. Several broadly neutralizing

stem monoclonal antibodies have been identified which provide heterosubtypic immunity, i.e. immunity to multiple influenza subtypes, in animal models, and some even exhibit pan-influenza binding [15,34–42]. Most reported broadly neutralizing stem antibodies target a single large epitope region within the HA_2 helical structure [39,43], although recent work has identified a new epitope near the transmembrane domain on HA that appears to be an additional common binding site of neutralizing stem antibodies [44]. The proposed mechanism of action for many broadly neutralizing stem antibodies is the inhibition of membrane fusion [39]. Because HA fusion activity is required for efficient infection, it has been suggested that stem antibody escape mutations are less likely to arise due to the functional constraints of this domain. Alternatively, the immunosubdominance of the stem domain, at least partially due to its less accessible location on the protein, may shield this region from intense selection pressure resulting in fewer escape mutations.

1.1.3 Examining the antigenic evolution of the HA stem domain

Directed evolution studies have been performed to try to identify mutations in the stem domain that confer escape from stem neutralizing antibodies. Given that mutations in the HA stem domain become fixed in nature less frequently than in the head domain [45,46], it may be unsurprising that selection of stem antibody escape mutation have been difficult to identify [47]. However, despite this barrier to selection, single mutations have been found that allow for escape from monoclonal stem-binding antibodies [31,48] and even polyclonal serum [46,49]. It is still unknown how naturally occurring mutations in the stem domain impact stem-binding antibodies which are not uncommon in human serum. Identifying whether the natural accumulation of mutations in the stem erode antibody binding will provide important implications for future stem-based vaccination strategies aimed at applying more potent stem antibody selection.

Further complicating stem immunity is the fact that different subtypes of HA appear to evolve antigenically at different rates. Specifically, H3N2 tends to antigenically drift faster than other circulating seasonal influenza A and B strains [50]. In addition, the enhanced evolvability of the H3N2 HA appears to extend beyond the antigenic regions of the head domain into neutralizing stem epitopes [48,51]. The greater ease

of escape from antibodies targeting H3 HA has important potential ramifications for influenza vaccine strategies especially those aimed at inducing broad stem-directed antibody responses. It is possible that, based on the above evidence, focusing immune selection on the stem domain may result in the rapid accumulation of escape mutations in H3N2 strains. This would degrade antibody immunity asymmetrically against this subtype while such stem antibodies may remain effective against H1N1 strains.

One vaccination strategy currently being explored for targeting antibodies to the HA stem domain is immunization with chimeric HA proteins. Specifically, a design is being explored that combines the stem domain from seasonal influenza strains with a head domain from an avian influenza strain to which humans have not been exposed [12–16]. The idea behind the chimeric HA vaccine strategy is that pre-existing antibodies against the more conserved seasonal HA stem domain will be boosted while head domain antibodies will not because the head domain is antigenically distinct from previous HA exposures. This method has been successfully used in animal models to elicit cross-protective immunity and has been tested for immunogenicity in human clinal trials [13,52,53,16,54]. Further supporting this stem antibody boosting method is the finding that infection by the 2009 pandemic H1N1 virus, which had an antigenically distinct HA head domain compared to strains circulating immediately prior to its emergence, elicited high levels of cross-reactive stem antibodies [55]. In our work, we have found that chimeric HA proteins are not only useful for eliciting stem immunity but also for detecting stem antibodies in human serum. As a research tool, chimeric HAs are useful for measuring the magnitude of stem-binding antibody levels. In chapter 1, I discuss my work utilizing chimeric HAs to examine the rate of antigenic drift for the stem domain.

1.1.4 Neuraminidase is a major target of infection-elicited antibodies

While neutralizing influenza antibodies have been the subject of intense investigation, non-neutralizing antibodies, such as those targeting neuraminidase (NA), also contribute to reduced viral shedding, less disease severity, and reduced length of illness [56–58,1,11,59]. NA plays a crucial role during the lifecycle of influenza virus by counteracting HA receptor binding. NA cleaves sialic acid receptors that are abundant in the mucin layer of the respiratory tract, known as the glycocalyx, and allows the virus to reach targets

cells [60,61]. Similar to how HAs have different binding preferences for α2,6 and α2,3 sialic acids [62], NA can also show cleavage preferences resulting in greater cleavage activity towards specific sialic acid types [63,64]. New evidence has shown how the distribution of NA on filamentous virions helps facilitate the mobility of virus particles by enabling virions to roll along the mucus layer in a linear direction [65,66]. In addition, NA is important for the release of newly formed virions on the cell surface. Without NA, the binding of HA to cellular sialic acid prevents the efficient release of viral particles and can cause the formation of viral aggregates [67].

Because NA performs several essential functions that promote infection and viral spread, NA has been examined as a potential anti-viral drug target and vaccine antigen. Most notably, the drug, oseltamivir, irreversibly binds and inhibits the NA active site and has been widely used to reduce the length and severity of disease [68]. Unfortunately, this drug is only effective if taken very early during infection before many individuals know that they are sick. Additionally, single mutations have been frequently identified in NA clinical isolates that make the virus resistant to oseltamivir inhibition [69–71]. Current seasonal vaccines contain NA and do elicit anti-NA antibodies. But unlike HA, the amount and structural integrity of NA proteins in vaccine batches are currently not carefully regulated [6]. This likely results in variable amounts of folded and unfolded NA protein in vaccines, and current evidence suggest NA that is not properly folded does not elicited a high-quality antibody response [72,73]. This is important because recent research demonstrated that antibodies against NA are more beneficial than originally thought, and currently new methods are being explored for quantifying NA activity in vaccine batches [74].

1.1.5 Anti-neuraminidase antibodies play a protective role against infection

The study of NA antibodies as a means of protection against influenza virus infection originally fell out of fashion after the H3N2 pandemic struck in 1968. This pandemic virus contained the same NA as the previously circulating H2N2 strains, yet the new H3N2 strain was still able to sweep through the population. There was some evidence, however, that individuals with prior exposure to H2N2 were more resistant to infection with the new H3N2 strain [75–77]. In addition, changes in the length of infection and the severity

of disease caused by H3N2 strains following prior H2N2 infection was only reported by a few studies and not well-understood at the time [57]. New evidence has identified anti-NA antibodies as an independent correlate of protection from infection [58]. One study demonstrated, in a mouse model of infection, that antibodies targeting residues near the NA active site are particularly protective against viral challenge [78]. A striking finding from this work was the breadth of binding shown by these antibodies which recognized group 1, group 2, and influenza B virus NAs [78]. Furthermore, it has been shown that such antibodies are not rare in human serum highlighting the potential of new immunization strategies directed at eliciting a broad immune response to NA [79].

The greater cross-reactivity of antibodies to NA than typical HA antibodies may not be totally surprising given that NA is more conserved than HA. Yet despite the greater breadth of many anti-NA antibodies, antigenic drift still erodes antibody binding to NA over time [80]. Intriguingly, recent evidence suggests that antigenic changes may oscillate between HA and NA such that they do not occur in at the same time [81]. Another group demonstrated that serum antibodies elicited by an old NA strain do not bind strongly to new strains, but antibodies raised against a new NA strain tend to recognize older NA strains as well [81]. This work highlights exciting findings in the relatively unexplored frontier of NA immune memory.

1.1.6 New methods for understanding anti-NA antibody responses

A large hurdle in the way of better understanding antibody responses to NA is the current lack of reagents and assays [6]. An abundance of assays has been developed for the study of HA targeting antibodies such has neutralization, hemagglutination inhibition, plaque inhibition, and hemolysis assays, but these assays are not applicable to the study of anti-NA antibodies and analogous assays do not exist. The recent renewed interest in anti-NA antibodies has spurred the development of few new methods. These include several standardized assays to measure NA catalytic activity and the inhibition of NA activity by antibody binding [82–86]. Since these assays are only useful for measuring NA inhibition (NI) for monovalent vaccine responses, other assays have been developed specifically to measure NA antibody responses to a wider range of influenza strains [74]. These include ELISAs which have long been used to identify antibody

responses to a variety of viral proteins. For neuraminidase, ELISAs can provide information on how much antibody in serum is able to bind to NA but not the functional impact of anti-NA antibodies on the viral lifecycle.

The NA catalytic assays mentioned above have been instrumental in detecting differences in NA activity between different influenza strains and the impact of antibody binding on catalytic activity. One limitation of these assays, however, is that the NA cleavage substrates used for existing assays may not be physiologically relevant. The substrates used in NA catalytic assays are typically small or bulky, heavily glycosylated oligosaccharides in a soluble solution which is dissimilar to the membrane bound receptors that influenza naturally interacts with on target cells. In my work outline in Chapter 3, I detail a new method for measuring the potency of NA antibodies targeting epitopes near the NA active site which differs from existing assays because detects antibody inhibition of NA activity towards complex cellular receptors.

1.2 Age, disease severity, and time since infection influence SARS-CoV-2 antibody levels

1.2.1 SARS-CoV-2 infection elicits neutralizing antibodies targeting the spike protein

At the time of this writing, the global pandemic caused by severe acute respiratory syndrome coronavirus 2 (SARS-CoV-2) is still ongoing resulting in 6 million deaths worldwide (Johns Hopkins Coronavirus Resource Center) and causing long term adverse health issues in many more. Only antibodies targeting the spike protein are known to neutralize viral infection of cells [87,88]. The importance of measuring the level of neutralizing antibodies in serum from infected or vaccinated individuals is based on evidence that neutralizing antibody titers correlate with protection from reinfection or infection, respectively [89,90,5,91].

Importantly, the spike protein of SARS-CoV-2 is divided in to two subunits: S_1 and S_2. Similar to hemagglutinin, these two subunits have distinct functions. The S_1 subunit contains the N-terminal domain (NTD) and the receptor-binding domain (RBD) which is responsible for interacting with angiotensin converting enzyme 2 (ACE2) on the surface of target cells [92–95]. Most neutralizing antibodies following infection and particularly after vaccination target the RBD or the NTD of the spike protein [20,96–101].

The S_2 domain is the fusogenic region of the protein which facilitates membrane fusion. Several broadly neutralizing antibodies have been recently identified that target conserved cryptic epitopes in the S_2 domain [102]. Broadly neutralizing S_2 antibodies appear to be rare, but may be important for protecting against new SARS-CoV-2 variants.

1.2.2 Anti-nucleocapsid antibodies are important for immune surveillance

Antibodies are also elicited against other viral proteins following infection, most notably nucleocapsid (N) and open reading frame 8 (ORF8) [87]. The N protein is highly abundant during infection and is responsible for encapsidating and protecting the viral RNA genome until its release in host cells [103]. Several antibody tests have focused on anti-N antibodies which have become an important target for the study of seroprevalence at the population level since antibodies against N are elicited by infection and not by most currently available vaccines [104]. A protective role for antibodies targeting N has not been firmly established, and more work is needed determine any potential disease mitigating impacts.

1.2.3 Factors influencing the magnitude of infection elicited antibodies

Thanks to the tireless efforts of the scientific community, we have gained insight into the immune responses elicited by SARS-CoV-2 at an unprecedented speed. For example, there are now many studies that show that disease severity and viral load are important factors that induce a higher magnitude antibody response following infection [3,105–109]. Other work has demonstrated that neutralizing antibodies tend to wane gradually over time but still remain detectable [3,106,108,110–113,4,109,114–116]. Nearly all of this work, however, has focused only on antibody responses in adults who tend to experience the most severe disease and for whom clinical studies are easier to perform than for other age groups. Yet regardless of the overall lower disease severity observed for children compared to adults, SARS-CoV-2 infection now causes more hospitalization and deaths in children than many other childhood illnesses [117]. Furthermore, disease severity in children ranges as widely as in adults with some pediatric patients experiencing life-threatening illness and long-lasting negative health affects [118]. Children are also susceptible to multisystem inflammatory syndrome in children (MIS-C) that can surface weeks after infection leading to medical

emergencies. The factors leading to MIS-C development remain unknown, and it is unclear if and/or how the antibody response infection may play a role. For all of the above reasons, further investigation into the pediatric immune responses is needed to better understand protection from reinfection and overall population immunity.

1.2.4 Current understanding of the pediatric SARS-CoV-2 antibody response

A few studies, have investigated the level of antibody responses following SARS-CoV-2 infection in children for relatively short timeframes. One such study, measured virus-specific antibodies by ELISA for adults and children for up to 60 days following infection [107]. Individuals were only sampled one time and not longitudinally. Analysis of antibody levels revealed lower levels of anti-N antibody titers in children than adults. It was also shown that anti-S titers increased for samples taken at later time points post-symptom onset for both the adult and pediatric cohorts [107]. Furthermore, when neutralizing antibody titers were measured, pediatric participants tended to have lower titers than adults [107]. In addition, this work found no detectable difference between antibody titers for children who developed MIS-C compared to those who did not [107]. In another study that did sample the same children longitudinally, the total amount of antibody against N and S proteins increased over an average of 62 days [119].

The longest period of time for which antibodies have been measured over time in children, thus far, has been six- to eight-months post-symptom onset [120,121]. Both studies report the persistence of robust neutralizing antibody responses. Of the two studies, one further analyzes neutralizing titers by pediatric age group and finds that children under the age of six have higher titers than older children and adults [120]. Another study corroborates these findings demonstrating higher neutralizing titers in young children than adults and even greater levels of RBD binding antibodies than in adults [122].Only Dowell et al. investigates the magnitude anti-N antibodies longitudinally in children finding low but sustained responses and reporting no differences between children and adults [121]. The limited number of pediatric longitudinal studies performed to date and variability in reported results necessitates additional investigation of SARS-CoV-2 infection-elicited antibody features.

1.2.5 Pseudotyped lentivirus neutralization assay measurement of serum antibody inhibition

At this time, many iterations of pseudoneutralization assays have been developed to measure *in vitro* antibody inhibition of viral infection without having to work with live SARS-CoV-2 virus in a biosafety level 3 setting. Our lab, very early during the pandemic, developed such an assay using lentivirus pseudotyped with SARS-CoV-2 spike [19]. Work with similar systems has shown that neutralization titers measured in the pseudoneutralization assay correlate well with assays performed with live virus [123]. The pseudotyped lentivirus platform used in the Bloom lab has now resulted in numerous publications from one of the first studies of seroprevalence in children and the dynamics of infection elicited antibodies in adults out to 90 days to the validation of monoclonal antibody and serum escape mutations just to name a few [3,20,96,124,125]. In my work, we again utilize the pseudoneutralization assay, as well as the Abbott Laboratories SARS-CoV-2 IgG assay, to measure pediatric antibody responses in children for up to a year after SARS-CoV-2 infection.

1.3 Layout of dissertation

The chapters that follow detail my work investigating three aspects of the interactions between antibodies and their viral targets. Specifically, I examine the antibody responses elicited by SARS-CoV-2 and influenza viral antigens. First, I examine viral evolution in response to antibody selection, then develop a new method for measuring viral antibody responses, and finally explore how the antibody response to viral infection changes over time.

Throughout **Chapter 2**, I probe the natural antigenic evolution of the influenza A virus hemagglutinin (HA) stem domain. We hypothesize that because the HA of H3N2 strains accumulates mutations at a faster rate in the stem domain than the HA of H1N1 strains, antibodies targeting the stem domain will lose reactivity to the H3N2 HA faster than to the H1N1 HA. To test this hypothesis, we employ an ELISA-based assay with chimeric HAs made up of an avian HA head domain to which humans are immunologically naïve combined with several different seasonal stem domains circulating at disparate points in time. Contrary to

my hypothesis, we find no detectable differences in the rate at which stem antibody-binding is lost between H3N2 and H1N1 strains.

In **Chapter 3**, I build on previous work in the lab to create an *in vitro* neutralization assay to measure the potency of anti-neuraminidase (NA) antibodies. This assay is analogous to traditional neutralization assays used to measure the potency of anti-HA antibodies. I used a virus that was previously engineered in our lab to confer receptor binding to NA via the mutation G147R [17]. This virus was further modified to ablate HA binding creating a virus dependent on NA for binding to target cell receptors [17]. We hypothesized that infection by this virus could be inhibited by anti-NA antibodies which I demonstrated for multiple antibodies. I was further able to select for an escape mutation from one of these antibodies demonstrating the utility of this model for *in vitro* study of NA targeting antibodies.

With the emergence of a global pandemic caused by severe acute respiratory syndrome coronavirus 2, my research transitioned to work on this new pathogen. In **Chapter 4**, I examined the dynamics of infection elicited antibodies in children. I measured neutralizing antibodies targeting the spike protein and nucleocapsid-binding antibodies for up to 52-weeks following symptom onset. I found that compared to adults, children have lower levels of neutralizing antibodies early after infection that then become similar to adults by 24 weeks. Strikingly, nucleocapsid-binding antibodies were present at much lower levels and waned faster over time in children than adults. In sum, this work highlights age-related differences in the antibody response following infection with SARS-CoV-2.

Chapter 2.

Similarly slow rates of antigenic evolution in the stem domains of human influenza virus H1 and H3 hemagglutinins

Lauren E Gentles, Katharine H D Crawford, Michael Murphy, Deleah Pettie, Terry Stevens-Ayers, and Jesse D Bloom

2.1 Abstract

The durability of the antibody response elicited by current seasonal influenza vaccines is limited because the head domain of the hemagglutinin (HA) receptor binding protein rapidly accumulates mutations that erode antibody immunity. New vaccine strategies aim to combat this challenge by eliciting antibodies to the more conserved stem domain of HA, but to date it is unknown whether antigenic drift may also erode the binding of antibodies to the stem domain. Furthermore, the head domain of human H3N2 influenza evolves faster than the head domain of H1N1, but it is unknown if there could be similar disparities in the rates of antigenic evolution in the stem domains. Here, we utilize a chimeric HA (cHA) design to measure the binding of serum antibodies to the HA stem by ELISA. Using soluble cHAs containing stem domains from the human seasonal H1N1 and H3N2 subtypes over a 17-year timeframe, we directly quantify how mutations that naturally accumulate in the stem domain reduce the binding of human serum antibodies. Our findings demonstrate that despite a somewhat faster rate of sequence evolution in the H3 stem domain compared to H1, the rate at which this evolution erodes binding by human serum antibodies is similarly slow for both subtypes.

2.2 Introduction

Antigenic drift is the process by which influenza virus accumulates mutations to escape antibody binding or neutralization [29,126–129]. This phenomenon has been well characterized for the immunodominant and mutationally tolerant head domain of the virus's surface glycoprotein hemagglutinin (HA) but not the membrane proximal stem domain [126,127,29,129–131]. Antigenic drift is distinct from sequence evolution which may include amino-acid changes that do not directly impact viral antigenicity. Phylogenetic analysis of influenza HA sequence evolution has revealed that the head domain evolves faster than the stem domain at the amino-acid level [46,45]. The greater conservation of the stem domain makes it an attractive target for vaccines aimed at eliciting more durable immunity [33,132]. In support of this theory, many studies have highlighted stem-binding antibodies with broad heterosubtypic reactivity [55,133–135,79,15]. However, despite several studies investigating *in vitro* selection of antibody escape

mutations in the stem [46,31,136,49], no direct measurements of how mutations that naturally accumulate in the stem domain impact polyclonal serum antibody binding have been made.

Previous studies combining antigenic cartography and phylogenetic analysis have shown that the H3N2 HA head domain undergoes more rapid antigenic evolution than that of the H1N1 HA [50]. This work relies on antigenic data from hemagglutination inhibition (HAI) assay measurements which only detect changes in the binding of antibodies that directly block HA binding to receptors on the surface of red blood cells. Many stem binding antibodies do not block HA receptor binding and are, therefore, not accounted for in these antigenic measurements. Using deep mutational scanning, work by Lee et al. 2018 investigated the mutational tolerance of the entire HA protein for both H1N1 and H3N2 strains [51]. The findings of this study suggest that while the H1 HA head domain is much more mutationally tolerant than the H1 HA stem, the H3 HA head and stem domains have more similar mutational tolerance. These results indicate that the stem domain of the H3 HA may be more evolvable than the H1 HA stem. Supporting this hypothesis, Wu et al. demonstrated that broadly neutralizing stem antibodies more easily selected for escape mutations in H3N2 HA than H1N1 HA [48]. In sum, this evidence led us to investigate changes in antibody binding to the stem domains of H1N1 and H3N2 HAs over time to compare the rate of antigenic drift.

Here, we use an ELISA-based method to detect changes in polyclonal serum antibody binding to the stem domain over a 17-year timeframe and compare the rate of antigenic drift in the stem domains of the H1N1 and H3N2 HA subtypes. To accomplish this, we utilize a chimeric HA design that has been tested as a vaccine antigen in Phase 1 human clinical trials as a method to boost stem antibodies [16]. For the chimeric HA antigens, we combine an immunologically irrelevant avian head domain with the seasonal H3N2 and H1N1 stem domains from the early 1990s and the late 2000s. We measure the changes in the binding of human serum collected in the early 1990s to these two constructs for each subtype. Our findings suggest that despite a higher rate of sequence evolution in the H3N2 stem domain compared to H1N1, the rate of antigenic drift across both subtypes is similar.

2.3 Materials and Methods

2.3.1 Plasmids

The plasmid constructs encoding the chimeric HA coding sequence were designed based on previously published work with some minor modifications [12]. Briefly, we designed GeneBlocks containing the first 177 (H1) or 204 (H3) of nucleotides coding for the C terminus seasonal influenza HA2 domain followed by the sequence of immunologically irrelevant head domain inserted between cysteines 59 and 290 for H1 HA and 68 and 293 for H3 HA followed by the remaining HA2 N-terminal domain. We deleted the transmembrane domain (nucleotide H1 1557-1701 and H3 1561-1701) in order to create a soluble protein. To facilitate trimerization, we added a flexible linker followed by a FoldOn trimerization domain. We included Y98F in the head domain coding sequence to limit HA binding and facilitate better protein production. These GeneBlocks were inserted into the pHW2000 plasmid vector. Plasmid sequences are available at the following accession number and plasmids are available by request.

2.3.2 Phylogenetic analysis

The influenza H3N2 and H1N1 full-length hemagglutinin phylogenetic tree sequences were curated as previously published [51]. Briefly, Nextstrain's augur pipeline was used to generate trees[137]. TreeTime was employed for ancestral reconstruction and branch length timing inferences[138]. We first analyzed all the unique seasonal H3N2 HA sequences from 1968 to 2017 and the seasonal H1N1 HA sequences from 1977 to 2009 in order to generate phylogenetic trees as outlined in previous work [51] (**Figure 2.1A&B**). We then used these trees to determine the number of mutations that occur along the trunk of the tree over this time period. We found that between 1968 and 2013, 36 mutations fixed in the stem domain of H3 HA, and between 1977 and 2007, 10 mutations fixed in the stem domain of H1 HA. Three reversions to previous amino-acid identities occurred during this timeframe in the H3 lineage at sites 3 in HA1 and at 46 and 121 in HA2 using H3 numbering. No reversions to previous amino-acid identities were observed in the H1 lineage.

2.3.3 Human serum samples

Serum samples were collected between 1993 to 1994 from healthy donors in compliance with Fred Hutchinson Cancer Research Center IRB approved protocols. The serum samples were heat inactivated for 30 minutes at 56ºC prior to use in experiments.

2.3.4 Antibodies

As positive controls for ELISA assays, convalescent ferret anti-A/human/Canada/RV444/2004 (H7N3) serum (CEIRS Reagent# F.2014-1) was used at a 1:10,000 dilution and mouse anti-A/Vietnam/1203/2004 (H5N1) HA monoclonal antibody, clone 11F4 (BEI Resources Cat# NR-13449) and used at a 1:5,000 dilution. As an additional control, the broadly neutralizing, stem-binding monoclonal antibody FI6v3 [34] was included in ELISAs at a concentration of 0.008ug/mL.

2.3.5 Chimeric HA ELISAs

To perform ELISAs with the chimeric HA constructs, we coated Thermo Fisher Scientific Clear Flat-Bottom Immuno Nonsterile 96-Well Plates with 1ug per well of each protein in coating buffer (0.05 M Carbonate-Bicarbonate, pH 9.6). Protein was allowed to bind to the plates overnight at 4ºC. Excess protein was removed by rinsing 5 times with wash buffer solution (50 mM Tris, 0.14 M NaCl, 0.05% Tween 20, pH 8.0) using the Tecan® Hydroflex® ELISA Plate Washer. The plates were then filled with blocking buffer (50mM Tris, 0.14M NACl, 1% BSA, pH 8.0) and incubated for 2 hours at room temperature before being washed 5 times again. Serum samples were added at a 1:100 dilution in blocking buffer to the first column of the plate and 3-fold dilutions generated across the plate. Anti-HA head domain antibodies were included as controls for each plate at the concentrations noted above. The primary antibodies were incubated with the plate antigen overnight at 4ºC. After washing 5 times, the appropriate HRP conjugated anti-human (Bethyl Labs Cat#A80-104P), anti-ferret (Bethyl Labs Cat#A140-108P), or anti-mouse (Bethyl Labs Cat#A90-131P) Fc secondary antibody was added at a 1:100,000 dilution. The plate was then incubated overnight at 4ºC then washed 5 times and developed for 5 minutes with Sigma TMB/E Single

Reagent Horseradish Peroxidase Substrate. 1N HCl Stop Solution was used to quench the reaction before reading the plate at 450nm on a Tecan® Infinite® M1000 PRO plate reader.

2.3.6 Analysis of ELISA data

OD450 measurements of the serum dilution series were plotted and a best-fit curve generated for the data. We then calculated the area under the curve (AUC) above zero for all samples including the head antibody controls. To compare across replicates and serum samples, we normalized the AUCs to the head antibody binding response by taking the ratio of the serum AUC to the head antibody controls. The fold change in AUC over time was calculated as the 2007 serum normalized AUC divide by the 1990 serum normalized AUC.

2.4 Results

2.4.1 Phylogenetic analysis reveals differences in the rate of sequence evolution in H1 and H3 hemagglutinin stem domain.

To examine the evolution of the influenza A virus HA stem domain, we analyzed the sequences of H1N1 HA and H3N2 HA from the time these strains began to cocirculate in humans in 1977. The goal of this analysis was to identify mutations that may have arisen in order to escape stem-binding antibodies. We generated sequence alignments from which we inferred phylogenetic trees as previously described [51]. Characterization of H1N1 and H3N2 trees revealed that a similar proportion of total mutations fixed in the stem domain compared to the head domain in the H1 and H3 lineages (0.20 and 0.25 respectively). However, H3 accumulates mutations more rapidly overall [45], and therefore, the H3 stem accumulated mutations at a higher rate of 0.79 per year compared to the H1 stem which fixed mutations at a rate of 0.33 mutations per year. From these rates, it is clear that H3 HA stem gains mutations more frequently than H1, specifically 2.4-fold more mutations per year.

Limiting our analysis only to the years in which H3N2 and H1N1 strains co-circulated, we still observe a substantial difference in the rate of sequence evolution. Between 1977 and 2007, 18 mutations fixed in the H3 stem domain while only 10 mutations fixed in H1 during this same time frame (**Figure 2.1C**). To date,

it has not been shown whether the mutations naturally accumulating in the stem domain contribute to the antigenic drift of stem epitopes. We set out to determine if over time serum antibodies lose reactivity to the H1 and H3 stem as more mutations fix in this domain. Based on the faster rate of sequence evolution, we hypothesized that the H3 stem is drifting antigenically faster than the H1 lineage.

H3 HA lineage **H1 HA lineage**

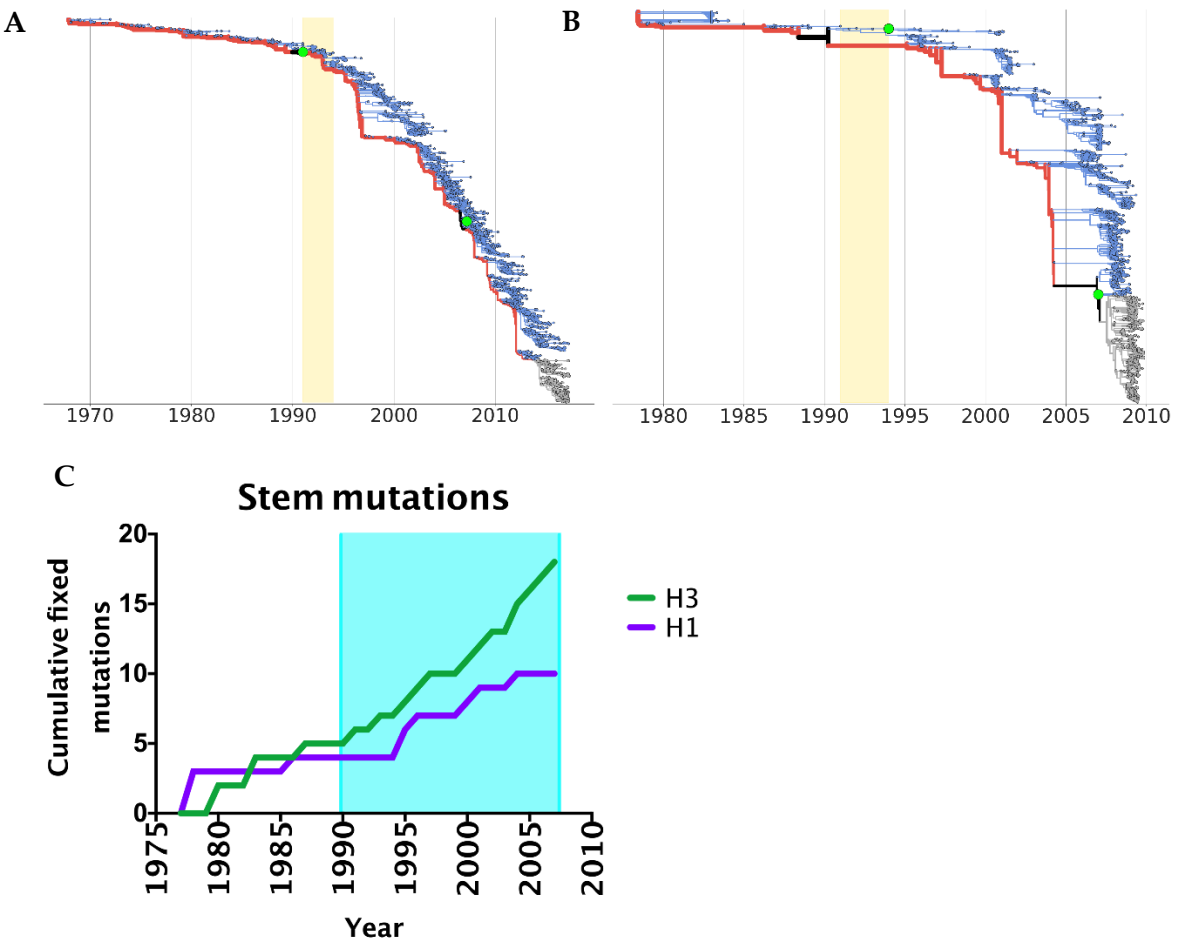

Figure 2.1 Phylogenetic analysis of the H1N1 and H3N2 hemagglutinin sequences

Phylogenetic trees were generated using all the unique **A**) H3N2 HA sequences from 1968 - 2013 and **B**) H1N1 HA sequences from 1977 - 2009 The resolved trunks of the trees are shown in red while the branches are shown in blue. Nodes in gray indicate areas where the trunk sequences could not be resolved. The green circles indicate the strains selected for the stem domains of the chimeric HA constructs used throughout this study. Trunk sequences with stems identical to the stem sequence of the strains selected are shown in black. The area in yellow indicates the timeframe of serum collection. **C**) The cumulative number of mutations that have fixed in the stem domain of the H1N1 and H3N2 HA since the start of their co-circulation in 1977 until 2007 is shown. The area highlighted in light blue indicates the timeframe examined in this study.

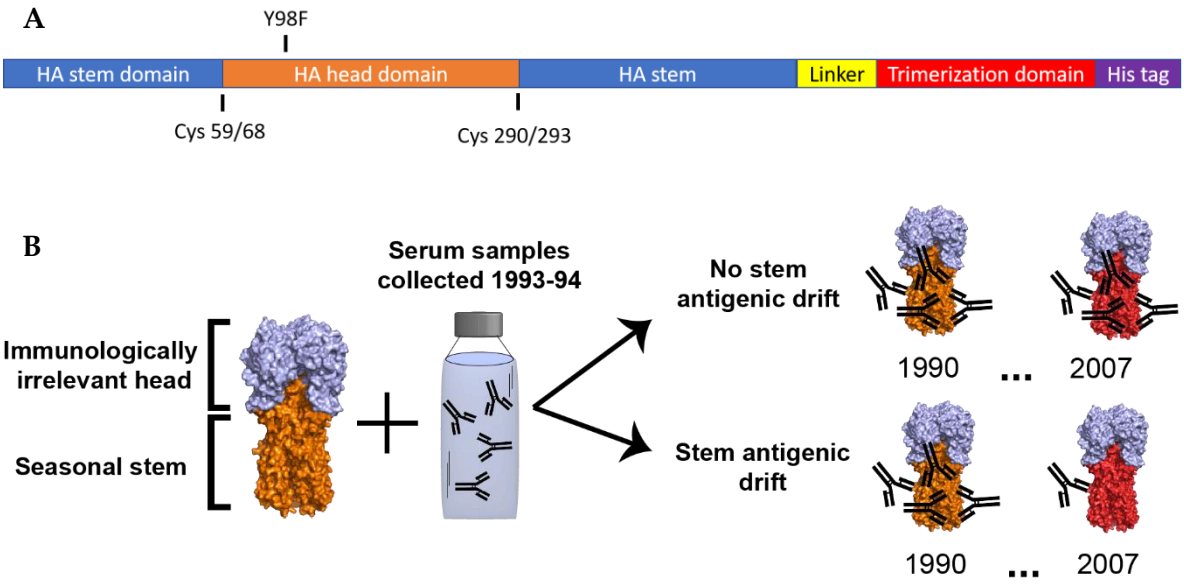

Figure 2.2 Chimeric hemagglutinin ELISA-based method for measuring the binding of stem antibodies in human serum.

The design of chimeric HAs is based on previous work [8] illustrating that the two highly conserved cysteine disulfide bonds that delineate the head domain from the stem can allow for the insertion of different head domains while still forming properly folding HA structures. We build on this design by adding the Y98F mutation that partially abrogates HA binding and allows for higher protein yield in transfected 293F cells. The transmembrane domain was replaced by a FoldOn trimerization domain linked to the HA construct followed by an N-terminal His tag. **B**) Experimental design for testing antigenic drift of stem-binding antibodies in human serum is shown. ELISAs measuring the binding of human serum to chimeric HAs generated with stem domains from seasonal influenza strains were performed. One of the selected strains for both the H1N1 and H3N2 stems circulated just prior to serum collection while the second strain selected circulated 17-years later and contains all stem mutations that fixed during the intervening time.

2.4.2 Development of an ELISA-based method to detect changes in serum antibody reactivity to the HA stem domain over time using chimeric HAs.

In order to detect changes in stem antibody binding, we performed ELISAs with chimeric HA proteins containing seasonal H1 and H3 stem domains (**Figure 2.2**). This design pairs an immunologically irrelevant avian HA head domain with a seasonal stem domain [12,14,139]. The immunologically irrelevant head domain of the chimeric proteins ensures that serum antibodies primarily recognize the stem domain and

any changes in ELISA signal between the two chimeric constructs are due to changes in binding to the stem domain only. By using these constructs in ELISAs, we are able to measure binding of seasonal stem targeting antibodies in human serum. Importantly, this method allows for the detection of drift at both neutralizing and non-neutralizing epitopes within the stem domain unlike traditional neutralization or HAI based antigenic measurements.

To test the longevity of serum reactivity to the stem domain as mutations accumulate over time, we created chimeric HAs with stem domains from H1N1 and H3N2 strains isolated approximately 17-years apart. Stem domains were paired with group 1 or group 2 avian influenza head domains according to the group of the stem domain. For the H1 constructs, we used the stem domains from A/Florida/2/1993 and A/England/557/2007 paired with an avian H5 head domain from A/Viet Nam/1203/2004. Of note, the stem sequence from A/Florida/2/1993 is identical to the stem sequence on the trunk of the tree in 1990 and is thus referred to as the 1990 strain throughout (**Figure 2.1**). For all chimeric constructs, we use the nomenclature which indicates the subtype of the head domain followed by the subtype of the stem domain (e.g., a chimeric HA with the H5 head domain + H1 stem = cH5/1). For the H3 constructs, the stem domains originated from A/Shanghai/24/1990 and A/Colorado/UR06-0534/2007 and contain an avian H7 head domain from A/mallard/Alberta/24/2001. Between the selected time points, six mutations fixed in the H1 stem and thirteen fixed in the H3 stem (**Supplemental Figure 6.1**). By performing ELISAs with these antigens using serum collected in the early 1990s, we can measure whether the mutations that naturally occurred during this 17-year time frame impact the binding of stem antibodies in human serum.

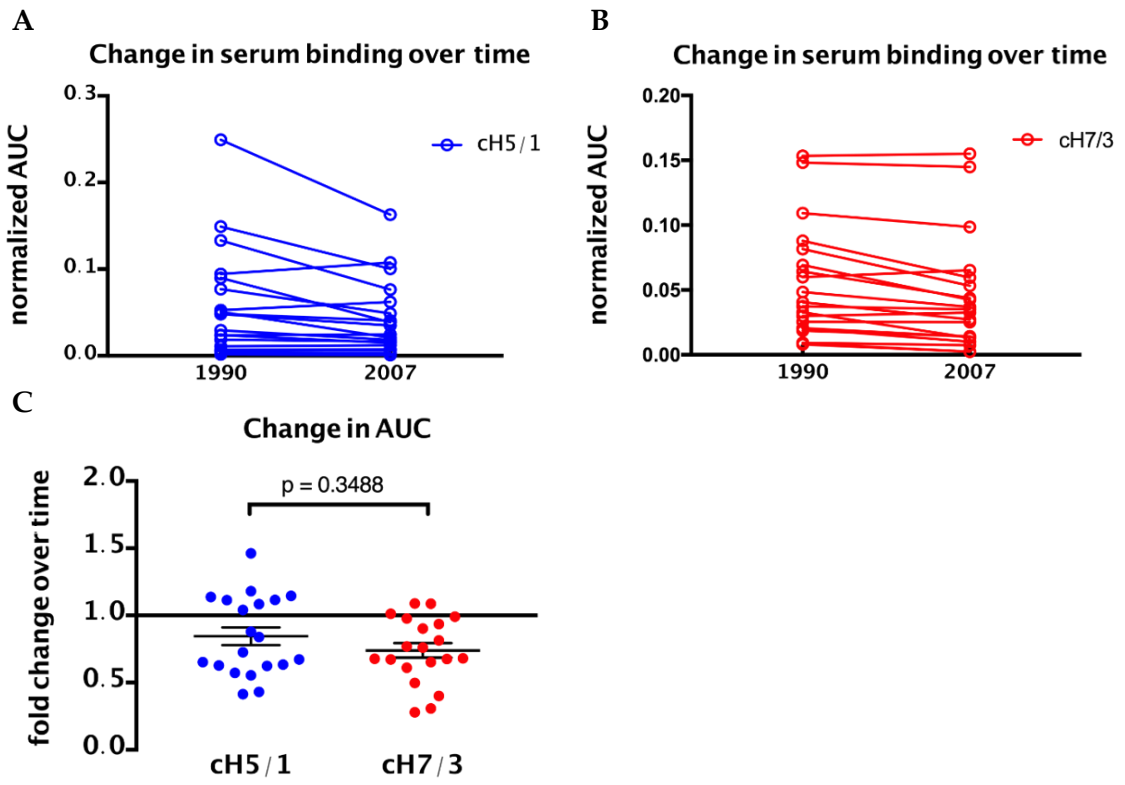

Figure 2.3 Serum antibody binding to chimeric HA constructs over time.

ELISA curves were generated for each serum sample collected between 1993-4 and for antibodies targeting the constant head domain. The area under these curves (AUC) above zero was calculated and the serum AUC was normalized by the head domain antibody AUC to account for any assay-to-assay variation in ELISA antigen. Lines connect the AUCs for a single serum sample against either a chimeric HA with an H5 head domain and an H1 stem domain **A)** or an H7 head domain and an H3 stem domain **B)** and show the change in binding over time. **C**) From the calculated AUCs, we determined the fold change over time in the ELISA serum antibody binding for the cH5/1 and cH7/3 constructs. Statistical significance was determined using Wilcoxon matched-pairs signed rank test.

2.4.3 Serum reactivity to seasonal H1 and H3 stem wanes slightly over time to a similar degree.

We tested 20 serum samples collected between 1993-1994, which was contemporary to the stem domains to which we chose to measure initial reactivity. The serum samples were collected from healthy donors across a wide range of ages to ensure that potential imprinting from the strains donors were first exposed to did not bias our results [140,141]. We hypothesized that serum samples collected in the early 1990s would react strongly with the stem domain from the seasonal strains circulating prior to sample collection, yet these same serum samples would have reduced reactivity to stem domains of strains from 17-years later

due to the accumulation of mutations. We generated ELISA curves for serial dilutions of each serum sample against each chimeric construct and calculated the area under the curve (AUC) for comparison across samples (**Supplemental Figure 2**). We simultaneously performed ELISAs using H5 or H7 head-specific antibodies to normalize for differences between experiments by dividing the AUC from the serum samples by the AUC of the head-binding monoclonal antibodies (**Figure 2.3A & B**). To determine changes in stem antibody binding, the fold change in the AUC was calculated between the 1990 stem chimeras and the 2007 chimeras (**Figure 2.3C**). From this analysis, we found that serum antibodies against H1 and H3 HA stem domains retained a mean of 85% and 74% reactivity respectively over 17-years of accumulated mutations. The difference between the waning of serum reactivity between H1 and H3 strains was not statistically significant. These results suggest that despite the increased rate at which mutations fix in the H3 lineage, these mutations do not lead to a greater rate of antigenic drift in the stem domain compared to the H1 stem.

2.5 Discussion

This study provides the first direct evidence of antigenic drift in the HA stem of seasonally circulating influenza A viruses. Our examination of mutations that accumulated over nearly two decades in the H1N1 and H3N2 HA stem domain reveals a similar rate of antigenic drift. This finding is surprising given the higher rate of sequence evolution observed in the H3N2 HA and highlights the need for serological binding-based assays in conjunction with phylogenetic analysis to detect antigenic variation in the stem domain.

Prior work focusing on HA antigenic drift has been unable to accurately detect antigenic changes in the stem domain because traditional methods rely on HAI and/or neutralization assays. While some broadly neutralizing stem antibodies are easily measured in these serological assays, many HA stem-binding antibodies often go completely undetected [142]. To more directly measure changes HA stem antigenicity, we employed an ELISA based method. Our cHA ELISA detects changes in the binding of both neutralizing and non-neutralizing antibodies providing a more complete measurement of antigenic drift. Furthermore, previous studies of serum antibody binding to HA have not been sensitive to changes in stem-binding

antibodies. This is because this work typically measures total serum binding to the entire protein rather than just the stem domain, and the immunodominance of the HA head domain could bury relatively smaller signal changes due to stem-binding antibodies. By performing ELISAs with cHAs containing an immunologically irrelevant avian head domain, our experiments were designed to largely eliminate antibody binding to the HA head domain. These experiments do not, however, examine the functional role of stem-binding antibodies or the consequences of their loss of binding. Future work is needed to better understand biological impact of stem natural antigenic drift and loss of antibody binding during the virus lifecycle. For example, measuring changes in serum neutralization of past and future influenza viruses with only naturally occurring stem mutations could provide insight into functional antigenic drift of the HA stem domain. It is also worth noting here that we do not attempt to compare the rate at which the HA stem domain antigenically drifts in relation to the head domain. It is of future interest to understand whether there is a relationship between the rate of antigenic drift between these two domains.

Previous work has shown that the stem is slow to acquire mutations in vitro that abrogate stem antibody binding and that antibodies with broader binding are typically more resistant to escape mutations [31,45,47,49]. Given the potential such broadly reactive antibodies may hold as therapeutics and vaccine targets, it is important try to understand the impact of not just laboratory selected escape mutations but mutations that have accumulated naturally as a result of seasonal circulation. Here, we find limited change in stem antibody binding over 17-years of accumulated mutations. This observation adds to existing evidence that the stem may be a stable target for more durable vaccine responses. Moreover, our results suggest that stem constructs used as vaccine antigens may not need to be updated at different frequencies for H1N1 and H3N2 strains given that they appear to drift antigenically at similar rates.

Author Contributions

Conceptualization, L.E.G. and J.D.B.; investigation, L.E.G.; resources, H.W. and M.C.E.; writing—original draft preparation, L.E.G. and J.D.B.; writing—review and editing, all authors. All authors have read and agreed to the published version of the manuscript.

Funding

This work was supported by R01 AI127893 from the NIH/NIAID. J.D.B. is an Investigator of the Howard Hughes Medical Institute. This material is based upon work supported by the National Science Foundation Graduate Research Fellowship Program under Grant No. DGE-1762114. Any opinions, findings, and conclusions or recommendations expressed in this material are those of the author(s) and do not necessarily reflect the views of the National Science Foundation. The funders had no role in study design, data collection, or the decision to submit the work for publication.

Acknowledgments

We thank Allie Greaney and Andrea Loes for manuscript review, and the FHCRC Flow Cytometry Core for technical assistance.

Conflicts of Interest

J.D.B consults for Moderna and Flagship Labs 77 on topics related to viral evolution.

Chapter 3.

Antibody Neutralization of an Influenza Virus that Uses Neuraminidase for Receptor Binding

Lauren E. Gentles, Hongquan Wan, Maryna C. Eichelberger, and Jesse D. Bloom

3.1 Abstract

The influenza virus infection elicits antibodies against the receptor-binding protein hemagglutinin (HA) and the receptor-cleaving protein neuraminidase (NA). Because HA is essential for viral entry, antibodies targeting HA often potently neutralize the virus in single-cycle infection assays. However, antibodies against NA are not potently neutralizing in such assays, since NA is dispensable for single-cycle infection. Here we show that a modified influenza virus that depends on NA for receptor binding is much more sensitive than a virus with receptor-binding HA to neutralization by some anti-NA antibodies. Specifically, a virus with a receptor-binding G147R N1 NA and a binding-deficient HA is completely neutralized in single-cycle infections by an antibody that binds near the NA active site. Infection is also substantially inhibited by antibodies that bind NA epitopes distant from the active site. Finally, we demonstrate that this modified virus can be used to efficiently select mutations in NA that escape antibody binding, a task that can be laborious with typical influenza viruses that are not well neutralized by anti-NA antibodies. Thus, viruses dependent on NA for receptor binding allow for sensitive in vitro detection of antibodies binding near the catalytic site of NA and enable the selection of viral escape mutants.

3.2 Introduction

Neuraminidase (NA) and hemagglutinin (HA) are the two major proteins on the surface of influenza virions, and play opposing roles during the viral life cycle. HA mediates viral attachment and entry into cells, while NA cleaves sialic-acid receptors to release newly formed virions and prevent their aggregation [67]. NA also plays an important role in vivo by helping the virus penetrate mucus barriers to reach target cells [60,61]. Because only HA is needed for viral entry, anti-NA antibodies are not strongly neutralizing in infection assays where viruses are only allowed to undergo a single cycle of growth [79,143]. However, many studies have shown that anti-NA antibodies are associated with reduced disease severity in humans [1,57,58].

Recently, several exceptions to the classic role of NA as a receptor-cleaving but not a receptor-binding protein have been uncovered. Beginning in 2003, several groups identified mutations at NA site 151 in

H3N2 clinical isolates that had been passaged in cell culture [69,144–149]. It was soon discovered that the mutations D151G/N allow N2 NA to bind sialic-acid receptors, but ablate NA catalytic receptor-cleaving activity [144,147,149,150]. It was subsequently shown that because D151G/N NA lacks enzymatic activity, viruses carrying these mutations can only grow in mixed "cooperating" populations with viruses encoding NA that retains receptor-cleaving activity [151]. Importantly, the D151G/N mutations appear to only arise in cell culture, and have not been found in actual human infections [146,148,152].

Shortly after the identification of D151G/N in N2 NA, it was discovered that the G147R mutation enables N1 NA to bind to cellular receptors while maintaining its receptor-cleaving function [17]. Viruses carrying this NA mutation can grow as a clonal population unaided by wildtype virions [17]. Unlike D151G/N mutations that only arise in N2 NA in tissue culture, the G147R mutation has been identified at low frequency in several naturally occurring H1N1 and H5N1 isolates [18]. Importantly, viruses with the G147R N1 NA can grow efficiently in cell culture even if the receptor-binding activity of HA is completely ablated by engineered mutations [17,18].

Here, we utilize the G147R NA in conjunction with a binding-deficient HA to develop a sensitive neutralization assay for anti-NA antibodies. Specifically, we test the susceptibility of this NA-binding-dependent virus to neutralization by four monoclonal antibodies targeting distinct epitopes of N1 NA [143], and find that some of these antibodies neutralize the NA-binding-dependent virus much better than they neutralize a virus that can bind cells via HA. We then leveraged this discovery to select an in vitro escape mutation to one of the antibodies, demonstrating the value of these viruses for antigenic mapping. Overall, our work suggests that NA-binding-dependent viruses may be a useful tool for studying antibodies targeting NA.

3.3 Materials and Methods

3.3.1 Viruses and Reverse Genetics Plasmids

The viruses used in this study all had internal genes derived from A/WSN/1933. The NA was derived from A/California/7/2009 (H1N1). The binding-competent HA was also derived from A/California/7/2009

(H1N1). The binding-deficient HA is referred to as “PassMut” HA in the original reference [17] describing its creation. This HA is derived from the A/Hong Kong/1968 H3N2 strain, and has the following mutations: Y98F, H183F, and L194A at receptor binding residues; seven potential N-linked glycosylation sites added at residues 45, 63, 122, 126, 133, 144, and 246; deletion of the receptor binding proximal loop spanning residues 221–228; and mutation K62E in the HA2 stem (all mutations in H3 numbering).

All viruses packaged eGFP in place of the PB1 coding sequence in the PB1 segment to enable easy detection by fluorescence, and so were propagated in cells expressing PB1 as described previously [71]. Briefly, the PB1flank-eGFP segment retains the non-coding regions of PB1 and the last 80 terminal nucleotides which allows for efficient packaging of this segment into virions and replication to high titers when complemented by PB1 constitutively expressing cells. These viruses were generated from the following reverse genetics plasmids: for the WSN internal genes, pHW181-PB2, pHW183-PA, pHW185-NP, pHW187-M, and pHW188-NS [153]; for the PB1 segment, pHH-PB1flank-eGFP [71]; for the NA segment either pHWCA09tc-NA or pHWCA09tc-G147R; and for the HA segment either pHW-CA09tc-HA or pHWX31-HA-NGly12-Y98F-L194A-H183F-del221to228-K62EHA2. Here, “tc” indicates that these segments were originally cloned from tissue culture-derived virus.

For experiments with the S364N mutant of NA, we introduced S364N into pHWCA09tc-NA-G147R to create pHWCA09tc-G147R-S364N.

3.3.2 Virus Rescue and Titering

All viruses were rescued in PB1flank-eGFP format by reverse genetics as previously described with minor modifications [71]. Briefly, in 2 mL DMEM, supplemented with 10% heat-inactivated fetal bovine serum (FBS) and 2 mM L-glutamine, we transfected co-cultures of 2 × 105 293T-CMV-PB1 [71] and 2.5 × 104 MDCK-SIAT1-CMV-PB1-TMPRSS2 cells [51] per well in six well plates with 200 ng of each of the eight plasmids encoding the influenza gene segments plus a PB1 protein expression plasmid, pHAGE2-CMV-PB1-IRES-mCherry-W, and a TMPRSS2 expression plasmid, pHAGE2-EF1aInt-TMPRSS2-IRES-mCherry [51] to augment viral growth. At 14–16 hours post-transfection, the media was changed to 1mL

of Opti-MEM supplemented with 100 ug/mL CaCl2, 0.3% bovine serum albumin (BSA), and 0.01% FBS, here referred to as influenza growth media (IGM). At 48 h post-transfection, the supernatant was collected, clarified by centrifugation, and frozen at −80˚C. All viruses were then expanded in 10 cm dishes at a low multiplicity of infection (MOI) (<0.1) in MDCK-SIAT1-CMV-PB1-TMPRSS2 cells that allow for multiple rounds of replication since PB1 protein is provided in trans and TMPRSS2 cleaves HA into its active form. Viruses were grown for 72 h and then collected, clarified, and stored at −80 ˚C.

Infectious particles were titered as described [17] with minor modifications. Briefly, 5 × 105 MDCK-SIAT1-CMV-PB1 cells per well in a 12-well plate were infected with serial dilutions of viral supernatant for 14–16 h. The cells were then harvested by trypsinization and fixed for 1 h in 1% paraformaldehyde in PBS at room temperature before being washed twice and resuspended in a 1% BSA solution in PBS. The cells were then analyzed by flow cytometry to determine the % GFP positive cells, and this measurement was used to calculate the concentration of infectious particles in the viral stocks.

3.3.3 Antibodies

The antibodies used in this study were originally described in the references [143,154,155].

3.3.4 NA Microneutralization Assay

Micro-neutralization assays were performed as previously described with some modifications [17,18,27,156]. Briefly in 96-well flat-bottom plates, 5-fold dilutions of each antibody were made across each plate in low autofluorescent media (Medium 199 supplemented with 0.01% FBS, 0.3% BSA, 100ug/mL CaCl2, and 25mM HEPES buffer). We then added either the NAbind / HAΔbind virus, NAbind+S364N / HAΔbind virus, NAbind / HA wt virus, or NAwt / HA wt virus using an infectious dose determined to be within the linear range of detection. This infection dose was determined by making 2-fold serial dilutions of the viruses in 96-well flat bottom plates and infecting 4 × 104 MDCK-SIAT1-CMV-PB1 cells per well to find the highest viral dose producing a GFP signal at 15–17 h post-infection within the linear range of detection (i.e., the highest dose where the signal still increased linearly with the virus concentration). To measure infectivity in the presence of each antibody, the virus/antibody mixtures were

incubated at 37 ˚C for 1 h before adding 4 × 104 MDCK-SIAT1-CMV-PB1 cells per well. Viral growth was measured 15–17 h post-infection on a Tecan® Infinite® M1000 PRO plate reader to detect the eGFP signal from infected cells. The background signal from wells containing virus and media only was subtracted from all measurements. All neutralization curves represent the mean and standard error of the mean from three technical replicates read from a single plate.

3.3.5 Selection of Escape Mutants

Escape mutations were selected by first incubating 106 infectious particles of the NAbind / HAΔbind virus with 4ug/mL of the antibody HF5 at 37˚C for 1 h. The total volume of the virus-antibody mixtures was 1 mL in IGM. We then added the mixture to a 6-well plate containing 5 × 103 MDCK-SIAT1-CMV-PB1-TMPRSS2 cells per well, rocking the plate every 15 min for 1 h to promote infection. After the 1-hour incubation, we removed the remaining virus/antibody mixture and added 2 mL of fresh IGM. At 71 h post-infection, viral supernatant was collected from the selected sample, clarified by centrifugation, and stored at −80 ˚C. The selected viruses were then expanded twice by infecting MDCK-SIAT1-CMV-PB1-TMPRSS2 cells with the selected viral supernatant, allowing the virus to grow for 72 h. After this expansion step, the selection was repeated as above to deplete residual wildtype virus. One final expansion of the selected virus was done as above prior to sequencing.

3.3.6 Sanger Sequencing

Viral RNA was extracted from bulk selected virus supernatant using a Qaigen QIAmp® Viral RNeasy Mini Kit according to manufacturer instructions. We then used the SuperScript™ III First-Strand Synthesis System to generate cDNA using a universal influenza RT primer with U12-G4 homology - 5’ TATTGGTCTCAGGGAGCGAAAGCAGG 3’ [157]. HA and NA gene segments were then further amplified by PCR using KOD Hot Start Master Mix and the following primers: NA forward primer—5’ TATTGGTCTCAGGGAGCAAAAGCAGGAGT 3’ [157] and NA reverse primer—3’ ATATGGTCTCGTATTAGTAGAAACAAGGAGTTTTTT 3’ [157]; HAΔbind forward primer—5’ ATGAAGACCATCATTGCTTTGAGCTACATTTTC 3’ and HAΔbind reverse primer—5’

AGTAGAAACAAGGGTGTTTTTAATTACTAATACACTCA 3' that we designed. The PCR products were then Sanger sequenced. The consensus sequencing was compared to the original NA sequence and selected mutations were identified as those arising to the majority (>50% frequency) in chromatograms.

3.4 Results

3.4.1 Anti-NA Monoclonal Antibodies Neutralize an NA-Binding-Dependent Virus but not an HA-Binding Viruses in Single-Cycle Infection Assays

We generated three influenza viruses with differing dependencies on HA and NA for viral entry. The first virus contains the wild type HA and NA from the pandemic H1N1 vaccine strain A/California/7/2009 (Cal09). This virus has an HA that binds receptors and an NA that cleaves receptors, and will be referred to as NAwt / HAwt throughout the rest of this paper. We expected this virus to be unaffected by NA antibodies in a single-cycle infection assay (**Figure 3.1**).

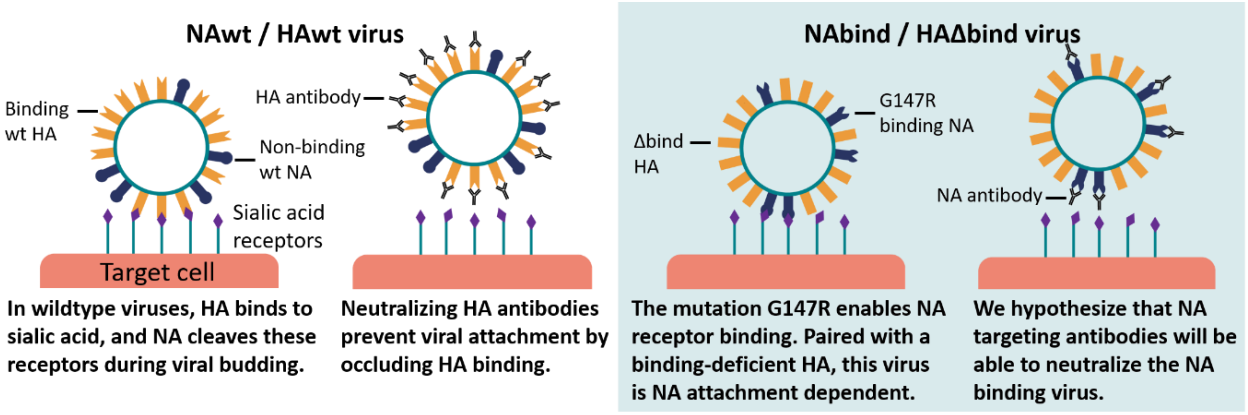

Figure 3.1 Proposed mechanism of neuraminidase (NA)-binding-dependent viruses by anti-NA antibodies. Most influenza viruses use hemagglutinin (HA) to bind and enter cells (left panel), so antibodies targeting HA can prevent infection while NA antibodies only inhibit the release of new virions. But in our engineered NA-binding-dependent virus (right panel), antibodies against NA can inhibit infection.

The second virus has the unmutated Cal09 HA, but the NA has the G147R mutation relative to the Cal09 sequence. As described in the Introduction, the G147R mutation enables NA to bind receptor while retaining its catalytic receptor-cleaving activity [17,18]. This virus will be referred to as NAbind / HAwt throughout the rest of this paper. We expected this virus to also be largely unaffected by NA antibodies in

a single-cycle infection assay, since HA can mediate an attachment to cells even when NA binding is blocked.

Finally, we generated a virus that is totally dependent on NA for receptor binding. To do this, we used a previously described engineered binding-deficient version of the HA from the H3N2 strain A/Hong Kong/1968 [17,18]. This engineered HA contains amino-acid mutations at key residues in the receptor binding pocket (Y98F, H183F, and L194A in H3 numbering [158]), deletion of residues 221-228 that form a loop near the receptor-binding pocket [159], and the addition of seven potential N-linked glycosylation sites (at residues 45, 63, 122, 126, 133, 144, and 246) that decrease HA receptor avidity [160]. The HA also contains the mutation K62E in the HA stem domain, which has previously been shown to enhance viral growth in the context of the other HA mutations [17,18]. Note that unlike the other HAs in this paper, this binding-deficient HA is H3 rather than H1—our rationale for using it is that it has been shown to completely lack receptor binding activity [17,18], whereas most characterized point mutants of HA in the receptor binding pocket (e.g., the widely used Y98F mutant) still retain a sufficient binding activity to enable HA-mediated infection in cell culture [161]. This binding-deficient HA was paired with the G147R mutant of the Cal09 NA to create a virus that we will refer to as NAbind / HAΔbind. We expect that anti-NA antibodies may neutralize this virus in single-cycle infection assays, since it depends on NA to attach to cells (**Figure 3.1**).

We tested neutralization of all three viruses using several well-characterized antibodies (HF5, CD6, 1H5, and 4E9) targeting different epitopes on NA's membrane-distal head domain [143]. These antibodies all bind to Cal09 NA and inhibit NA catalytic activity to varying degrees. HF5 and CD6 are strain-specific antibodies that each target distinct epitopes, and strongly inhibit NA activity as measured by enzyme-linked lectin assays (ELLA) which detect NA cleavage of the large glycoprotein substrate, fetuin [86,143]. Antibodies 1H5 and 4E9 recognize a similar epitope on the lateral surface of the NA head that is conserved across the N1 subtype, but these antibodies only weakly inhibit NA activity in ELLA assays [143].

We tested neutralization by each antibody in a single-cycle infection assay using a previously described method that uses viruses packaging eGFP in the PB1 segment [17,18,156,27]. The antibodies were pre-

incubated with the virus for one hour at 37 ˚C, and then the virus/antibody mix was used to infect cells for 15–17 hours before reading the fluorescent signal. In order to ensure only a single-cycle of viral growth, we performed the infections in the absence of trypsin, thereby precluding the proteolytic activation of newly formed HA that is necessary to enable secondary infection [32,162].

As expected, none of the antibodies substantially neutralized the NAwt / HAwt virus (Figure 2). However, several antibodies partially neutralized and one completely neutralized the NAbind / HAΔbind virus (**Figure 3.2**). The antibody that completely neutralized the NAbind / HAΔbind virus was HF5, which binds to the top of the NA near the active site [143]. Interestingly, HF5 also partially neutralized the NAbind / HAwt virus, suggesting that it uses both NA and HA to bind to cells.

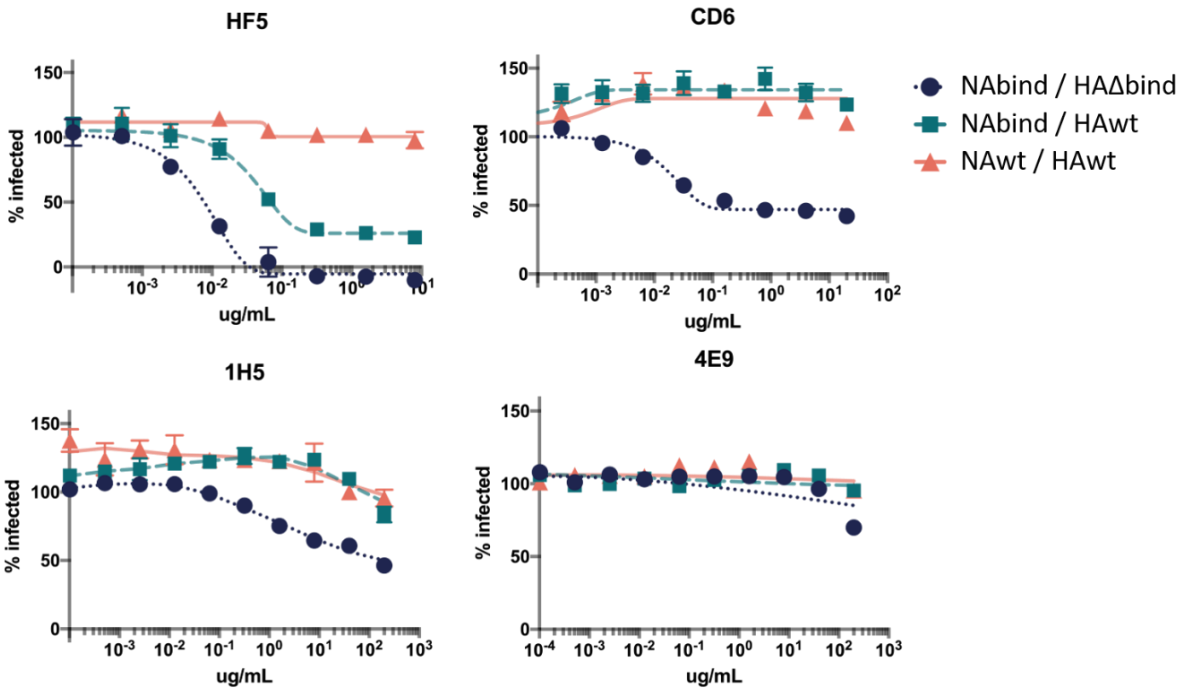

Figure 3.2 Neutralization of viruses with different dependencies on HA and NA for receptor binding by anti-NA antibodies in single-cycle infection assays.

Neutralization curves show the percentage of the NAwt / HAwt, NAbind / HAwt, or NAbind / HAΔbind virus infection that is inhibited by each antibody over a range of concentrations compared to the no-antibody control infection. Points represent the mean of three technical replicates with error bars showing the standard error of the mean.

The extent to which antibodies neutralized the NAbind / HAΔbind virus paralleled with their ability to inhibit NA catalytic activity in previously reported ELLA assays (**Table 3.1**) [143]. Specifically, HF5 has the strongest ELLA activity and was the most potent in our neutralization assay, CD6 has intermediate ELLA activity and partially neutralized in our assay, and 4E9 and 1H5 have little impact on NA catalytic activity in ELLA assays and do not neutralize [143]. We speculate that the correlation between neutralization of NAbind / HAΔbind and inhibitory activity in the ELLA assay reflects the fact that the G147R receptor-binding NA binds to cells using the NA active site [17]. Therefore, an antibody that blocks NA activity would also be expected to block binding.

Table 3.1 NA antibody inhibition by epitope location.

Antibody	Amino-Acids Targeted	ELLA Inhibition	Neutralization
HF5	364, 369, 397	+++	+++
CD6	95, 449, 451	++	++
1H5	273, 338, 339	+	+
4E9	273, 338, 339	+	-

(−) no activity, (+) weak activity, (++) moderate activity, (+++) strong activity. Enzyme-linked lectin assay (ELLA)

3.4.2 Selecting Antibody-Escape Mutations Using the NA-Binding Virus

One classic approach to map the epitopes of neutralizing antibodies is to select viral mutants that escape neutralization. This approach has been widely and successfully applied to neutralizing anti-HA antibodies where it works very well because it directly selects for viral mutants that can enter cells in the presence of the antibody [126,163,127,130]. We tested whether our NAbind / HAΔbind virus could similarly be used to select antibody viral escape mutants in NA. To accomplish this, we pre-incubated a stock of the NAbind / HAΔbind virus with the HF5 antibody at an excess of the amount needed to totally neutralize this virus, and then infected the cells with the antibody/virus mix to select for mutants that escaped antibody binding. The resulting virus was then passaged to produce appreciable titers before performing a second round of selection to deplete any parental virus remaining in the population.

Upon Sanger sequencing of the selected virus population in bulk, we discovered two mutations that were present in the consensus sequence after the antibody selection. One of the selected mutations, S364N, had previously been identified as an HF5 escape mutation in cell-based ELISAs using a panel of mutants and again after the passage of Cal09 virus in passively immunized animals [143]. The second mutation was D151N—as discussed in the Introduction, this mutation confers receptor-binding properties on N2 NA [144,147,149,150]. We speculate that D151N indirectly increases antibody resistance by enhancing NA's affinity for receptors, similar to the "avidity" mutations that sometimes arise in HA under antibody pressure [164]. Therefore, D151N might allow the virus to outcompete antibody binding by increasing NA binding avidity to cells, allowing rapid attachment and therefore reducing sensitivity to antibodies in a similar fashion to that shown for HA [164]. Since D151N ablates NA catalytic activity, it is not possible to rescue this virus as a clonal population [151], so we only tested the S364N mutation in subsequent validation. Based on prior work [151], it may be possible to generate D151N as a mixed cooperating population, but we did not attempt that here.

To validate that S364N is an HF5 escape mutation in the NAbind / HAΔbind virus, we performed neutralization assays with the parental NAbind / HAΔbind virus and a reverse-genetics generated virus with S364N introduced into this background. As expected, S364N greatly increased the resistance of the virus to HF5 neutralization (**Figure 3.3**). This observation illustrates the utility of the NAbind / HAΔbind virus for identifying escape mutants from antibodies that target regions of NA near the active site.

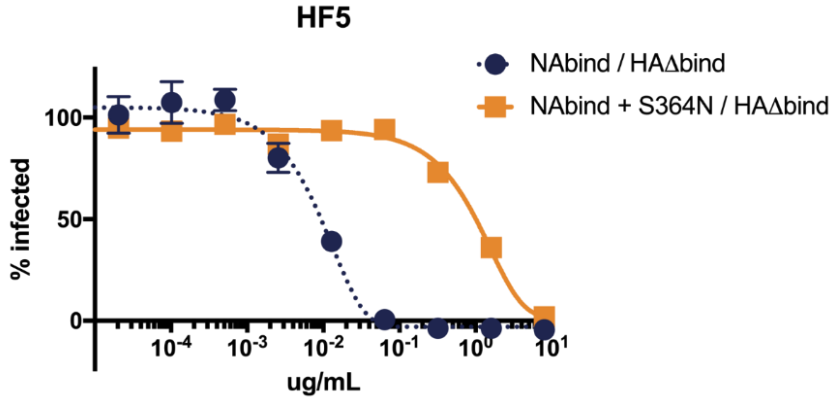

Figure 3.3 S364N increases resistance to neutralization by antibody HF5 in single-cycle infections for viruses that are dependent on NA for receptor-binding.

Results are shown as the percent infection at each concentration compared to the no-antibody infection control. Points represent the mean of three technical replicates with error bars showing the standard error of the mean.

3.5 Discussion

We have shown that engineered influenza viruses that use NA for receptor-binding are potently neutralized by some anti-NA antibodies. This contrasts with the typical situation for viruses that bind receptors using HA, where the inhibitory activity of anti-NA antibodies only becomes strongly apparent after multicycle growth [79,165].

Notably, neutralization of NA receptor-binding-dependent viruses is strongest for antibodies that bind to the top of the NA head near the active site where receptor binding also occurs. A similar trend occurs for HA, with the most potent antibodies often directly blocking the interaction between HA and cellular sialic acid receptors [28,130,163,166]. Because the neutralization of the NA-binding-dependent virus likely depends on blocking receptor binding by residues in NA's catalytic site, neutralization by anti-NA antibodies parallels their ability to inhibit NA catalytic activity in ELLA assays. Of interest, a recent study identified NA antibodies that are broadly protective in mice and bind near the active site of NA [78], suggesting that the types of NA antibodies that are highly active against NA receptor-binding viruses in vitro can also be protective in vivo.

We also show that NA-binding-dependent viruses can be used to easily select for anti-NA antibody escape mutations in vitro. Previous in vitro methods of selecting escape mutants to anti-NA antibodies require selection in multi-cycle growth conditions or by passaging the virus in passively immunized animals [143,167]. Therefore, we suggest that in some cases, NA receptor-binding viruses could be a useful tool to simplify the mapping of anti-NA antibody epitopes via escape-mutant selections.

Chapter 4.

Longitudinal dynamics of infection-elicited SARS-CoV-2 antibodies in children

Lauren E. Gentles, Leanne Kehoe, Katharine H.D. Crawford, Kirsten Lacombe, Jane Dickerson, Caitlin Wolf, Joanna Yuan, Susanna Schuler, John T. Watson, Sankan Nyanseor, Melissa Briggs-Hagen, Sharon Saydah, Claire M. Midgley, Kimberly Pringle, Helen Chu, Jesse D. Bloom, and Janet A. Englund

4.1 Abstract

Severe acute respiratory syndrome coronavirus 2 (SARS-CoV-2) infection elicits an antibody response that targets several viral proteins including spike (S) and nucleocapsid (N); S is the major target of neutralizing antibodies. Here, we assess levels of anti-N binding antibodies and anti-S neutralizing antibodies in unvaccinated children compared with unvaccinated older adults following infection. Specifically, we examine neutralization and anti-N binding by sera collected up to 52 weeks following SARS-CoV-2 infection in children and compare these to a cohort of adults, including older adults, most of whom had mild infections that did not require hospitalization. Neutralizing antibody titers were lower in children than adults early after infection, but by 6 months titers were similar between age groups. The neutralizing activity of the children's sera decreased modestly from one to six months; a pattern that was not significantly different from that observed in adults. However, infection of children induced much lower levels of anti-N antibodies than in adults, and levels of these anti-N antibodies decreased more rapidly in children than in adults, including older adults. These results highlight age-related differences in the antibody responses to SARS-CoV-2 proteins and, as vaccines for children are introduced, may provide comparator data for the longevity of infection-elicited and vaccination-induced neutralizing antibody responses.

4.2 Introduction

SARS-CoV-2, the causative agent of coronavirus disease 2019 (COVID-19), elicits an antibody response targeting multiple viral proteins following infection. Anti-spike (S) antibodies are of particular importance because S is the major target of neutralizing antibodies and neutralizing anti-S antibody titers correlate with protection [3–5,168]. For this reason, currently authorized vaccines only include the S antigen and specifically induce anti-S responses. Additionally, SARS-CoV-2 neutralization assays are designed to measure the potency of antibodies that block viral binding and entry to cells, including via inhibiting S binding to host angiotensin converting enzyme 2 (ACE2) on host cells, and/or inhibiting S fusion. Nucleocapsid (N) protein is also highly immunogenic during SARS-CoV-2 infection and is a predominant

target of binding antibodies making it a robust marker of infection. In adults, circulating antibodies rise to peak titers within 3-5 weeks after infection and then gradually begin to wane [3,4,106,108–116]. Studies have shown a strong positive correlation between neutralizing antibody titers and protection from subsequent infection [5,90,91,169–171].

COVID-19 in children tends to be milder than in adults, resulting in lower risk of progression to hospitalization and death [172,173]. However, clinical manifestations of COVID-19 vary widely in children as in adults and can range from asymptomatic infections to illness lasting for several months [118]. Furthermore, infection by SARS-CoV-2 in children causes a greater burden of hospitalization and death than pre-vaccine burden of some other childhood illnesses, including varicella [117]. Previous work has documented the acute and convalescent dynamics of the SARS-CoV-2 antibody response in adults across a wide range of ages and disease severities [3,4,105–109,116], but few data are available detailing the longevity of circulating antibodies in the pediatric population [107,119,120].

Here, we follow a cohort of 32 SARS-CoV-2-infected convalescent children <18 years old up to 52 weeks post-symptom onset, measuring anti-S neutralizing antibody levels with a pseudoneutralization assay, and anti-N binding antibody levels. We compare the pediatric antibody response to those in a previously characterized cohort of adults [3].

4.3 Materials and Methods:

4.3.1 Pediatric Participants

Our IRB-approved study enabled us to enroll children, defined as <18 years old at enrollment, including children with underlying medical conditions, and obtain sera for the assessment of immune responses to SARS-CoV-2 infection at Seattle Children's Hospital, Seattle, WA, beginning in April 2020. Informed consent was obtained from parents and assent from children over 7 years of age. The REDCap electronic data collection tool was used to acquire demographics, hospitalization data; clinical information including respiratory support, ICU admission, length of stay; laboratory studies including viral testing results, and

medical history including chronic underlying medical conditions [174]. This study was reviewed and approved by the Seattle Children's Hospital IRB[§].

Children with confirmed or presumed SARS-CoV-2 infection were recruited to our study between April 2020 and January 2021. Children were considered to have a confirmed SARS-CoV-2 infection if they tested positive for SARS-CoV-2 by RT-PCR. Children were presumed to have SARS-CoV-2 infection if they did not have documentation of a positive RT-PCR, but had detectable SARS-CoV-2-specific antibodies and either 1) presented with confirmed Multisystem Inflammatory Syndrome in Children (MIS-C), or 2) were symptomatic and had an RT-PCR-positive household contact.

All children were recruited from the Seattle metropolitan area. Enrollment included hospitalized children, children who were tested for SARS-CoV-2 using RT-PCR as outpatients as determined by their provider, and children who did not receive medical care but were recruited from the community, including community-based surveillance platforms [175]. Children were recruited during acute illness with sera drawn at approximately 4-8 weeks (1-2 months), 24 weeks (6 months), and 52 weeks (12 months) following symptom onset for confirmed or presumed infection. Only children who provided at least two specimens by May 2021 were included in this analysis. In addition, only presumed cases with at least one positive serological result were included (**Supplemental Table 7.1**). For asymptomatic cases, weeks post-positive RT-PCR test result was used as a substitute for weeks post-symptom onset. For children who developed MIS-C, "weeks post-symptom onset" refers to acute infection symptoms prior to MIS-C onset. No children in this study were vaccinated prior to specimen collection.

4.3.2 Adult Participants

Adult specimens were collected as a part of the Hospitalized or Ambulatory Adults with Respiratory Viral Infections (HAARVI) cohort at the University of Washington Department of Medicine [3,96,176]. Adults were enrolled from March through May of 2020. A convenience sample of adults who provided specimens at roughly eight- and twenty-four-weeks post-symptom onset were included in this analysis. Study

enrollment and specimen collection are detailed elsewhere [3,96,176]. Briefly, adults were enrolled in the study following RT-PCR confirmed SARS-CoV-2 infection. Inpatients were recruited for enrollment during their hospital stay at Harborview Medical Hospital, University of Washington Medical Center, or Northwest Hospital in Seattle, Washington in 2020. Asymptomatic adults were identified as participants who responded "None" to a symptom questionnaire and tested positive for SARS-CoV-2 infection via outpatient or community testing. Informed consent was provided by all participants or their legally authorized representatives. No adults in this study were vaccinated prior to specimen collections since no vaccines were available during the collection period, and no adults in this study were enrolled in ongoing vaccine clinical trials. Weeks post-positive RT-PCR test result was used in lieu of weeks post-symptom onset for asymptomatic adults.

4.4 Laboratory Methods

4.4.1 Pediatric specimen collection

Whole blood collection was scheduled for 4 to 8-weeks, 24-weeks, and 52-weeks post-symptom onset for the pediatric cohort (**Supplemental figure 7.1**). Blood specimens were collected in serum separator tubes, stored at 5°C, and spun within 24 hours before being aliquoted and stored at -80°C. Heat inactivation of all specimens was performed at 56°C for 30 minutes before performing serological assays.

4.4.2 Adult specimen collection

Whole blood collection was scheduled for 8- and 24-weeks post-symptom onset for the adult cohort. Blood specimens were immediately added to acid citrate dextrose tubes upon collection which were then spun down to separate out the red blood cell fraction. Within 6 hours following collection, aliquots of these specimens were frozen at -20°C for storage. Prior to use in serological assays, all specimens were heat inactivated at 56°C for one hour.

4.4.3 Neutralization assays

Neutralization assays were performed as previously reported using spike-pseudotyped lentiviral particles [3]. The spike protein used is based on Wuhan-Hu-1 (GenBank: MN908947) with a 21 base pair deletion (delta21) at the terminus of the cytoplasmic tail that enhances viral titers [177–182]. The spike also contains the mutation D614G that has become predominant in circulating strains [183]. Plasmid HDM_Spikedelta21_D614G encoding this spike protein is available from AddGene (no. 155130) or BEI Resources (NR-53765) along with the full annotated sequence. To perform neutralization assays, $1.25x10^4$ HEK-293T-ACE2 cells [19] (BEI resources NR-52511) are added in 50ul per well of a 96-well poly-L-lysine coated plate (Greiner; no. 655936). Our limit of detection for the neutralization assay is 1:20 since this is the starting serum dilution. All assays included pre-pandemic pooled serum collected between 2015 to 2018 as a negative control. No substantial neutralization was observed for a pool of pre-pandemic sera at a dilution of 1:20. SARS2 Spike-D614G-delta21 pseudotyped lentivirus particles encoding luciferase were added at a dilution of 200,000 RLU per well as determined by titering. The virus-antibody plate was then incubated for 1 hour at 37°C before being added to the plate with cells. Neutralization titers were determined using a plate reader to measure luciferase activity at 50 hours post-infection. Measurements were given as the reciprocal dilution of sera at which viral infection was inhibited by 50% (NT_{50}). NT_{50} values were calculated using the neutcurve python package version 0.5.3 available here: https://github.com/jbloomlab/neutcurve which fit a Hill curve to our data to determine the 50% inhibitory concentration (IC_{50}). NT_{50} values reported here were the reciprocal of the IC_{50}.

4.4.4 SARS-CoV-2 IgG assay

The SARS-CoV-2 IgG assay, an FDA Emergency Use Authorized immunoassay, which utilizes a chemiluminescent test to assess immunoglobulin G (IgG) binding to nucleocapsid (N) protein, was performed according to manufacturer specifications. Anti-N IgG index values were assessed; higher index values reflected higher antibody levels. An index value of > 1.40 is considered a positive result for this

assay. Sensitivity and specificity of the SARS-CoV-2 IgG assay have been reported elsewhere [105,184–188].

4.4.5 Comparison of antibody levels in a subset of immunocompetent children and adults

For comparison of antibody levels between pediatric participants and adults, we limited our analysis to only specimens that were collected within a similar range of weeks post-onset between 8-13 (first collection period) and 24-29 (second collection period) weeks for both cohorts. In this sub-analysis, we excluded participants with MIS-C development, complicating immunocompromising conditions, or receipt of multiple blood transfusions. We assessed changes in antibody titers over time among a limited number of children and adults with two specimens collected within these comparative time frames. Statistical significance was determined by Mann Whitney test.

4.5 Results

4.5.1 Study participants.

From April 2020 through June 2021, we enrolled 97 pediatric participants of whom 42 had completed at least 6-months of follow-up with two blood draws obtained by May 2021 (**Figure 4.1**). Thirty-two of the 42 children had evidence of confirmed or presumed infection and were included in the pediatric analysis: 27 of 32 had a confirmed positive RT-PCR test, including one of two children who presented with MIS-C; one of 32 had a positive serological test result and presented with MIS-C; and four of 32 had a positive serological test result and a known RT-PCR-positive household member (**Supplemental Table 7.1**). Among the 32 children included in this analysis, median age was 12 years, 6 (19%) were female, 5 (16%) were symptomatic and hospitalized, 25 (78%) were symptomatic but not hospitalized, and 2 (6%) were asymptomatic during acute infection (**Table 4.1, Figure 4.2**). Of the two children who developed MIS-C: one (C27) had an asymptomatic acute infection (identified through RT-PCR) and subsequently required ICU admission and supplemental oxygen in the form of bilevel positive airway pressure upon the onset of MIS-C symptoms; the other (C15) had an initial SARS-CoV-2 respiratory infection managed as an

outpatient but was subsequently hospitalized with MIS-C, during which time C15 was SARS-CoV-2 RNA-negative and antibody-positive. Five children had underlying immunocompromising conditions or received multiple blood transfusions; four of whom were hospitalized. Among the 25 children who were not immunocompromised, did not received multiple blood transfusions, and did not present with MIS-C (**Figure 4.2A**), one child was hospitalized, 22 children were symptomatic but not hospitalized, and two children were asymptomatic.

Table 4.1 Pediatric and adult cohort demographics by disease severity.

Pediatric cohort

Characteristic	Asymptomatic n=2	Symptomatic non-hospitalized n=25	Symptomatic hospitalized n=5	Overall n=32
Age, median (range)	10 (9.3-10.7)	11.8 (0.2-17.8)	16 (3.6-17.7)	12 (0.2-17.8)
Sex, no. (%)				
Female	0 (0)	4 (16)	2 (40)	6 (19)
Male	2 (100)	21 (84)	3 (60)	26 (81)
Immunocompromised or received multiple blood transfusions*	0	1	4	5

*No other children reported chronic conditions.

Adult cohort

Characteristic	Asymptomatic n=4	Symptomatic non-hospitalized n=8	Symptomatic hospitalized n=2	Overall n=14
Age, median (range)	69.5 (60-79)	65 (47-76)	59 (54-64)	65 (47-79)
Sex, no. (%)				
Female	3 (75)	4 (50)	1 (50)	8 (57)
Male	1 (25)	4 (50)	1 (50)	6 (43)

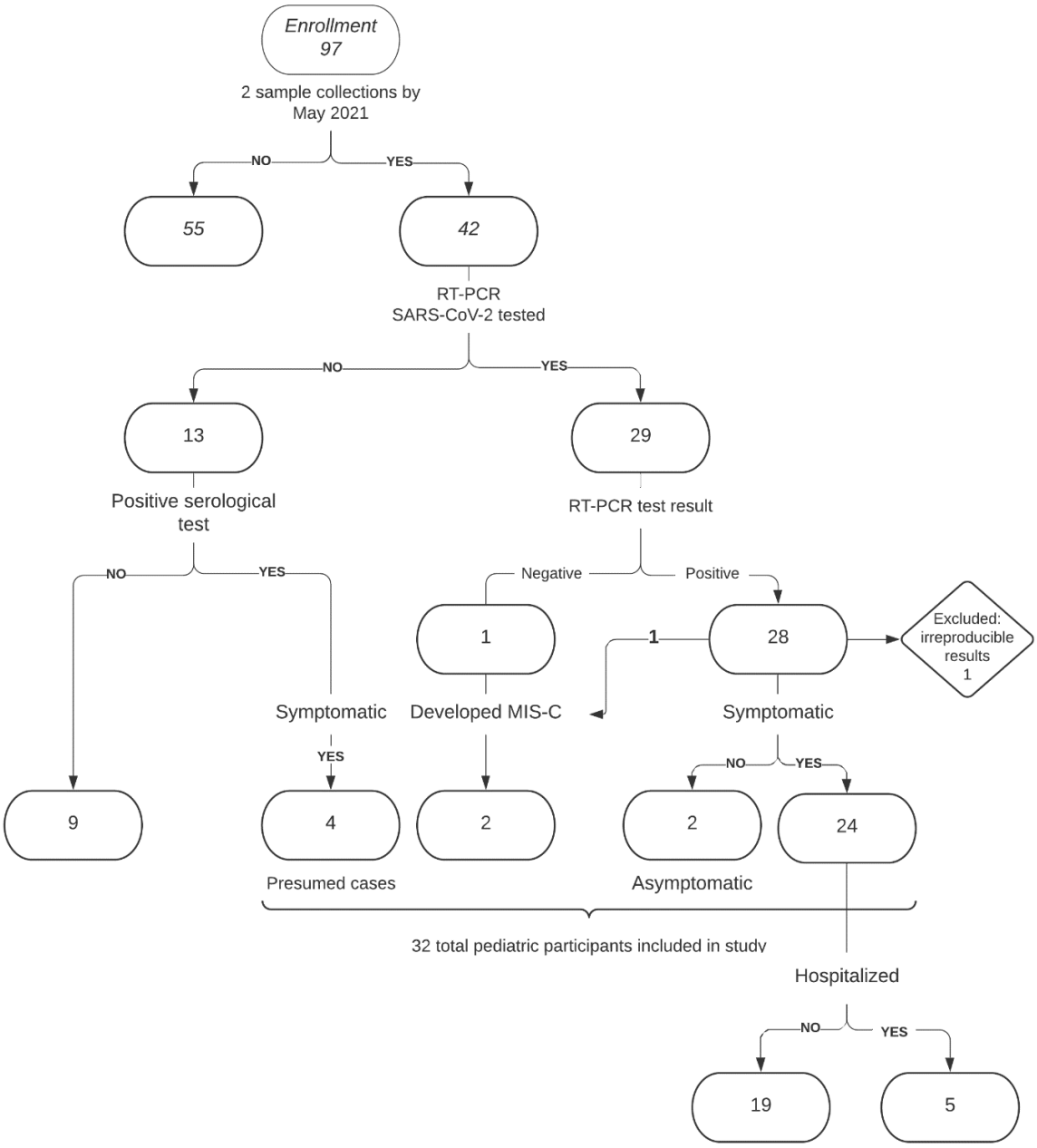

Figure 4.1 Pediatric study inclusion criteria flowchart.

Evidence of infection included a PCR-positive test (n=28) or positive serological test result following a known RT-PCR-positive household exposure (n=4) and/or presentation with MIS-C (n=2).

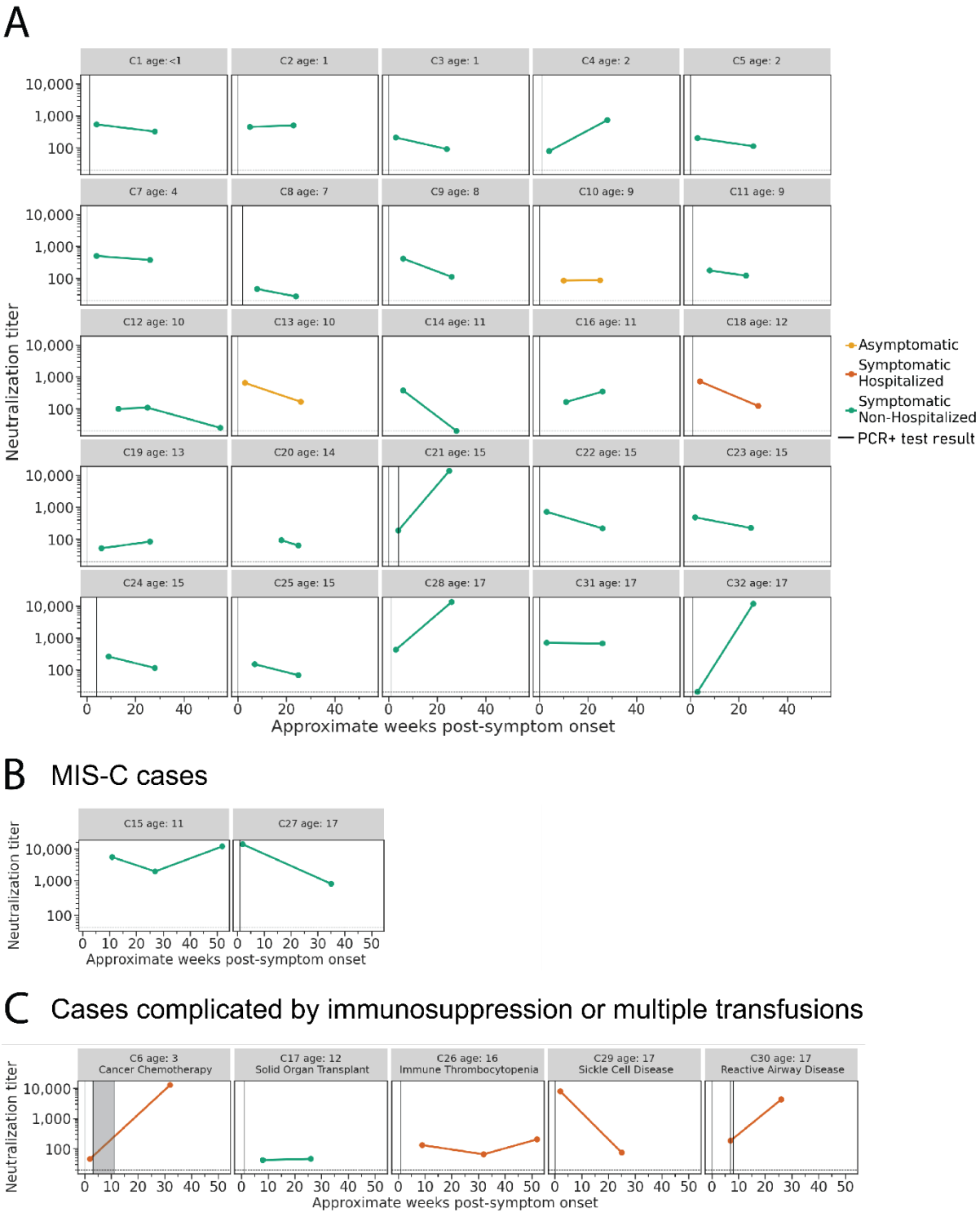

Figure 4.2 Neutralization titers in children over time.

Neutralizing antibody titers (NT_{50}) in **A**) 25 children with confirmed SARS-CoV-2 infection, **B**) children who developed MIS-C following acute infection and **C**) cases complicated by immunosuppression (N = 4) or multiple blood transfusions (N = 1) in 5 children with confirmed SARS-CoV-2 infection followed

prospectively over time shown as weeks. Vertical lines represent the week of positive RT-PCR test result(s), and shaded areas indicate weeks with consecutive positive PCR test results. Colors show disease severity during acute infection. Dotted horizontal lines indicate the limit of detection (20).

A second cohort of 14 SARS-CoV-2-infected unvaccinated immunocompetent adults between the ages of 47 and 79 years (median: 65) was included in this study as a comparator group. We previously profiled neutralizing antibody dynamics for all these adults out to 90 days post-symptom onset [3] (See **Supplemental Table 7.2**). Here we performed additional assays for the same adult participants to enable direct comparison with the pediatric cohort in a sub-analysis. This convenience sample of 14 adults included two who were symptomatic and hospitalized, 8 who were symptomatic non-hospitalized, and 4 who were asymptomatic. Eight (57%) adults were female. Two adult participants reported underlying conditions: one participant (A3) was recorded as having diabetes, chronic obstructive pulmonary disease, asthma, and obstructive sleep apnea; and another (A13) had hypertension.

4.5.2 Specimen collection.

During the first and second collection period, specimens were collected from the 32 children at a median of 4.5 weeks (IQR: 2.5weeks; range: 2-18weeks) and 26 weeks (IQR: 1.25weeks; range: 23-35weeks), respectively; 3 children also had blood collected at 52 weeks. At 8- and 24-weeks, specimens were collected from the 14 adults at a median of 9.5 (range: 8-13weeks, IQR:1wk) and 25 weeks (range: 24-29weeks, IQR: 1wk), respectively. To compare pediatric and adult responses, we performed a sub-analysis which included specimens collected within two collection periods: the first at 8-13 weeks, and the second at 24-29 weeks. This sub-analysis included specimens from all 14 adults; for children, 7 children had blood drawn in the first collection period (median = 9.5 weeks; IQR = 2.5) and 24 children had blood drawn in the second collection period (median 26 weeks; IQR=1) Five children and 14 adults, with specimens collected at both timepoints, were included in fold-change analyses.

4.5.3 Neutralization dynamics over time in children.

We measured neutralization titers for the pediatric specimens collected at each time period (**Figure 4.2A, B, & C**). All children with confirmed or presumed infections had measurable neutralizing antibody titers for at least one specimen. For the 25 children without MIS-C or immunocompromising conditions or multiple blood transfusions, overall neutralization titers changed very little over the course of 24 weeks from a geometric mean NT_{50} of 214 and 244 for the first and second collection period, respectively. Interestingly, a greater than 4-fold increase in neutralization titer between the first and second collection period was seen for four children all of whom were symptomatic but not hospitalized. If these four children are excluded, the geometric mean NT_{50} decreases by 1.86-fold from the first to the second collection period (from 245 to 132, respectively). For two of the 25 children without immunocompromising conditions, a decrease of greater than 4-fold between 4 and 24 weeks was observed. Both children were symptomatic of whom one was hospitalized. For 19 (76%) of the 25 children, less than 4-fold (range 3.86- to 1.02-fold) changes in neutralization titers were observed. One child with increasing titers, (C32), had no detectable neutralization titer at 3 weeks post-symptom onset despite testing positive by RT-PCR, but subsequently developed high neutralization titers by 26 weeks. Despite the variability among individual immunocompetent children, some trends in the overall antibody dynamics were observed (**Figure 4.3A**). Nearly all immunocompetent children had neutralizing activity at all timepoints, and the majority of children (15 out of the 25 total) exhibited at least a 25% decrease in neutralization titers over 24 weeks.

For further clinical and laboratory data on children with underlying immunocompromising conditions, multiple blood transfusions, or MIS-C, please refer to Figures 2B & C. Three children with specimens at 52 weeks had detectable neutralizing antibodies (**Figure 4.2A, B, & C**). Of note, one child (C26) with blood collected at 52 weeks reported a febrile illness, with negative SARS-CoV-2 RT-PCR, between the 24- and 52- week specimen collection (**Figure 4.2C**).

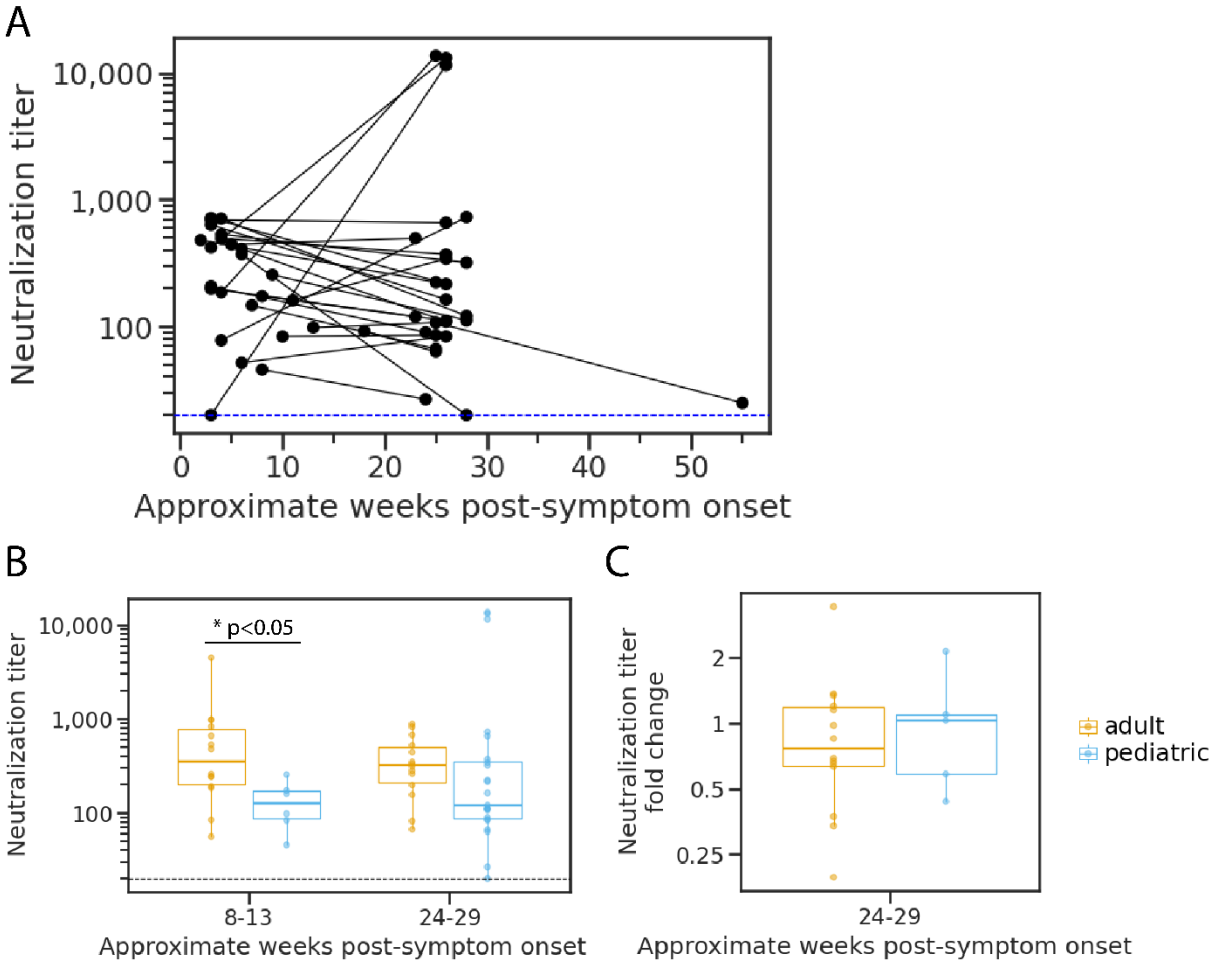

Figure 4.3 Neutralization potency kinetics in children compared to adults.

A) Aggregated trajectories of pediatric neutralization titers (NT50) longitudinally with lines connecting specimens from the same individual for the 25 pediatric participants without underlying immunosuppression, receipt of multiple blood transfusions, or MIS-C. **B**) Comparison of adult and pediatric neutralization titers collected within the time periods 8 to 13 weeks and 24 to 29 weeks for the participants without underlying immunosuppression, receipt of multiple blood transfusions, or MIS-C. **C**) Analysis of fold change in neutralization titers at 24 to 29 weeks relative to titers at 8 to 13 weeks for adults and children without underlying immunosuppression, receipt of multiple blood transfusions, or MIS-C. Significance determined by Mann Whitney test.

4.5.4 Comparison of neutralization dynamics in immunocompetent children and adults.

We next compared neutralization titers and their longitudinal dynamics in children and adults. To accomplish this, we measured plasma neutralizing antibody levels from adults over a 24-week period. Neutralization titers for specimens collected at 8- to 13-weeks post-symptom onset (first collection period) were previously reported using the same spike pseudotyped lentivirus neutralization assay but without the

D614G spike mutation [3]. Here, we repeated the neutralization assays using spike pseudotyped lentivirus encoding D614G as well as performing neutralization assays for the first time on specimens collected between 24 and 29 weeks (second collection period). Neutralization titers had a geometric mean of 385 (range: 56 - 4,487) and 302 (range: 67 – 880) at the first and second collection period, respectively (**Supplemental figure 7.2**). Of the 14 participants in our adult cohort, only one demonstrated a greater than 4-fold decrease in neutralization titer over the observation period, and no adults showed an increase greater than 4-fold. There were no adults for whom neutralization titers fell below the limit of detection during the timeframe tested.

For comparison of neutralization titers between the children and adults including older adults, we restricted our analysis to only specimens collected in the same timeframe for both cohorts, as well as only including children without immunocompromising conditions, those who did not receive multiple blood transfusions, and those without MIS-C. In this sub-analysis, we found that children had significantly lower neutralization potency (geometric mean titer [GMT] = 118, range: 46-256, N=7, $p<0.05$) than adults (GMT = 385, range: 56-4,487, N=14) during the first collection period, but titers were not significantly different between age groups by the second collection period (children: GMT= 244, range: 27-13,694, N=22; adults: GMT = 302, range: 67-880, N=14; $p = 0.23$) (**Figure 4.3B**). If the four children with neutralization titers that increased by greater than 4-fold are excluded, the children's GMT for the second collection period is 2.46-fold lower than the adults' (123 compared to 302 in children and adults, respectively). We calculated the fold change in titers for each individual measured at the first collection period relative to those measured for the same individual during the second time period. Fold change analysis was limited to 5 children with specimens collected at both first and second collection period; no difference in the fold change between children (geometric mean fold decrease = 1.12, N=6, $p = 0.893$) and adults (geometric mean fold decrease = 1.28, N=14) was detectable. (**Figure 4.3C**)**.**

4.5.5 Anti-nucleocapsid antibody dynamics over time in children.

Anti-N antibody levels were determined for all pediatric specimens (**Figure 4.4A, B, & C**). Among the 25 children without immunocompromising conditions, multiple blood transfusions, or MIS-C, 23 and 14 had detectable anti-N antibodies at the first and second collection periods, respectively; 2 children with confirmed infection by RT-PCR (C1 and C32) did not have detected anti-N antibodies at either timepoint. Anti-N antibody levels dropped dramatically from a geometric mean index of 3.7 to 1.3 over 24 weeks. Eighteen of the 23 children, who were positive for anti-N antibodies at the first collection period, exhibited a decrease in index values of greater than 2-fold, and an additional five changed less than 2-fold. No children showed an increase in anti-N antibodies. In totality, the children without immunocompromising conditions showed very similar declining trends in anti-N antibody levels across time (**Figure 4.5A**). Of the children with a positive index at 4 weeks, values ranged from 1.9 to 8.0 and from undetectable to 7.3 by the first and second collection periods, respectively.

For anti-N antibody levels and clinical information for the children with underlying immunocompromising conditions, multiple blood transfusions, or MIS-C refer to Figure 4B & C. The antibody dynamics out to 52-weeks post-symptom onset were measured for three children all of whom had levels below the limit of detection by this later time period (**Figure 4.4A, B, &C**).

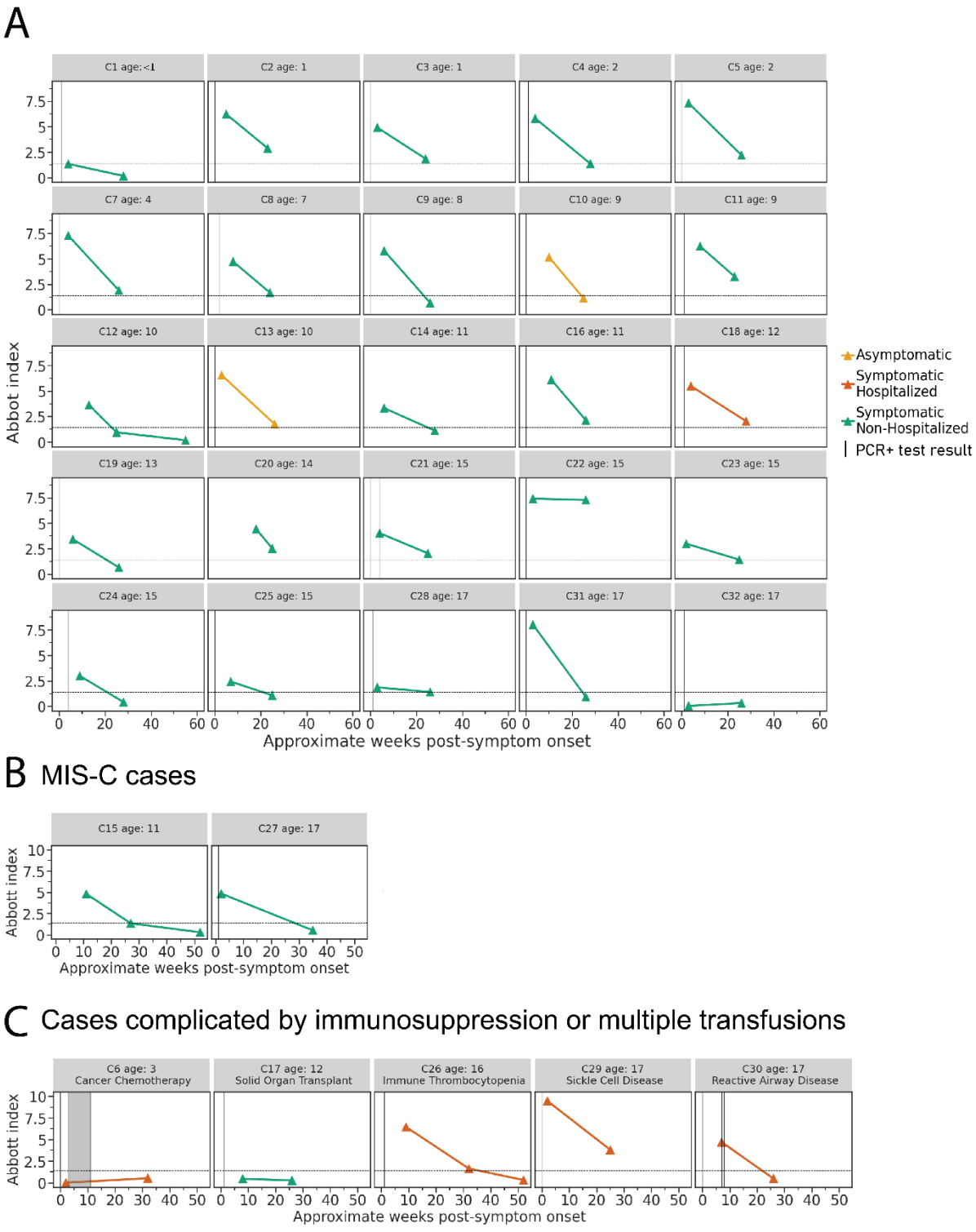

Figure 4.4 Anti-nucleocapsid antibody binding in children over time.

Anti-N antibody titers in **A**) 25 children with confirmed SARS-CoV-2 infection, **B**) children who developed MIS-C following acute infection, and **C**) cases complicated by immunosuppression or multiple blood transfusions in 5 children with confirmed SARS-CoV-2 infection followed prospectively over time shown

as weeks. Vertical lines represent the week of positive RT-PCR test result(s), and shaded areas indicate weeks with consecutive positive PCR test results. Colors show disease severity during acute infection. Dotted horizontal lines indicate the limit of detection for the Abbott Architect assay (1.40).

4.5.6 Comparison of pediatric and adult anti-nucleocapsid antibody dynamics.

Next, we compared anti-N antibody dynamics in children and adults. We first measured anti-N antibody levels for all adult specimens in our cohort (**Supplemental figure 7.3**). Overall, geometric mean values fell from 6.0 to 3.3 between the first and second collection period, respectively. One adult (A12) had values below the limit of detection at both 8- and 24-weeks post-symptom onset. Of the adults with a positive index at 8 weeks, values ranged from 4.2 to 9.4 and from 1.9 to 7.7 by the first and second collection period, respectively. No adults with positive index values at the first timepoint fell below the limit of detection by the later timepoint. This is in stark contrast to the pediatric cohort where many fell below detectable levels over the course of the study. Furthermore, only 3 adults showed a greater than 2-fold decrease in index values.

Compared to the pediatric cohort, adults had higher anti-N antibody levels at both timepoints measured although not quite reaching statistical significance at 8-13 weeks (children: GMT = 4.7, range: 3.0-6.2, p=0.053; adults: GMT = 6.0, range: 0.8-9.4) (**Figure 4.5B**). The difference between adult and child index values was greatest at the later 24- to 29-week timepoint (children: GMT = 1.2, range: 0.2-7.3, $p<0.0005$; adults: GMT = 3.3, range: 0.2-7.7) suggesting that anti-N antibodies may wane faster in children than adults. To test this, we compared the fold change between the first and second collection periods in in children and adults. We found a greater decrease for the pediatric cohort (geometric mean decrease of 4-fold) demonstrating that these children lost N antibody binding at a faster rate than the adult cohort (geometric mean decrease of 1.8-fold) (**Figure 4.5C**).

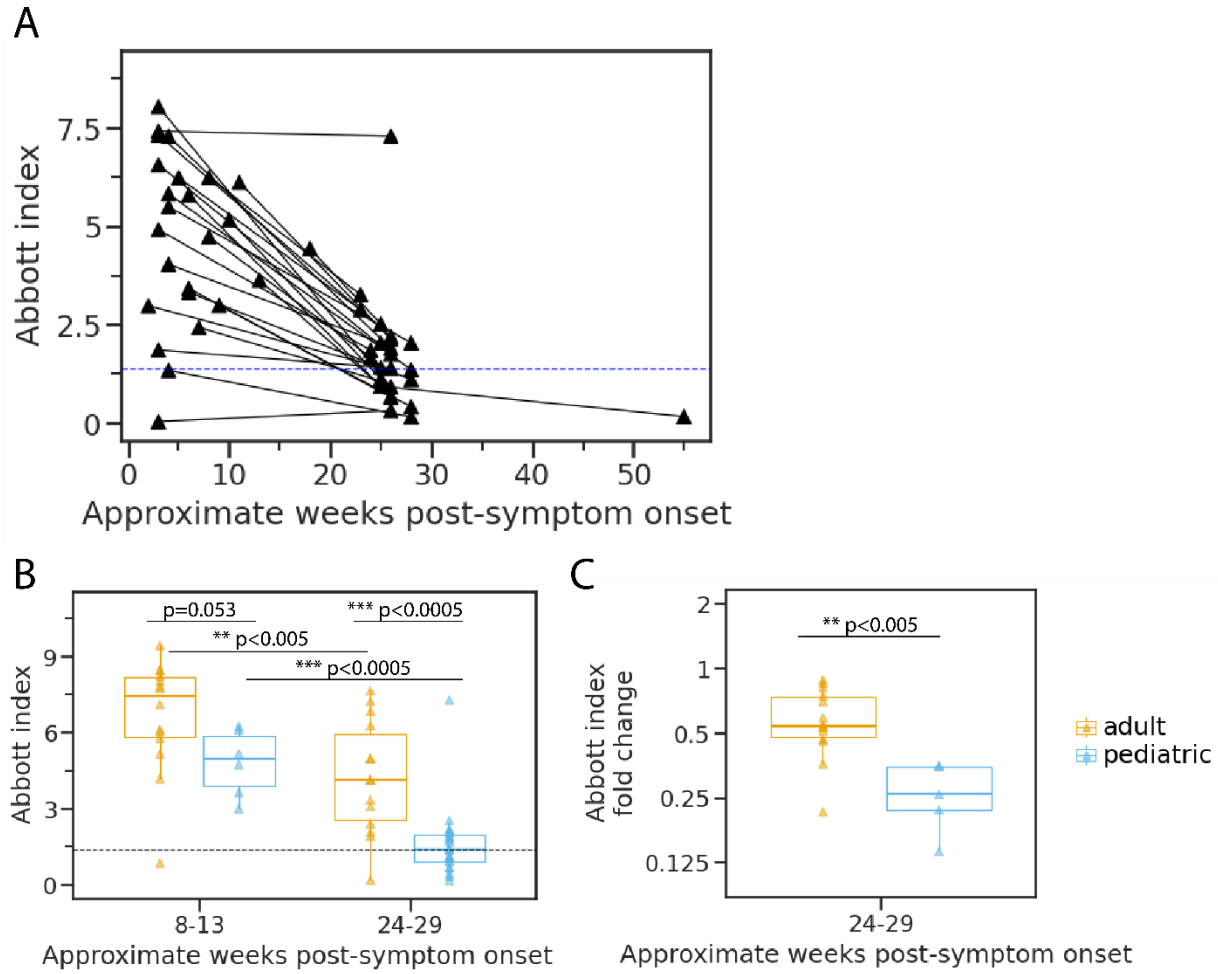

Figure 4.5 Change in nucleocapsid-binding antibody levels longitudinally in children and adults.

A) Aggregated Abbott index values for children without immunocompromising conditions over one-year post-symptom onset with lines connecting specimens from the same individual for the 25 pediatric participants without underlying immunosuppression, receipt of multiple blood transfusions, or MIS-C. **B**) Comparison of Abbott index values between pediatric and adult cohorts restricted to the same time periods of collection for participants without underlying immunosuppression, receipt of multiple blood transfusions, or MIS-C. **C**) Change in Abbott index values at 24 to 29 weeks relative to specimens collected at 8 to 13 weeks for children and adults with specimens collected within both timeframes for participants without underlying immunosuppression, receipt of multiple blood transfusions, or MIS-C. Significance determined by Mann Whitney test. Dotted lines indicate the limit of detection for the Abbott Architect assay (1.40).

4.6 Discussion

In this study, we describe the kinetics of serum antibodies over time in children after infection with SARS-CoV-2. In our convenience samples of unvaccinated children and adults with confirmed or presumed

SARS-CoV-2 infection, we found that pediatric serum neutralizing titers were maintained over 24 weeks while anti-N-binding antibodies waned quickly. Importantly, neutralizing antibody titers were highly variable among individual children as has been previously observed in adults [3,4,105–109,111,189]. Other studies have demonstrated that greater disease severity and higher viral load are associated with higher antibody levels in adults [3,106,190]. The limited number of asymptomatic, hospitalized, and MIS-C cases in our cohort prevented analysis of the role that disease severity may play in this variability. While further investigation is needed, the wide range of neutralization titers and anti-N antibody levels observed in our group of 22 immunocompetent, non-MIS-C presenting children, who were symptomatic but not hospitalized, suggests that disease severity may not entirely explain the observed heterogeneity.

There are several reasons why antibody responses to SARS-CoV-2 infection could be different in children compared to adults, including disease typically being less severe in children [173,191–195] as well as immune senescence and greater burden of comorbidities in older adults [196–202]. Further, primary infections with respiratory pathogens tend to occur early in life leaving uncertainty about how antibody responses to primary infection may differ with age. One example of how age can impact the antibody development was demonstrated following the 2009 H1N1 influenza pandemic where infection elicited a more cross-reactive antibody response in adults compared to children [203]. With regards to SARS-CoV-2, children are also susceptible to life threatening MIS-C following infection, and it remains unclear if and/or how the immune response following infection may impact development of such sequelae.

Interestingly, only a modest and non-significant decrease in neutralizing antibody level was detected for pediatric specimens collected out to six months. A similar persistence in neutralization potency was also observed in the adult cohort, suggesting that there might be long term maintenance of neutralizing antibodies regardless of age following SARS-CoV-2 infection. This finding is in line with several other bodies of work demonstrating the persistence of neutralizing antibodies over many months [113,120,204–206]. We did, however, detect lower levels of neutralization in children's serum compared to adults early after infection. This finding is perhaps surprising given recent work, in the context of vaccination, showing

that older adults, similar to the age group of adults reported here, develop lower neutralizing titers than younger adults[207]. Antibody dynamics across ages may be different between infection and vaccination, and other factors such as specimen collection time or disease severity could also contribute the difference between this study and ours. Interestingly, by 24 weeks, a difference in neutralization titers between children and adults was no longer detectable. This leveling of neutralization titers over time has also been observed for some [3] but not all [109] studies of adults who have disease of different severity: adults with severe disease have higher initial titers at early, but not later, timepoints [3]. Overall, the neutralizing antibody kinetics that we observe for children are similar to adults with mild infections [3,116]. Our findings corroborate a previous study which show lower pediatric neutralization titers early after infection by measuring neutralization titers in children and adults out to 60 days [107], and another study looking at only hospitalized children and adults reported the same [208]. However, one study [120] found that younger children had higher titers than older children and adults. Differences in study population and sampling timepoints could explain these differences.

The most striking difference in SARS-CoV-2 antibody levels between children and adults was seen for anti-N antibodies. Although not statistically significant, children tended to have lower levels than adults early after infection and a significantly lower level after six months. Lower anti-N antibody levels in children than adults have been reported in another study as well [107]. Those authors speculated that, since nucleocapsid protein is disseminated during infection through the lysis of infected cells, children may experience lower levels of N antigen expression due to their reduced duration of illness and potentially lower levels of viral replication [107]. Alternatively, the cumulative lifetime exposure to betacoronavirus infections in adults may repeatedly boost antibodies to the more conserved nucleocapsid proteins that are cross-reactive to SARS-CoV-2, as has been observed in for conserved influenza proteins [209]. It is important to note that several studies have found that the SARS-CoV-2 IgG assay used for this study decreases in sensitivity over time faster than in other assays [105,115,184–188]. In addition, the SARS-

CoV-2 IgG assay only has emergency use authorization for qualitative assessment of antibodies and not quantitative.

The underlying mechanism behind why we observe relatively little waning of neutralizing antibody titers but a strong decrease in N-binding antibody levels remains unknown. There are several potential factors, however, that may help to explain this finding. First, the titers from neutralization assays result from both the concentration of neutralizing antibodies and their affinity while the N-binding antibody measurements we make primarily account for the concentration not affinity. Therefore, while the absolute amount of the S-targeting neutralizing antibodies in serum may actually decline overtime, we might not detect a decrease in the neutralizing titer due to an increase in antibody affinity. This phenomenon would not be detected in our anti-N antibody assay.

Limitations of our study include small sample size and limited number of children with follow-up at 52-weeks. Follow-up is ongoing with children who had not yet reached 52-weeks post-symptom onset at the time of this analysis. Furthermore, blood volume obtained from younger children is limited and therefore the number of assays utilized was also limited. The adult comparative specimens were obtained from the same geographic location and analyzed in the same laboratory, although not necessarily collected from the same families or at the same time. Additionally, the adults in this study were a convenience sample of a broader study, and approximately half were older adults, over 65 years of age, meaning that the data presented here may not be representative of all adults across wider age ranges. Likewise, our pediatric cohort was also a convenience sample and may also not be representative of the broader population. Furthermore, unlike the pediatric cohort, adults were only enrolled following RT-PCR confirmed infection without enrollment based on household RT-PCR positive contacts. Of note, both children and adult cohorts were enrolled prior to the widespread introduction of the SARS-CoV-2 Delta variant.

Overall, our results suggest that although neutralizing antibody responses to SARS-CoV-2 are broadly similar between adults and children, anti-N antibodies are elicited at lower levels in children than adults.

These results contribute to our knowledge of pediatric immune responses to SARS-CoV-2 over time, and the data on the longevity of neutralizing antibodies may prove valuable for comparison investigations of immunity induced by vaccines in children.

4.7 Acknowledgements:

The authors would like to acknowledge Andrea Loes for her supportive role in this study. This work was supported by CDC BAA75D301-20-R-67897 and also by the NIAID/NIH R01AI141707 and R01AI127893 grant to J.D.B. The findings and conclusions in this report are those of the author(s) and do not necessarily represent the official position of the Centers for Disease Control and Prevention (CDC). In addition, J.D.B. is an Investigator of the Howard Hughes Medical Institute. This material is based upon work supported by the National Science Foundation Graduate Research Fellowship Program under Grant No. DGE-1762114 to L.E.G. Any opinions, findings, and conclusions or recommendations expressed in this material are those of the author(s) and do not necessarily reflect the views of the National Science Foundation. The funders had no role in study design, data collection, or the decision to submit the work for publication.

J.D.B consults for Moderna and Flagship Labs 77 on topics related to viral evolution. J.A.E. consults for AstraZeneca, Sanofi Pasteur, Meissa Vaccines, Teva Pharmaceuticals, and receives research support from AstraZeneca, Merck, Novavax, and Pfizer. H.Y.C. receives research support from Gates Ventures, NIH, CDC, DARPA, Sanofi-Pasteur, and Cepheid and serves on the advisory boards for Merck, Pfizer, Ellume, and the Gates Foundation. All other authors report no additional competing interests.

Pediatric study design, patient enrollment and data acquisition, and specimen collection were completed by J.A.E., L.K., J.Y., and S.S. Adults study design, patient enrollment and data acquisition, and specimen collection was completed by H.Y.C. and L.W. Neutralization assays, data analysis, and manuscript writing were performed by L.E.G. All work was performed under the direction of J.D.B. and J.A.E. SARS-CoV-2

IgG assay were performed by J.D. Manuscript editing and review was completed by J.D.B, J.A.E., H.Y.C., L.K., S.N., S.S., K.P., M.B.H, and C.M.M.

Chapter 5.

Conclusions and Future Directions

Antibodies that are elicited following infection represent a crucial component of our adaptive immune response which serve to protect us from infection by many different pathogens whether bacterial, viral, fungal, or parasitic. In this body of work, I have focused on investigating the robust antibody response that is generated upon infection by the respiratory pathogens, influenza A virus and SARS-CoV-2. This antibody response is highly effective at preventing reinfection by antigenically similar strains. As these viruses evolve to evade antibody recognition, however, it is important to explore how we can broaden antibody responses to multiple conserved viral targets to combat antigenic drift. In order to move towards this goal, we need to understand how our antibody response changes over time following infection. To accomplish this, new tools are need for measuring antibody responses to a wide array of viral targets and to measure the impact of such antibodies on viral replication. In the preceding chapters, I described my work to advance these goals, and here I review the main findings discussed in my dissertation along with potential future directions to continue this work.

5.1 Seasonal group 1 and group 2 influenza A virus hemagglutinin stem domains show a similar rate of antigenic evolution.

Based on phylogenetic analysis of HA sequences, we observed that H3N2 viruses have a faster rate of sequence evolution in the HA stem domain than H1N1 viruses. Combined with evidence that stem antibodies more easily select escape mutations in the H3N2 HA than H1N1 [31,48], we hypothesized that over time acquired mutations may be degrading antibody binding to the HA stem domain faster for H3N2 viruses than H1N1 viruses.

By utilizing a chimeric HA design where human serum only recognizes the stem domain, I was able to measure the amount of antibody binding to the stem by ELISA. The chimeric construct is a critical component of our experimental design to examine natural antigenic drift in the stem domain. Because the HA stem domain generates a subdominant antibody response compared to the head domain, using full-length HA for serum ELISAs would overwhelm the signal from antibodies targeting the stem. The intense signal from antibodies binding to the head domain makes small changes in stem antibody binding undetectable. Thus, using a chimeric HA design with an immunologically foreign head domain eliminates this problem.

To test our hypothesis, I measured the binding of a set of serum samples to chimeric HAs with stem domains from H3N2 and H1N1 strains spanning 17 years. This experimental design allowed me to test whether the mutations that accumulate in the stem domain over this timeframe lead to a loss of antibody binding. Unlike hemagglutination inhibition and neutralization assays which have been traditionally used to measure antigenic drift of the HA head domain, this method allows us to detect a loss of antibody binding regardless of function. This is important because stem-binding antibodies do not block agglutination of red blood cells and non-neutralizing HA antibodies have been shown to also provide protection against infection [10,7–9].

For both H3N2 and H1N1 strains, I found very little change in the binding of serum antibodies over time. I further examined whether the stem domain of H3N2 strains lost binding at a faster rate than H1N1 strains since the stem of H3N2 HA accumulates mutations at a faster rate. I found no detectable difference in the rate at which stem antibody binding was lost between the H3N2 and H1N1 HAs tested. This suggests that despite the H3N2 HA stem accumulating more mutations over time, relatively few of these mutations lead to antigenic changes such that a similar loss in binding was observed compared to the less mutated H1N1 HA stem domain.

My findings provide evidence that the HA stem domain undergoes minimal antigenic evolution under selection by stem-binding antibodies elicited by seasonal infection and/or vaccination. These results bode well for the durability of vaccination strategies aimed at directing antibody responses towards the stem

domain. However, it remains to be seen whether stronger selection pressure from more a more directed stem antibody response may lead to more substantial antigenic drift. Future work to address this open question may include directed evolution studies that assess the evolvability of the stem domain by measuring the ease of escape from serum collected during clinical studies of chimeric HA vaccination [16]. Deep mutational scanning studies, like those performed in the Bloom lab, would allow for massively parallel experimental testing of all possible single mutations in the stem to measure ease of escape which has been demonstrated to work previously for human serum primarily targeting the head domain [156]. Further, new libraries under development have the potential to measure the effects of multiple mutations on antibody binding that will allow measurement of how combinations of mutations impact stem antibody binding.

5.2 Anti-NA antibody potency can be measured in a neutralization-based assay.

Recent evidence of anti-NA antibody efficacy against infection has created renewed interest in NA as a potential target of disease mitigating and durable antibodies. A lack of reagents and NA specific assays currently hampers investigation into anti-NA antibody responses [6]. Prior work in the Bloom lab and our interest in influenza antibody responses allowed me to take an interesting approach to address this technological gap. Using an influenza virus engineered to bind to host receptors exclusively through NA interactions, I developed a neutralization-like assay for measuring anti-NA antibody potency.

With four previously characterized monoclonal antibodies targeting different NA epitopes [143], I showed that it is possible to inhibit infection of an NA binding-dependent virus. Neutralization of the NAbind virus was strongest for the antibody HF5 which, of the four antibodies tested, binds closest to site 147 where the binding activity of this NA is thought to occur. This region is near the catalytic active site of NA, and antibodies binding near this epitope, including HF5, have been shown to also inhibit NA catalytic activity [143]. In addition, recent work has shown that antibodies targeting the NA catalytic site tend to have broad reactivity and are protective in animal models [78] highlighting the utility of the NAbind virus neutralization assay for measuring the potency of such important antibodies.

In addition to demonstrating the utility of this assay for measuring anti-NA antibody potency, I used the NAbind virus to perform a classical directed evolution experiment with the HF5 antibody. Through minimal serial passaging of the virus in the presence of HF5, I selected for a mutation that enabled antibody escape. Such experiments with traditional influenza viruses have required either numerous sequential passaging with high antibody concentrations limiting feasibility, passaging in an animal model of infection, or have not been possible at all for many anti-NA antibodies. Thus, the NAbind virus provides a feasible method for mapping anti-NA antibody epitopes and mutations that allow for antibody escape.

While the current neutralization assay that I developed works well for monoclonal antibodies, there are limitations that prohibit the use of this assay for accurately measuring the inhibition of NA antibodies in serum that could be addressed by future studies. The current design of our anti-NA antibody neutralization assay may overestimate the potency of anti-NA antibodies in serum. Two independent studies have demonstrated that antibodies targeting the HA stem domain can also inhibit NA activity likely through steric hinderance [210,211]. While these results suggest an added protective benefit to eliciting an HA stem antibody response, it does mean that antibodies in serum that do not target NA can still inhibit NA activity and may also inhibit infection of the NAbind virus used in our neutralization assay. Thus, while the neutralization assay that I developed may perform well at measuring overall NA inhibiting serum potency, modification is required to strictly determine the inhibition due to NA antibodies alone.

One potential next step for future development of the anti-NA antibody neutralization assay, is to create this virus with a non-binding HA from an avian strain that has not circulated in humans. Using such an avian HA would minimize stem antibody recognition, and therefore ensure that any inhibition measured from serum in our anti-NA antibody neutralization assay comes from anti-NA antibodies alone. Creating a new non-binding HA for an avian influenza strain is not trivial, however. The mutation Y98F which has been reported to abrogate HA binding does not completely remove all binding [158,161]. Thus, additional careful engineering is required to completely ablate HA binding while still retaining the membrane fusion properties of HA [17]. Effort to further developing this assay in this way for use in screening human serum

is justified, however, since an anti-NA serum antibody neutralization assay could provide key information about the potency of antibodies elicited by infection or vaccination.

5.3 Children have variable antibody dynamics following SARS-CoV-2 infection that are distinct from adults.

With the pandemic caused by SARS-CoV-2 still ongoing and the rise of new variants of concern, it is crucial to understand antibody responses following infection in order to gauge the longevity of protective immunity. In chapter 4, I described my efforts in collaboration with Seattle Children's hospital to measure the trajectory of SARS-CoV-2 infection elicited antibody responses in the pediatric population for up to one-year post-infection. We examined neutralizing and nucleocapsid (N)-binding antibodies in children over time and found that the dynamics of each were dissimilar with interesting differences compared to the same antibodies in adults.

In children and adults, neutralizing antibodies were largely maintained over the timeframe of investigation, although exclusion of a few children who showed increasing titers resulted in a waning of titers over time. Overall, I did not detect a difference in neutralizing antibody titers over time for either cohort, but when I compare neutralizing titers between children and adults early after infection, we observed slightly lower levels in children. It is unclear what factors contribute to this early difference in neutralization titers, and by 24-weeks post-symptom onset a difference was no longer detectable between the children and adults.

Our results were determined using a pseudoneutralization assay where the spike expressed on the pseudotyped lentivirus originated from Wuhan-1 with the additional infection enhancing mutation D614G. Thus, while my longitudinal analysis of neutralizing antibody responses suggests that robust neutralizing antibody responses are sustained following infection, it remains to be seen how effective infection elicited antibodies are against new variants of SARS-CoV-2 that have become predominant. This is a particularly pressing question in light of the recent emergence of the highly transmissible omicron SARS-CoV-2 variant which appears to evade antibody immunity through a number of antigenic mutations at sites targeted by neutralizing antibodies [100,212–214].

Further investigation is needed not only to address the issue of the impact of infection elicited neutralizing antibodies on new antigenic variants, but also to query the differences between infection and vaccination elicited neutralizing antibody responses in children over time. Very young children are a particularly important population to study, in this regard, as infection or vaccination against SARS-CoV-2 may be their first exposure to a coronavirus. Original antigenic sin, also known as antigenic imprinting, has been a topic of intense study for influenza virus, dengue virus, and HIV and will likely play an important role in how our antibody response against SARS-CoV-2 evolves. The phenomena of original antigenic sin hinges on how the antibody response to a given virus is biased towards in individual's first exposure. For example, an individual that was first infected with an H3N2 influenza virus early in life will tend to boost antibodies against this strain during subsequent infections even when later infected with another subtype such as H1N1 [25,215]. This immunological memory tends to make antibodies less likely to be as effective against new strains compared to antibodies elicited from a primary infection. This mechanism may pose a significant problem for tackling future SARS-CoV-2 variants as most individuals in the U.S. have been vaccinated against the original Wuhan-1 strain. Supporting this hypothesis, recent work has demonstrated antigenic imprinting is possible for *Sarbecoviruses* in a mouse model [216,217]. Furthermore, as an individual ages, this immune memory has the effect of shifting antibody responses to more conserved non-neutralizing antibody targets [141,142,209]. Some studies have begun to suggest similar trends in adults infected or vaccinated with SARS-CoV-2 [87,218]. Now that SARS-CoV-2 has become the first coronavirus exposure for many children, longitudinal studies of vaccinated or infected children and adults may reveal differences in the immunodominance of viral epitopes in an age dependent manner in part due to original antigenic sin.

In chapter 4, we also measured the magnitude and longevity of anti-nucleocapsid (N) antibodies in children. Our results from this set of experiments were striking: children showed a steep drop in anti-N antibodies by 24-weeks post-symptom onset. In fact, the rate at which anti-N antibodies declined was much greater in children when compared to adults. Further, at both early and late time points following infection, children showed much lower anti-N antibody levels than adults. The cause of this age-related difference in antibody

targeting is unknown, and as discussed in the previous chapters, has been noted in several other studies. It is possible that the answer may lie in original antigenic sin and the back boosting of cross-reactive antibodies against previous betacoronavirus N proteins. Current evidence suggests that anti-N antibodies to hCoV are boosted upon SARS-CoV-2 infection [219], but more work is needed to determine if this boosting affect is associated with age. To investigate a potential role of prior exposures to betacoronaviruses in the boosting of hCoV antibodies following SARS-CoV-2 infection, B cell sequencing to identity cross-reactive anti-N antibody lineages in SARS-CoV-2 convalescent patients from different birth cohorts may prove fruitful.

Another hypothesis is that higher levels of N protein are present during adult infection compared to children which could result in a stronger anti-N antibody response. Chung et al. measured SARS-CoV-2 viral RNA levels as a surrogate for viral load for a large cohort of children and adults [172]. They found that, while there were no differences in RNA levels between asymptomatic children and adults or between symptomatic children and adults, children had slightly lower duration of symptoms [172]. These results suggest that the levels of N protein are not higher during adult infection compared to children but may indicate a faster resolution of infection in children compared to adults. This could result a reduced period of antigen exposure. A future study might test for age-related differences in N antigen persistence, in young and aged hamsters by examining N staining in infected lungs to determine whether there are differences in nucleocapsid antigen abundance or duration and test potential impacts on antibody targeting.

Chapter 6. Appendix A:

Supplementary Material for Chapter 2

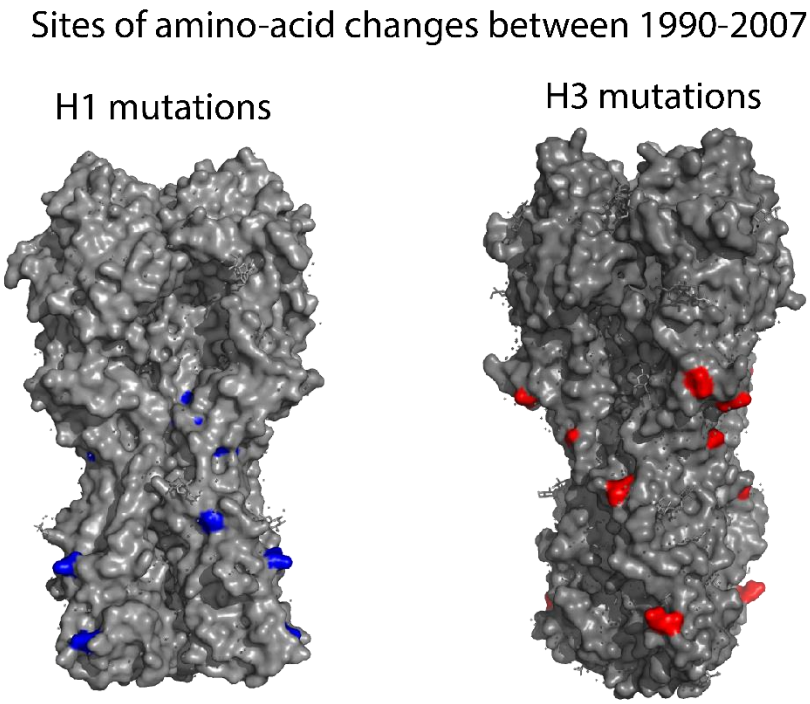

Supplemental Figure 6.1 Structural location of mutations accumulated in the stem domain of the H1N1 and H3N2 HA between 1990 and 2007.

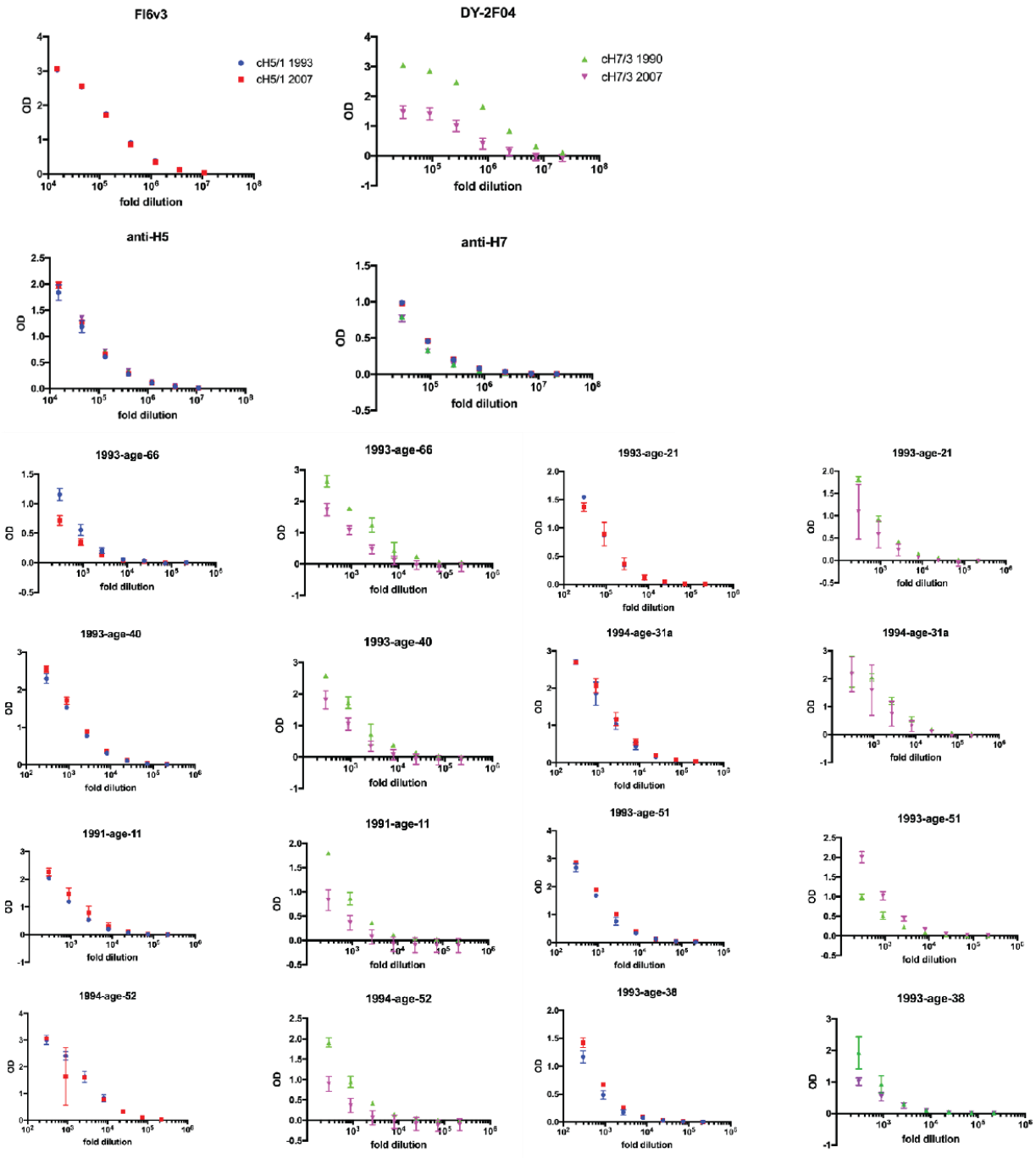
FI6v3
cH5/1 1993
cH5/1 2007
OD
fold dilution
DY-2F04
cH7/3 1990
cH7/3 2007
OD
fold dilution
anti-H5
OD
fold dilution
anti-H7
OD
fold dilution
1993-age-66
OD
fold dilution
1993-age-66
OD
fold dilution
1993-age-21
OD
fold dilution
1993-age-21
OD
fold dilution
1993-age-40
OD
fold dilution
1993-age-40
OD
fold dilution
1994-age-31a
OD
fold dilution
1994-age-31a
OD
fold dilution
1991-age-11
OD
fold dilution
1991-age-11
OD
fold dilution
1993-age-51
OD
fold dilution
1993-age-51
OD
fold dilution
1994-age-52
OD
fold dilution
1994-age-52
OD
fold dilution
1993-age-38
OD
fold dilution
1993-age-38
OD
fold dilution

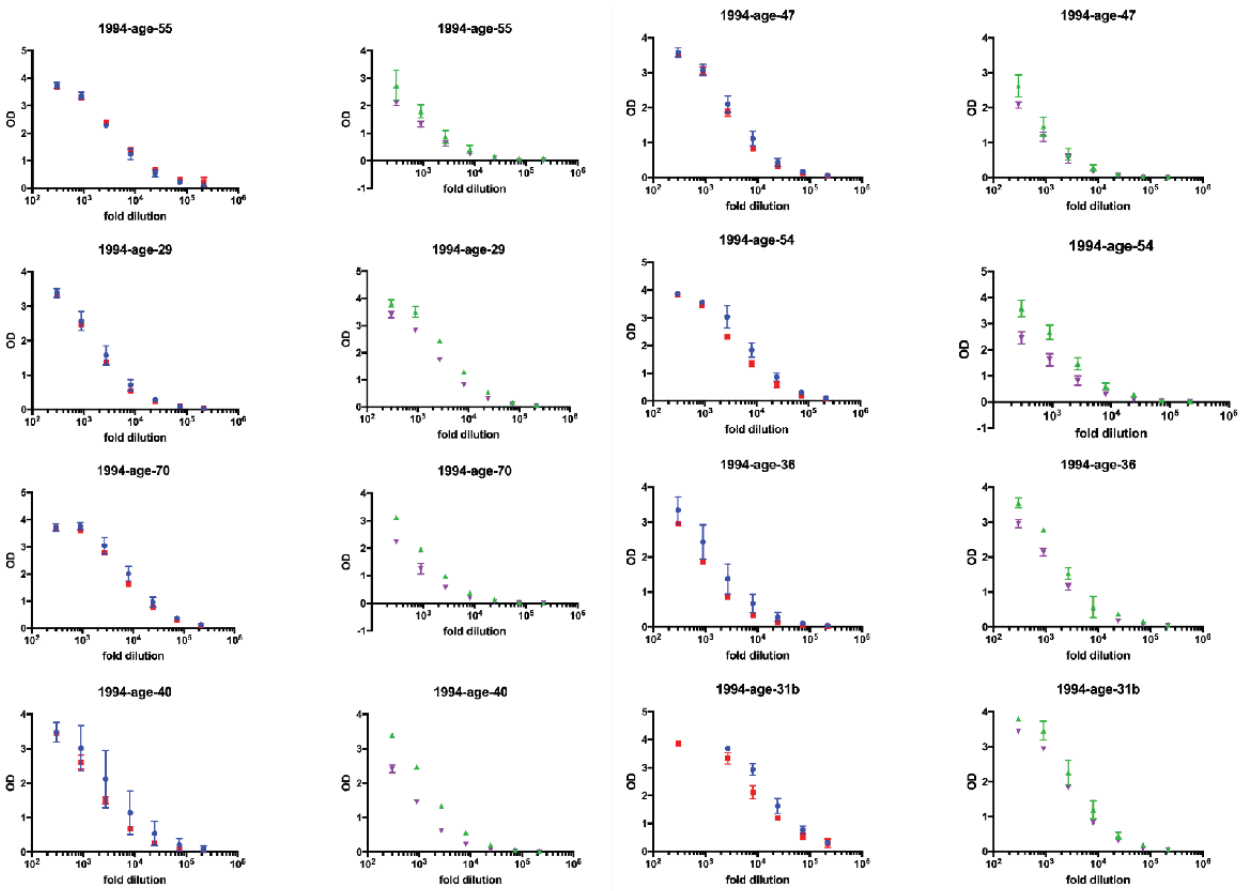

Supplemental Figure 6.2 ELISA curves generated for each human serum sample collected between 1993 to 1994 against cH5/1 and cH7/3 proteins. Representative stem and head domain antibody control ELISA curves shown in top two rows.

Chapter 7. Appendix B:

Supplementary Material for Chapter 4

Supplemental Table 7.1 Evidence of SARS-CoV-2 infection among patients without a confirmed SARS-CoV-2 RT-PCR.

Patient ID	Evidence of SARS-CoV-2 infection	Epi-week of household RT-PCR test	Epi-week of participant symptom onset
C15	Experienced syptomatic infection, developed MIS-C, neutralization and nucleocapsid antibodies confirmed through serological testing; this child is listed un the MIS-C subset in inclusion flowchart.	not applicable	2020 week 11 - acute 2020 week 18 - MIS-C
C12	Known PCR-positive household infection (family member with long COVID who was not tested until well after initial household outbreak), entire family experienced symptoms consistent with SARS-CoV-2 infection, neutralization and nucleocapsid antibodies confirmed through serological testing	2020 week 20	2020 week 11
C20	Known PCR-positive household infection, experienced symptoms consistent with SARS-CoV-2 infection, neutralization and nucleocapsid antibodies confirmed through serological testing	unknown	2020 week 12
C23	Known PCR-positive household infection, experienced symptoms consistent with SARS-CoV-2 infection, neutralization and nucleocapsid antibodies confirmed through serological testing	two family members positive both in 2020 week 49	2020 week 49
C14	Known PCR-positive contacts, experienced symptoms consistent with SARS-CoV-2 infection, neutralization and nucleocapsid antibodies confirmed through serological testing	2020 week 48	2020 week 48

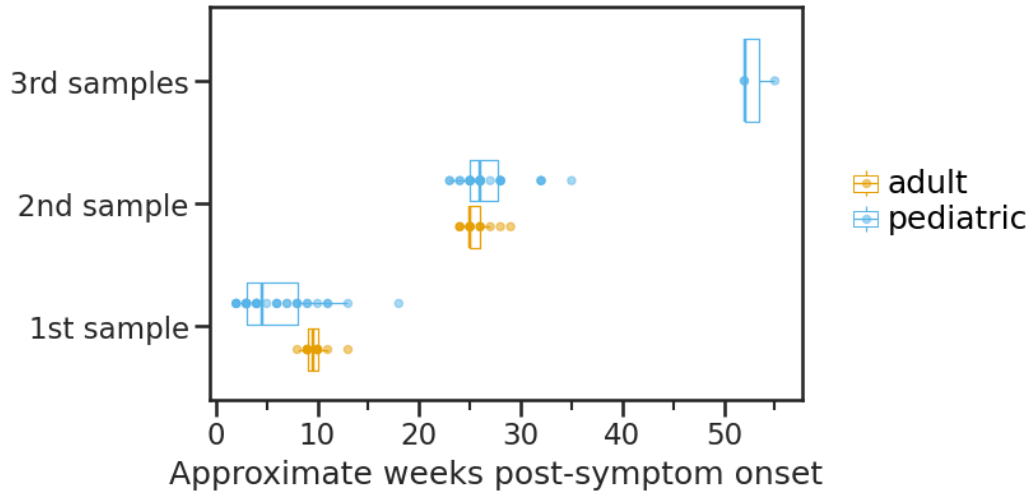

Supplementary Figure 7.1 Distribution of specimen collections in children and adults.

Supplemental Table 7.2 Naming of adults across publications.

Naming in Crawford et al. 2020 (3)	**Naming in the present study**
PID 13	A3
PID 3C	A1
PID 4C	A2
PID 6C	A6
PID 7C	A7
PID 11C	A4
PID 12C	A10
PID 22C	A9
PID 23C	A8
PID 24C	A13
PID 103C	A12
PID 113C	A14
PID 117C	A11
PID 200C	A5

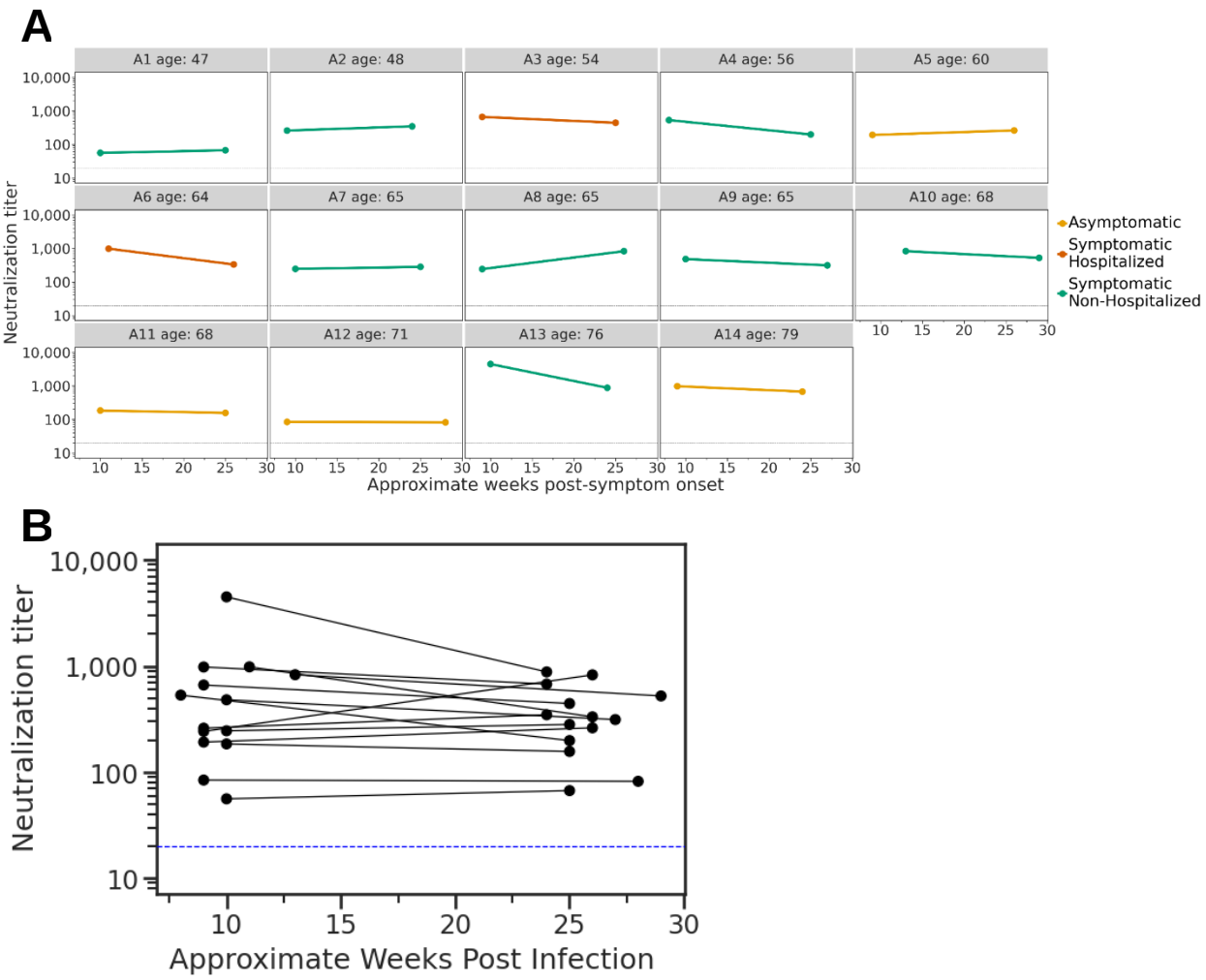

Supplemental Figure 7.2 Neutralization titers in adults over time.

A) Neutralizing antibody titers in 14 adults with confirmed SARS-CoV-2 infection followed prospectively over time shown as weeks post-symptom onset, x axis. **B**) Aggregated neutralization titers for all adults. Dotted horizontal lines indicate the limit of detection (20).

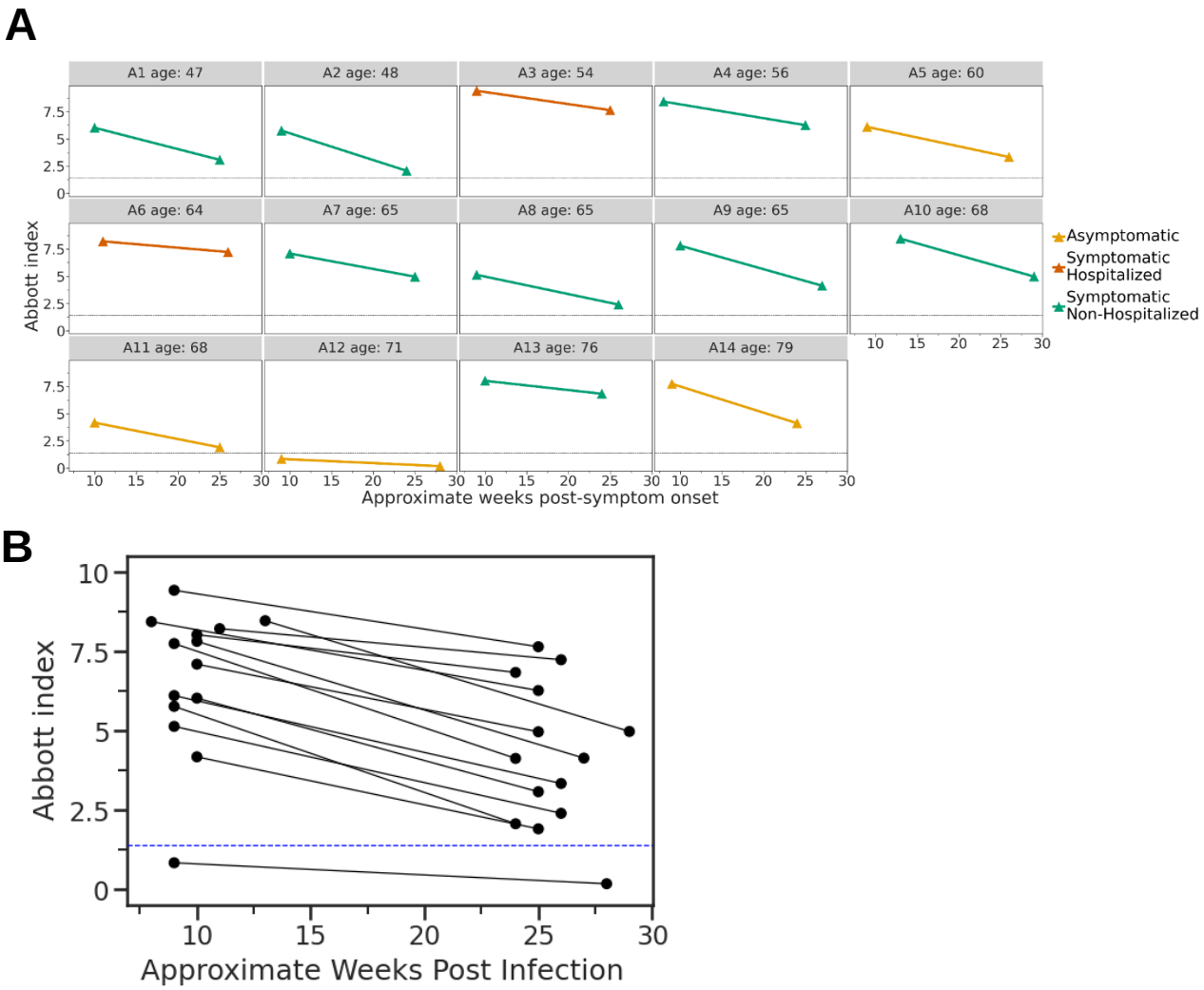

Supplemental Figure 7.3: Nucleocapsid-binding antibody levels in adults over time.

A) The Abbott Architect assay was used to determine SARS-CoV-2 nucleocapsid-binding antibody in 14 adults followed prospectively over time shown as weeks post-symptom onset, x axis. **B**) Aggregated Abbott index values for all adults. Dotted horizontal lines indicate the limit of detection for the Abbott Architect assay (1.40).

Chapter 8. Bibliography

1. Memoli, M.J.; Shaw, P.A.; Han, A.; Czajkowski, L.; Reed, S.; Athota, R.; Bristol, T.; Fargis, S.; Risos, K.; Powers, J.H.; et al. Evaluation of Antihemagglutinin and Antineuraminidase Antibodies as Correlates of Protection in an Influenza A/H1N1 Virus Healthy Human Challenge Model. *mBio* **2016**, *7*, doi:10.1128/mBio.00417-16.

2. Padilla-Quirarte, H.O.; Lopez-Guerrero, D.V.; Gutierrez-Xicotencatl, L.; Esquivel-Guadarrama, F. Protective Antibodies Against Influenza Proteins. *Front Immunol* **2019**, *10*, doi:10.3389/fimmu.2019.01677.

3. Crawford, K.H.D.; Dingens, A.S.; Eguia, R.; Wolf, C.R.; Wilcox, N.; Logue, J.K.; Shuey, K.; Casto, A.M.; Fiala, B.; Wrenn, S.; et al. Dynamics of Neutralizing Antibody Titers in the Months After Severe Acute Respiratory Syndrome Coronavirus 2 Infection. *The Journal of Infectious Diseases* **2020**, doi:10.1093/infdis/jiaa618.

4. Wu, J.; Liang, B.; Chen, C.; Wang, H.; Fang, Y.; Shen, S.; Yang, X.; Wang, B.; Chen, L.; Chen, Q.; et al. SARS-CoV-2 Infection Induces Sustained Humoral Immune Responses in Convalescent Patients Following Symptomatic COVID-19. *Nature Communications* **2021**, *12*, 1813, doi:10.1038/s41467-021-22034-1.

5. Gilbert, P.B.; Montefiori, D.C.; McDermott, A.; Fong, Y.; Benkeser, D.; Deng, W.; Zhou, H.; Houchens, C.R.; Martins, K.; Jayashankar, L.; et al. *Immune Correlates Analysis of the MRNA-1273 COVID-19 Vaccine Efficacy Trial*; 2021; p. 2021.08.09.21261290;

6. Krammer, F.; Fouchier, R.A.M.; Eichelberger, M.C.; Webby, R.J.; Shaw-Saliba, K.; Wan, H.; Wilson, P.C.; Compans, R.W.; Skountzou, I.; Monto, A.S. NAction! How Can Neuraminidase-Based Immunity Contribute to Better Influenza Virus Vaccines? *mBio* **2018**, *9*, doi:10.1128/mBio.02332-17.

7. Dunand, C.J.H.; Leon, P.E.; Huang, M.; Palese, P.; Krammer, F.; Wilson, P.C.; Dunand, C.J.H.; Leon, P.E.; Huang, M.; Choi, A.; et al. Both Neutralizing and Non-Neutralizing Human H7N9 Confer Protection Article Both Neutralizing and Non-Neutralizing Human H7N9 Influenza Vaccine-Induced Monoclonal Antibodies Confer Protection. *Cell Host and Microbe* **2016**, *19*, 800–813, doi:10.1016/j.chom.2016.05.014.

8. Kim, J.H.; Reber, A.J.; Kumar, A.; Ramos, P.; Sica, G.; Music, N.; Guo, Z.; Mishina, M.; Stevens, J.; York, I.A.; et al. Non-Neutralizing Antibodies Induced by Seasonal Influenza Vaccine Prevent, Not Exacerbate A(H1N1)Pdm09 Disease. *Scientific Reports* **2016**, *6*, 37341, doi:10.1038/srep37341.

9. Ko, Y.-A.; Yu, Y.-H.; Wu, Y.-F.; Tseng, Y.-C.; Chen, C.-L.; Goh, K.-S.; Liao, H.-Y.; Chen, T.-H.; Cheng, T.-J.R.; Yang, A.-S.; et al. A Non-Neutralizing Antibody Broadly Protects against Influenza Virus Infection by Engaging Effector Cells. *PLoS Pathog* **2021**, *17*, e1009724, doi:10.1371/journal.ppat.1009724.

10. McLain, L.; Dimmock, N.J. Protection of Mice from Lethal Influenza by Adoptive Transfer of Non-Neutralizing Haemagglutination-Inhibiting IgG Obtained from the Lungs of Infected Animals Treated with Defective Interfering Virus. *Journal of General Virology* **1989**, *70*, 2615–2624, doi:10.1099/0022-1317-70-10-2615.

11. Maier, H.E.; Nachbagauer, R.; Kuan, G.; Ng, S.; Lopez, R.; Sanchez, N.; Stadlbauer, D.; Gresh, L.; Schiller, A.; Rajabhathor, A.; et al. Pre-Existing Antineuraminidase Antibodies Are Associated With Shortened Duration of Influenza A(H1N1)Pdm Virus Shedding and Illness in Naturally Infected Adults. *Clinical Infectious Diseases* **2019**, doi:10.1093/cid/ciz639.

12. Hai, R.; Krammer, F.; Tan, G.S.; Pica, N.; Eggink, D.; Maamary, J.; Margine, I.; Albrecht, R.A. Influenza Viruses Expressing Chimeric Hemagglutinins : Globular Head and Stalk Domains Derived from Different Subtypes. **2012**, *88*, 5774–5781, doi:10.1128/JVI.00137-12.

13. Krammer, F.; Pica, N.; Hai, R.; Margine, I.; Palese, P. Chimeric Hemagglutinin Influenza Virus Vaccine Constructs Elicit Broadly Protective Stalk-Specific Antibodies. *J Virol* **2013**, *87*, 6542–6550, doi:10.1128/JVI.00641-13.

14. Chen, C.-J.; Ermler, M.E.; Tan, G.S.; Krammer, F.; Palese, P.; Hai, R. Influenza A Viruses Expressing Intra- or Intergroup Chimeric Hemagglutinins. *Journal of Virology* **2016**, *90*, 3789–3793, doi:10.1128/JVI.03060-15.

15. Isakova-Sivak, I.; Korenkov, D.; Smolonogina, T.; Kotomina, T.; Donina, S.; Matyushenko, V.; Mezhenskaya, D.; Krammer, F.; Rudenko, L. Broadly Protective Anti-Hemagglutinin Stalk Antibodies Induced by Live Attenuated Influenza Vaccine Expressing Chimeric Hemagglutinin. *Virology* **2018**, *518*, 313–323, doi:10.1016/j.virol.2018.03.013.

16. Bernstein, D.I.; Guptill, J.; Naficy, A.; Nachbagauer, R.; Berlanda-Scorza, F.; Feser, J.; Wilson, P.C.; Solórzano, A.; Van der Wielen, M.; Walter, E.B.; et al. Immunogenicity of Chimeric Haemagglutinin-Based, Universal Influenza Virus Vaccine Candidates: Interim Results of a Randomised, Placebo-Controlled, Phase 1 Clinical Trial. *The Lancet Infectious Diseases* **2020**, *20*, 80–91, doi:10.1016/S1473-3099(19)30393-7.

17. Hooper, K.A.; Bloom, J.D. A Mutant Influenza Virus That Uses an N1 Neuraminidase as the Receptor-Binding Protein. *Journal of Virology* **2013**, *87*, 12531–12540, doi:10.1128/JVI.01889-13.

18. Hooper, K.A.; Crowe, J.E.; Bloom, J.D. Influenza Viruses with Receptor-Binding N1 Neuraminidases Occur Sporadically in Several Lineages and Show No Attenuation in Cell Culture or Mice. *Journal of Virology* **2015**, *89*, 3737–3745, doi:10.1128/JVI.00012-15.

19. Crawford, K.H.D.; Eguia, R.; Dingens, A.S.; Loes, A.N.; Malone, K.D.; Wolf, C.R.; Chu, H.Y.; Tortorici, M.A.; Veesler, D.; Murphy, M.; et al. Protocol and Reagents for Pseudotyping Lentiviral Particles with SARS-CoV-2 Spike Protein for Neutralization Assays. *Viruses* **2020**, *12*, E513, doi:10.3390/v12050513.

20. Greaney, A.J.; Loes, A.N.; Gentles, L.E.; Crawford, K.H.D.; Starr, T.N.; Malone, K.D.; Chu, H.Y.; Bloom, J.D. Antibodies Elicited by MRNA-1273 Vaccination Bind More Broadly to the Receptor Binding Domain than Do Those from SARS-CoV-2 Infection. *Sci Transl Med* **2021**, *13*, eabi9915, doi:10.1126/scitranslmed.abi9915.

21. Influenza (Seasonal) Available online: https://www.who.int/news-room/fact-sheets/detail/influenza-(seasonal) (accessed on 7 December 2021).

22. Angeletti, D.; Gibbs, J.S.; Angel, M.; Kosik, I.; Hickman, H.D.; Frank, G.M.; Das, S.R.; Wheatley, A.K.; Prabhakaran, M.; Leggat, D.J.; et al. Defining B Cell Immunodominance to Viruses. *Nature Immunology* **2017**, *18*, 456–463, doi:10.1038/ni.3680.

23. Altman, M.O.; Angeletti, D.; Yewdell, J.W. Antibody Immunodominance: The Key to Understanding Influenza Virus Antigenic Drift. *Viral Immunol* **2018**, *31*, 142–149, doi:10.1089/vim.2017.0129.

24. Angeletti, D.; Yewdell, J.W. Understanding and Manipulating Viral Immunity: Antibody Immunodominance Enters Center Stage. *Trends in Immunology* **2018**, *39*, 549–561, doi:10.1016/j.it.2018.04.008.

25. Knight, M.; Changrob, S.; Li, L.; Wilson, P.C. Imprinting, Immunodominance, and Other Impediments to Generating Broad Influenza Immunity. *Immunological Reviews* **2020**, *296*, 191–204, doi:10.1111/imr.12900.

26. Doud, M.B.; Bloom, J.D. Accurate Measurement of the Effects of All Amino-Acid Mutations on Influenza Hemagglutinin. *Viruses* **2016**, *8*, doi:10.3390/v8060155.

27. Doud, M.B.; Hensley, S.E.; Bloom, J.D. Complete Mapping of Viral Escape from Neutralizing Antibodies. *PLoS Pathogens* **2017**, *13*, 1–20, doi:10.1371/journal.ppat.1006271.

28. Gerhard, W.; Yewdell, J.; Frankel, M.E.; Webster, R. Antigenic Structure of Influenza Virus Haemagglutinin Defined by Hybridoma Antibodies. *Nature* **1981**, *290*, 713–717, doi:10.1038/290713a0.

29. Das, S.R.; Hensley, S.E.; Ince, W.L.; Brooke, C.B.; Subba, A.; Delboy, M.G.; Russ, G.; Gibbs, J.S.; Bennink, J.R.; Yewdell, J.W. Defining Influenza a Virus Hemagglutinin Antigenic Drift by Sequential Monoclonal Antibody Selection. *Cell Host and Microbe* **2013**, doi:10.1016/j.chom.2013.02.008.

30. Matsuzaki, Y.; Sugawara, K.; Nakauchi, M.; Takahashi, Y.; Onodera, T.; Tsunetsugu-Yokota, Y.; Matsumura, T.; Ato, M.; Kobayashi, K.; Shimotai, Y.; et al. Epitope Mapping of the Hemagglutinin Molecule of A/(H1N1)Pdm09 Influenza Virus by Using Monoclonal Antibody Escape Mutants. *J Virol* **2014**, *88*, 12364–12373, doi:10.1128/JVI.01381-14.

31. Doud, M.B.; Lee, J.M.; Bloom, J.D. How Single Mutations Affect Viral Escape from Broad and Narrow Antibodies to H1 Influenza Hemagglutinin. *Nature Communications* **2018**, *9*, 1–12, doi:10.1038/s41467-018-03665-3.

32. Lazarowitz, S.G.; Compans, R.W.; Choppin, P.W. Proteolytic Cleavage of the Hemagglutinin Polypeptide of Influenza Virus. Function of the Uncleaved Polypeptide HA. *Virology* **1973**, *52*, 199–212, doi:10.1016/0042-6822(73)90409-1.

33. Fukuyama, H.; Shinnakasu, R.; Kurosaki, T. Influenza Vaccination Strategies Targeting the Hemagglutinin Stem Region. *Immunol Rev* **2020**, doi:10.1111/imr.12887.

34. Corti, D.; Voss, J.; Gamblin, S.J.; Codoni, G.; Macagno, A.; Jarrossay, D.; Vachieri, S.G.; Pinna, D.; Minola, A.; Vanzetta, F.; et al. A Neutralizing Antibody Selected from Plasma Cells That Binds to Group 1 and Group 2 Influenza A Hemagglutinins. *Science* **2011**, *333*, 850–856, doi:10.1126/science.1205669.

35. Dreyfus, C.; Laursen, N.S.; Kwaks, T.; Zuijdgeest, D.; Khayat, R.; Ekiert, D.C.; Lee, J.H.; Metlagel, Z.; Bujny, M.V.; Jongeneelen, M.; et al. Highly Conserved Protective Epitopes on Influenza B Viruses. *Science* **2012**, *337*, 1343–1348, doi:10.1126/science.1222908.

36. Dreyfus, C.; Ekiert, D.C.; Wilson, I.A. Structure of a Classical Broadly Neutralizing Stem Antibody in Complex with a Pandemic H2 Influenza Virus Hemagglutinin. *J Virol* **2013**, *87*, 7149–7154, doi:10.1128/JVI.02975-12.

37. Ekiert, D.C.; Bhabha, G.; Elsliger, M.-A.; Friesen, R.H.E.; Jongeneelen, M.; Throsby, M.; Goudsmit, J.; Wilson, I.A. Antibody Recognition of a Highly Conserved Influenza Virus Epitope. *Science* **2009**, *324*, 246–251, doi:10.1126/science.1171491.

38. Kashyap, A.K.; Steel, J.; Rubrum, A.; Estelles, A.; Briante, R.; Ilyushina, N.A.; Xu, L.; Swale, R.E.; Faynboym, A.M.; Foreman, P.K.; et al. Protection from the 2009 H1N1 Pandemic Influenza by an Antibody from Combinatorial Survivor-Based Libraries. *PLoS Pathog* **2010**, *6*, e1000990, doi:10.1371/journal.ppat.1000990.

39. Sui, J.; Hwang, W.C.; Perez, S.; Wei, G.; Aird, D.; Chen, L.; Santelli, E.; Stec, B.; Cadwell, G.; Ali, M.; et al. Structural and Functional Bases for Broad-Spectrum Neutralization of Avian and Human Influenza A Viruses. *Nat Struct Mol Biol* **2009**, *16*, 265–273, doi:10.1038/nsmb.1566.

40. Wang, T.T.; Tan, G.S.; Hai, R.; Pica, N.; Petersen, E.; Moran, T.M.; Palese, P. Broadly Protective Monoclonal Antibodies against H3 Influenza Viruses Following Sequential Immunization with Different Hemagglutinins. *PLoS Pathog* **2010**, *6*, e1000796, doi:10.1371/journal.ppat.1000796.

41. Okuno, Y.; Isegawa, Y.; Sasao, F.; Ueda, S. A Common Neutralizing Epitope Conserved between the Hemagglutinins of Influenza A Virus H1 and H2 Strains. *J Virol* **1993**, *67*, 2552–2558, doi:10.1128/JVI.67.5.2552-2558.1993.

42. Throsby, M.; Brink, E. van den; Jongeneelen, M.; Poon, L.L.M.; Alard, P.; Cornelissen, L.; Bakker, A.; Cox, F.; Deventer, E. van; Guan, Y.; et al. Heterosubtypic Neutralizing Monoclonal Antibodies Cross-Protective against H5N1 and H1N1 Recovered from Human IgM+ Memory B Cells. *PLOS ONE* **2008**, *3*, e3942, doi:10.1371/journal.pone.0003942.

43. Laursen, N.S.; Wilson, I.A. Broadly Neutralizing Antibodies against Influenza Viruses. *Antiviral Res* **2013**, *98*, 476–483, doi:10.1016/j.antiviral.2013.03.021.

44. Guthmiller, J.J.; Han, J.; Utset, H.A.; Li, L.; Lan, L.Y.-L.; Henry, C.; Stamper, C.T.; Stovicek, O.; Gentles, L.; Dugan, H.L.; et al. *A Public Broadly Neutralizing Antibody Class Targets a Membrane-Proximal Anchor Epitope of Influenza Virus Hemagglutinin*; 2021; p. 2021.02.25.432905;

45. Kirkpatrick, E.; Qiu, X.; Wilson, P.C.; Bahl, J.; Krammer, F. The Influenza Virus Hemagglutinin Head Evolves Faster than the Stalk Domain. *Sci Rep* **2018**, *8*, doi:10.1038/s41598-018-28706-1.

46. Anderson, C.S.; Ortega, S.; Chaves, F.A.; Clark, A.M.; Yang, H.; Topham, D.J.; DeDiego, M.L. Natural and Directed Antigenic Drift of the H1 Influenza Virus Hemagglutinin Stalk Domain. *Scientific Reports* **2017**, *7*, doi:10.1038/s41598-017-14931-7.

47. Roubidoux, E.K.; Carreño, J.M.; McMahon, M.; Jiang, K.; Bakel, H. van; Wilson, P.; Krammer, F. Mutations in the Hemagglutinin Stalk Domain Do Not Permit Escape from a Protective, Stalk-Based Vaccine-Induced Immune Response in the Mouse Model. *mBio* **2021**, *12*, doi:10.1128/mBio.03617-20.

48. Wu, N.C.; Thompson, A.J.; Lee, J.M.; Su, W.; Arlian, B.M.; Xie, J.; Lerner, R.A.; Yen, H.-L.; Bloom, J.D.; Wilson, I.A. Different Genetic Barriers for Resistance to HA Stem Antibodies in Influenza H3 and H1 Viruses. *Science* **2020**, *368*, 1335–1340, doi:10.1126/science.aaz5143.

49. Park, J.-K.; Xiao, Y.; Ramuta, M.D.; Rosas, L.A.; Fong, S.; Matthews, A.M.; Freeman, A.D.; Gouzoulis, M.A.; Batchenkova, N.A.; Yang, X.; et al. Pre-Existing Immunity to Influenza Virus Hemagglutinin Stalk Might Drive Selection for Antibody-Escape Mutant Viruses in a Human Challenge Model. *Nat. Med.* **2020**, doi:10.1038/s41591-020-0937-x.

50. Bedford, T.; Suchard, M.A.; Lemey, P.; Dudas, G.; Gregory, V.; Hay, A.J.; McCauley, J.W.; Russell, C.A.; Smith, D.J.; Rambaut, A. Integrating Influenza Antigenic Dynamics with Molecular Evolution. *eLife* **2014**, *3*, e01914, doi:10.7554/eLife.01914.

51. Lee, J.M.; Huddleston, J.; Doud, M.B.; Hooper, K.A.; Wu, N.C.; Bedford, T.; Bloom, J.D. Deep Mutational Scanning of Hemagglutinin Helps Predict Evolutionary Fates of Human H3N2 Influenza Variants. *Proceedings of the National Academy of Sciences* **2018**, *115*, E8276–E8285, doi:10.1073/pnas.1806133115.

52. Nachbagauer, R.; Miller, M.S.; Hai, R.; Ryder, A.B.; Rose, J.K.; Palese, P.; García-Sastre, A.; Krammer, F.; Albrecht, R.A. Hemagglutinin Stalk Immunity Reduces Influenza Virus Replication and Transmission in Ferrets. *Journal of Virology* **2016**, *90*, 3268–3273, doi:10.1128/JVI.02481-15.

53. Nachbagauer, R.; Kinzler, D.; Choi, A.; Hirsh, A.; Beaulieu, E.; Lecrenier, N.; Innis, B.L.; Palese, P.; Mallett, C.P.; Krammer, F. A Chimeric Haemagglutinin-Based Influenza Split Virion Vaccine Adjuvanted with AS03 Induces Protective Stalk-Reactive Antibodies in Mice. *npj Vaccines* **2016**, *1*, 16015, doi:10.1038/npjvaccines.2016.15.

54. Liu, W.-C.; Nachbagauer, R.; Stadlbauer, D.; Strohmeier, S.; Solórzano, A.; Berlanda-Scorza, F.; Innis, B.L.; García-Sastre, A.; Palese, P.; Krammer, F.; et al. Chimeric Hemagglutinin-Based Live-Attenuated Vaccines Confer Durable Protective Immunity against Influenza A Viruses in a Preclinical Ferret Model. *Vaccines* **2021**, *9*, 40, doi:10.3390/vaccines9010040.

55. Wrammert, J.; Koutsonanos, D.; Li, G.-M.; Edupuganti, S.; Sui, J.; Morrissey, M.; McCausland, M.; Skountzou, I.; Hornig, M.; Ian Lipkin, W.; et al. Broadly Cross-Reactive Antibodies Dominate the Human B Cell Response against 2009 Pandemic H1N1 Influenza Virus Infection Cor Rection. *The Journal of Experimental Medicine* **2011**, *208*, 181–193.

56. Kilbourne, E.D.; Laver, W.G.; Schulman, J.L.; Webster, R.G. Antiviral Activity of Antiserum Specific for an Influenza Virus Neuraminidase. *J. VIROL.* **1968**, *2*, 281–288.

57. Murphy, B.R.; Kasel, J.A.; Chanock, R.M. Association of Serum Anti-Neuraminidase Antibody with Resistance to Influenza in Man. *N. Engl. J. Med.* **1972**, *286*, 1329–1332, doi:10.1056/NEJM197206222862502.

58. Monto, A.S.; Petrie, J.G.; Cross, R.T.; Johnson, E.; Liu, M.; Zhong, W.; Levine, M.; Katz, J.M.; Ohmit, S.E. Antibody to Influenza Virus Neuraminidase: An Independent Correlate of Protection. *Journal of Infectious Diseases* **2015**, *212*, 1191–1199, doi:10.1093/infdis/jiv195.

59. Tan, J.; O'Dell, G.; Hernandez, M.M.; Sordillo, E.M.; Kahn, Z.; Kriti, D.; van Bakel, H.; Ellebedy, A.H.; Wilson, P.C.; Simon, V.; et al. Human Anti-Neuraminidase Antibodies Reduce Airborne Transmission of Clinical Influenza Virus Isolates in the Guinea Pig Model. *Journal of Virology* **2021**, JVI.01421-21, doi:10.1128/JVI.01421-21.

60. Cohen, M.; Zhang, X.-Q.; Senaati, H.P.; Chen, H.-W.; Varki, N.M.; Schooley, R.T.; Gagneux, P. Influenza A Penetrates Host Mucus by Cleaving Sialic Acids with Neuraminidase. *Virology Journal* **2013**, *10*, 321, doi:10.1186/1743-422X-10-321.

61. Matrosovich, M.N.; Matrosovich, T.Y.; Gray, T.; Roberts, N.A.; Klenk, H.-D. Neuraminidase Is Important for the Initiation of Influenza Virus Infection in Human Airway Epithelium. *Journal of Virology* **2004**, *78*, 12665–12667, doi:10.1128/JVI.78.22.12665-12667.2004.

62. Stevens, J.; Blixt, O.; Glaser, L.; Taubenberger, J.K.; Palese, P.; Paulson, J.C.; Wilson, I.A. Glycan Microarray Analysis of the Hemagglutinins from Modern and Pandemic Influenza Viruses Reveals Different Receptor Specificities. *Journal of Molecular Biology* **2006**, *355*, 1143–1155, doi:10.1016/j.jmb.2005.11.002.

63. Baum, L.G.; Paulson, J.C. The N2 Neuraminidase of Human Influenza Virus Has Acquired a Substrate Specificity Complementary to the Hemagglutinin Receptor Specificity. *Virology* **1991**, *180*, 10–15, doi:10.1016/0042-6822(91)90003-T.

64. Kobasa, D.; Kodihalli, S.; Luo, M.; Castrucci, M.R.; Donatelli, I.; Suzuki, Y.; Suzuki, T.; Kawaoka, Y. Amino Acid Residues Contributing to the Substrate Specificity of the Influenza A Virus Neuraminidase. *Journal of Virology* **1999**, doi:10.1128/JVI.73.8.6743-6751.1999.

65. Guo, H.; Rabouw, H.; Slomp, A.; Dai, M.; van der Vegt, F.; van Lent, J.W.M.; McBride, R.; Paulson, J.C.; de Groot, R.J.; van Kuppeveld, F.J.M.; et al. Kinetic Analysis of the Influenza A Virus HA/NA Balance Reveals Contribution of NA to Virus-Receptor Binding and NA-Dependent Rolling on Receptor-Containing Surfaces. *PLoS Pathog.* **2018**, *14*, e1007233, doi:10.1371/journal.ppat.1007233.

66. Vahey, M.D.; Fletcher, D.A. Influenza A Virus Surface Proteins Are Organized to Help Penetrate Host Mucus. *eLife* **2019**, *8*, e43764, doi:10.7554/eLife.43764.

67. Liu, C.; Eichelberger, M.C.; Compans, R.W.; Air, G.M. Influenza Type A Virus Neuraminidase Does Not Play a Role in Viral Entry, Replication, Assembly, or Budding. *Journal of virology* **1995**, *69*, 1099–1106, doi:10.1128/JVI.69.2.1099-1106.1995.

68. Welliver, R.; Monto, A.S.; Carewicz, O.; Schatteman, E.; Hassman, M.; Hedrick, J.; Jackson, H.C.; Huson, L.; Ward, P.; Oxford, J.S.; et al. Effectiveness of Oseltamivir in Preventing Influenza in Household ContactsA Randomized Controlled Trial. *JAMA* **2001**, *285*, 748–754, doi:10.1001/jama.285.6.748.

69. McKimm-Breschkin, J.; Trivedi, T.; Hampson, A.; Hay, A.; Klimov, A.; Tashiro, M.; Hayden, F.; Zambon, M. Neuraminidase Sequence Analysis and Susceptibilities of Influenza Virus Clinical Isolates to Zanamivir and Oseltamivir. *Antimicrobial Agents and Chemotherapy* **2003**, *47*, 2264–2272, doi:10.1128/AAC.47.7.2264-2272.2003.

70. Lee, N.; Hurt, A. Neuraminidase Inhibitor Resistance in Influenza: A Clinical Perspective. *Current Opinion in Infectious Diseases* **2018**, *31*, 520–526, doi:10.1097/QCO.0000000000000498.

71. Bloom, J.D.; Gong, L.I.; Baltimore, D. Permissive Secondary Mutations Enable the Evolution of Influenza Oseltamivir Resistance. *Science* **2010**, *328*, 1272–1275, doi:10.1126/science.1187816.

72. Sultana, I.; Yang, K.; Getie-Kebtie, M.; Couzens, L.; Markoff, L.; Alterman, M.; Eichelberger, M.C. Stability of Neuraminidase in Inactivated Influenza Vaccines. *Vaccine* **2014**, *32*, 2225–2230, doi:10.1016/j.vaccine.2014.01.078.

73. McMahon, M.; Strohmeier, S.; Rajendran, M.; Capuano, C.; Ellebedy, A.H.; Wilson, P.C.; Krammer, F. Correctly Folded - but Not Necessarily Functional - Influenza Virus Neuraminidase Is

Required to Induce Protective Antibody Responses in Mice. *Vaccine* **2020**, doi:10.1016/j.vaccine.2020.08.067.

74. Byrne-Nash, R.T.; Gillis, J.H.; Miller, D.F.; Bueter, K.M.; Kuck, L.R.; Rowlen, K.L. A Neuraminidase Potency Assay for Quantitative Assessment of Neuraminidase in Influenza Vaccines. *npj Vaccines* **2019**, *4*, 1–10, doi:10.1038/s41541-019-0099-3.

75. Hope-Simpson, R.E. Hong Kong Influenza Variant. *Br Med J* **1971**, *3*, 531.

76. Hope-Simpson, R.E. Protection against Hong Kong Influenza. *Br Med J* **1972**, *4*, 490–491.

77. Gill, P.W.; Murphy, A.M. Naturally Acquired Immunity to Influenza Type A: A Clinical and Laboratory Study. *Med J Aust* **1976**, *2*, 329–333, doi:10.5694/j.1326-5377.1976.tb130219.x.

78. Stadlbauer, D.; Zhu, X.; McMahon, M.; Turner, J.S.; Wohlbold, T.J.; Schmitz, A.J.; Strohmeier, S.; Yu, W.; Nachbagauer, R.; Mudd, P.A.; et al. Broadly Protective Human Antibodies That Target the Active Site of Influenza Virus Neuraminidase. *Science* **2019**, *366*, 499–504, doi:10.1126/science.aay0678.

79. Chen, Y.Q.; Wohlbold, T.J.; Zheng, N.Y.; Huang, M.; Huang, Y.; Neu, K.E.; Lee, J.; Wan, H.; Rojas, K.T.; Kirkpatrick, E.; et al. Influenza Infection in Humans Induces Broadly Cross-Reactive and Protective Neuraminidase-Reactive Antibodies. *Cell* **2018**, *173*, 417-429.e10, doi:10.1016/j.cell.2018.03.030.

80. Gao, J.; Couzens, L.; Burke, D.F.; Wan, H.; Wilson, P.; Memoli, M.J.; Xu, X.; Harvey, R.; Wrammert, J.; Ahmed, R.; et al. Antigenic Drift of the Influenza A(H1N1)Pdm09 Virus Neuraminidase Results in Reduced Effectiveness of A/California/7/2009 (H1N1pdm09)-Specific Antibodies. *mBio* **2019**, *10*, doi:10.1128/mBio.00307-19.

81. Sandbulte, M.R.; Westgeest, K.B.; Gao, J.; Xu, X.; Klimov, A.I.; Russell, C.A.; Burke, D.F.; Smith, D.J.; Fouchier, R.A.M.; Eichelberger, M.C. Discordant Antigenic Drift of Neuraminidase and Hemagglutinin in H1N1 and H3N2 Influenza Viruses. *Proceedings of the National Academy of Sciences* **2011**, *108*, 20748–20753, doi:10.1073/pnas.1113801108.

82. Warner, T.G.; O'Brien, J.S. Synthesis of 2'-(4-Methylumbelliferyl)-.Alpha.-D-N-Acetylneuraminic Acid and Detection of Skin Fibroblast Neuraminidase in Normal Humans and in Sialidosis. *Biochemistry* **1979**, *18*, 2783–2787, doi:10.1021/bi00580a014.

83. Potier, M.; Mameli, L.; Bélisle, M.; Dallaire, L.; Melançon, S.B. Fluorometric Assay of Neuraminidase with a Sodium (4-Methylumbelliferyl-Alpha-D-N-Acetylneuraminate) Substrate. *Anal Biochem* **1979**, *94*, 287–296, doi:10.1016/0003-2697(79)90362-2.

84. Buxton, R.C.; Edwards, B.; Juo, R.R.; Voyta, J.C.; Tisdale, M.; Bethell, R.C. Development of a Sensitive Chemiluminescent Neuraminidase Assay for the Determination of Influenza Virus Susceptibility to Zanamivir. *Anal Biochem* **2000**, *280*, 291–300, doi:10.1006/abio.2000.4517.

85. Marathe, B.M.; Lévêque, V.; Klumpp, K.; Webster, R.G.; Govorkova, E.A. Determination of Neuraminidase Kinetic Constants Using Whole Influenza Virus Preparations and Correction for Spectroscopic Interference by a Fluorogenic Substrate. *PLOS ONE* **2013**, *8*, e71401, doi:10.1371/journal.pone.0071401.

86. Gao, J.; Couzens, L.; Eichelberger, M.C. Measuring Influenza Neuraminidase Inhibition Antibody Titers by Enzyme-Linked Lectin Assay. *J Vis Exp* **2016**, doi:10.3791/54573.

87. Dugan, H.L.; Stamper, C.T.; Li, L.; Changrob, S.; Asby, N.W.; Halfmann, P.J.; Zheng, N.-Y.; Huang, M.; Shaw, D.G.; Cobb, M.S.; et al. Profiling B Cell Immunodominance after SARS-CoV-2 Infection Reveals Antibody Evolution to Non-Neutralizing Viral Targets. *Immunity* **2021**, *54*, 1290-1303.e7, doi:10.1016/j.immuni.2021.05.001.

88. Chen, X.; Li, R.; Pan, Z.; Qian, C.; Yang, Y.; You, R.; Zhao, J.; Liu, P.; Gao, L.; Li, Z.; et al. Human Monoclonal Antibodies Block the Binding of SARS-CoV-2 Spike Protein to Angiotensin Converting Enzyme 2 Receptor. *Cell Mol Immunol* **2020**, *17*, 647–649, doi:10.1038/s41423-020-0426-7.

89. Huang, A.T.; Garcia-Carreras, B.; Hitchings, M.D.T.; Yang, B.; Katzelnick, L.C.; Rattigan, S.M.; Borgert, B.A.; Moreno, C.A.; Solomon, B.D.; Trimmer-Smith, L.; et al. A Systematic Review of Antibody Mediated Immunity to Coronaviruses: Kinetics, Correlates of Protection, and Association with Severity. *Nat Commun* **2020**, *11*, 4704, doi:10.1038/s41467-020-18450-4.

90. Addetia, A.; Crawford, K.H.D.; Dingens, A.; Zhu, H.; Roychoudhury, P.; Huang, M.-L.; Jerome, K.R.; Bloom, J.D.; Greninger, A.L. Neutralizing Antibodies Correlate with Protection from SARS-CoV-2 in Humans during a Fishery Vessel Outbreak with a High Attack Rate. *Journal of Clinical Microbiology* **2020**, *58*, doi:10.1128/JCM.02107-20.

91. Khoury, D.S.; Cromer, D.; Reynaldi, A.; Schlub, T.E.; Wheatley, A.K.; Juno, J.A.; Subbarao, K.; Kent, S.J.; Triccas, J.A.; Davenport, M.P. Neutralizing Antibody Levels Are Highly Predictive of Immune Protection from Symptomatic SARS-CoV-2 Infection. *Nat Med* **2021**, doi:10.1038/s41591-021-01377-8.

92. Zhou, P.; Yang, X.-L.; Wang, X.-G.; Hu, B.; Zhang, L.; Zhang, W.; Si, H.-R.; Zhu, Y.; Li, B.; Huang, C.-L.; et al. A Pneumonia Outbreak Associated with a New Coronavirus of Probable Bat Origin. *Nature* **2020**, *579*, 270–273, doi:10.1038/s41586-020-2012-7.

93. Walls, A.C.; Park, Y.-J.; Tortorici, M.A.; Wall, A.; McGuire, A.T.; Veesler, D. Structure, Function, and Antigenicity of the SARS-CoV-2 Spike Glycoprotein. *Cell* **2020**, *181*, 281-292.e6, doi:10.1016/j.cell.2020.02.058.

94. Hoffmann, M.; Kleine-Weber, H.; Schroeder, S.; Krüger, N.; Herrler, T.; Erichsen, S.; Schiergens, T.S.; Herrler, G.; Wu, N.-H.; Nitsche, A.; et al. SARS-CoV-2 Cell Entry Depends on ACE2 and TMPRSS2 and Is Blocked by a Clinically Proven Protease Inhibitor. *Cell* **2020**, *181*, 271-280.e8, doi:10.1016/j.cell.2020.02.052.

95. Wang, Q.; Zhang, Y.; Wu, L.; Niu, S.; Song, C.; Zhang, Z.; Lu, G.; Qiao, C.; Hu, Y.; Yuen, K.-Y.; et al. Structural and Functional Basis of SARS-CoV-2 Entry by Using Human ACE2. *Cell* **2020**, *181*, 894-904.e9, doi:10.1016/j.cell.2020.03.045.

96. Greaney, A.J.; Loes, A.N.; Crawford, K.H.D.; Starr, T.N.; Malone, K.D.; Chu, H.Y.; Bloom, J.D. Comprehensive Mapping of Mutations in the SARS-CoV-2 Receptor-Binding Domain That Affect Recognition by Polyclonal Human Plasma Antibodies. *Cell Host & Microbe* **2021**, *29*, 463-476.e6, doi:10.1016/j.chom.2021.02.003.

97. Yuan, M.; Liu, H.; Wu, N.C.; Lee, C.-C.D.; Zhu, X.; Zhao, F.; Huang, D.; Yu, W.; Hua, Y.; Tien, H.; et al. Structural Basis of a Shared Antibody Response to SARS-CoV-2. *Science* **2020**, *369*, 1119–1123, doi:10.1126/science.abd2321.

98. Wu, Y.; Wang, F.; Shen, C.; Peng, W.; Li, D.; Zhao, C.; Li, Z.; Li, S.; Bi, Y.; Yang, Y.; et al. A Noncompeting Pair of Human Neutralizing Antibodies Block COVID-19 Virus Binding to Its Receptor ACE2. *Science* **2020**, *368*, 1274–1278, doi:10.1126/science.abc2241.

99. McCallum, M.; De Marco, A.; Lempp, F.A.; Tortorici, M.A.; Pinto, D.; Walls, A.C.; Beltramello, M.; Chen, A.; Liu, Z.; Zatta, F.; et al. N-Terminal Domain Antigenic Mapping Reveals a Site of Vulnerability for SARS-CoV-2. *Cell* **2021**, *184*, 2332-2347.e16, doi:10.1016/j.cell.2021.03.028.

100. Cerutti, G.; Guo, Y.; Liu, L.; Zhang, Z.; Liu, L.; Luo, Y.; Huang, Y.; Wang, H.H.; Ho, D.D.; Sheng, Z.; et al. *Structural Basis for Antibody Resistance to SARS-CoV-2 Omicron Variant*; 2021; p. 2021.12.21.473620;

101. Chi, X.; Yan, R.; Zhang, J.; Zhang, G.; Zhang, Y.; Hao, M.; Zhang, Z.; Fan, P.; Dong, Y.; Yang, Y.; et al. A Neutralizing Human Antibody Binds to the N-Terminal Domain of the Spike Protein of SARS-CoV-2. *Science* **2020**, doi:10.1126/science.abc6952.

102. Pinto, D.; Sauer, M.M.; Czudnochowski, N.; Low, J.S.; Tortorici, M.A.; Housley, M.P.; Noack, J.; Walls, A.C.; Bowen, J.E.; Guarino, B.; et al. Broad Betacoronavirus Neutralization by a Stem Helix–Specific Human Antibody. *Science* **2021**, *373*, 1109–1116, doi:10.1126/science.abj3321.

103. Zeng, W.; Liu, G.; Ma, H.; Zhao, D.; Yang, Y.; Liu, M.; Mohammed, A.; Zhao, C.; Yang, Y.; Xie, J.; et al. Biochemical Characterization of SARS-CoV-2 Nucleocapsid Protein. *Biochem Biophys Res Commun* **2020**, *527*, 618–623, doi:10.1016/j.bbrc.2020.04.136.

104. Whitaker, H.J.; Elgohari, S.; Rowe, C.; Otter, A.D.; Brooks, T.; Linley, E.; Hayden, I.; Ribeiro, S.; Hewson, J.; Lakhani, A.; et al. Impact of COVID-19 Vaccination Program on Seroprevalence in Blood Donors in England, 2021. *Journal of Infection* **2021**, *83*, 237–279, doi:10.1016/j.jinf.2021.04.037.

105. Peluso, M.J.; Takahashi, S.; Hakim, J.; Kelly, J.D.; Torres, L.; Iyer, N.S.; Turcios, K.; Janson, O.; Munter, S.E.; Thanh, C.; et al. SARS-CoV-2 Antibody Magnitude and Detectability Are Driven by Disease Severity, Timing, and Assay. *Science Advances* **2021**, *7*, eabh3409, doi:10.1126/sciadv.abh3409.

106. Wang, Y.; Zhang, L.; Sang, L.; Ye, F.; Ruan, S.; Zhong, B.; Song, T.; Alshukairi, A.N.; Chen, R.; Zhang, Z.; et al. Kinetics of Viral Load and Antibody Response in Relation to COVID-19 Severity. *J Clin Invest* **2020**, *130*, 5235–5244, doi:10.1172/JCI138759.

107. Weisberg, S.P.; Connors, T.J.; Zhu, Y.; Baldwin, M.R.; Lin, W.-H.; Wontakal, S.; Szabo, P.A.; Wells, S.B.; Dogra, P.; Gray, J.; et al. Distinct Antibody Responses to SARS-CoV-2 in Children and Adults across the COVID-19 Clinical Spectrum. *Nature Immunology* **2021**, *22*, 25–31, doi:10.1038/s41590-020-00826-9.

108. Seow, J.; Graham, C.; Merrick, B.; Acors, S.; Pickering, S.; Steel, K.J.A.; Hemmings, O.; O'Byrne, A.; Kouphou, N.; Galao, R.P.; et al. Longitudinal Observation and Decline of Neutralizing Antibody Responses in the Three Months Following SARS-CoV-2 Infection in Humans. *Nature Microbiology* **2020**, *5*, 1598–1607, doi:10.1038/s41564-020-00813-8.

109. Dan, J.M.; Mateus, J.; Kato, Y.; Hastie, K.M.; Yu, E.D.; Faliti, C.E.; Grifoni, A.; Ramirez, S.I.; Haupt, S.; Frazier, A.; et al. Immunological Memory to SARS-CoV-2 Assessed for up to 8 Months after Infection. *Science* **2021**, *371*, doi:10.1126/science.abf4063.

110. Beaudoin-Bussières, G.; Laumaea, A.; Anand, S.P.; Prévost, J.; Gasser, R.; Goyette, G.; Medjahed, H.; Perreault, J.; Tremblay, T.; Lewin, A.; et al. Decline of Humoral Responses against SARS-CoV-2 Spike in Convalescent Individuals. *mBio* **2020**, *11*, doi:10.1128/mBio.02590-20.

111. Iyer, A.S.; Jones, F.K.; Nodoushani, A.; Kelly, M.; Becker, M.; Slater, D.; Mills, R.; Teng, E.; Kamruzzaman, M.; Garcia-Beltran, W.F.; et al. Persistence and Decay of Human Antibody Responses to the Receptor Binding Domain of SARS-CoV-2 Spike Protein in COVID-19 Patients. *Sci. Immunol.* **2020**, *5*, eabe0367, doi:10.1126/sciimmunol.abe0367.

112. Wang, K.; Long, Q.-X.; Deng, H.-J.; Hu, J.; Gao, Q.-Z.; Zhang, G.-J.; He, C.-L.; Huang, L.-Y.; Hu, J.-L.; Chen, J.; et al. Longitudinal Dynamics of the Neutralizing Antibody Response to Severe Acute Respiratory Syndrome Coronavirus 2 (SARS-CoV-2) Infection. *Clinical Infectious Diseases* **2020**, doi:10.1093/cid/ciaa1143.

113. Wajnberg, A.; Amanat, F.; Firpo, A.; Altman, D.R.; Bailey, M.J.; Mansour, M.; McMahon, M.; Meade, P.; Mendu, D.R.; Muellers, K.; et al. Robust Neutralizing Antibodies to SARS-CoV-2 Infection Persist for Months. *Science* **2020**, *370*, 1227–1230, doi:10.1126/science.abd7728.

114. Gaebler, C.; Wang, Z.; Lorenzi, J.C.C.; Muecksch, F.; Finkin, S.; Tokuyama, M.; Cho, A.; Jankovic, M.; Schaefer-Babajew, D.; Oliveira, T.Y.; et al. Evolution of Antibody Immunity to SARS-CoV-2. *Nature* **2021**, *591*, 639–644, doi:10.1038/s41586-021-03207-w.

115. Muecksch, F.; Wise, H.; Batchelor, B.; Squires, M.; Semple, E.; Richardson, C.; McGuire, J.; Clearly, S.; Furrie, E.; Greig, N.; et al. Longitudinal Serological Analysis and Neutralizing Antibody Levels in Coronavirus Disease 2019 Convalescent Patients. *The Journal of Infectious Diseases* **2021**, *223*, 389–398, doi:10.1093/infdis/jiaa659.

116. Wheatley, A.K.; Juno, J.A.; Wang, J.J.; Selva, K.J.; Reynaldi, A.; Tan, H.-X.; Lee, W.S.; Wragg, K.M.; Kelly, H.G.; Esterbauer, R.; et al. Evolution of Immune Responses to SARS-CoV-2 in Mild-Moderate COVID-19. *Nat Commun* **2021**, *12*, 1162, doi:10.1038/s41467-021-21444-5.

117. Encinosa, W.; Figueroa, J.; Elias, Y. Severity of Hospitalizations from SARS-CoV-2 vs Influenza and Respiratory Syncytial Virus Infection in Children Aged 5 to 11 Years in 11 US States. *JAMA Pediatrics* **2022**, doi:10.1001/jamapediatrics.2021.6566.

118. Molteni, E.; Sudre, C.H.; Canas, L.S.; Bhopal, S.S.; Hughes, R.C.; Antonelli, M.; Murray, B.; Kläser, K.; Kerfoot, E.; Chen, L.; et al. Illness Duration and Symptom Profile in Symptomatic UK School-Aged Children Tested for SARS-CoV-2. *The Lancet Child & Adolescent Health* **2021**, S235246422100198X, doi:10.1016/S2352-4642(21)00198-X.

119. Roarty, C.; Tonry, C.; McFetridge, L.; Mitchell, H.; Watson, C.; Waterfield, T.; Waxman, E.; Fairley, D.; Roew-Setz, G.; McKenna, J.; et al. Kinetics and Seroprevalence of SARS-CoV-2 Antibodies in Children. *The Lancet Infectious Diseases* **2020**, doi:10.1016/S1473-3099(20)30884-7.

120. Bonfante, F.; Costenaro, P.; Cantarutti, A.; Chiara, C.D.; Bortolami, A.; Petrara, M.R.; Carmona, F.; Pagliari, M.; Cosma, C.; Cozzani, S.; et al. Mild SARS-CoV-2 Infections and Neutralizing Antibody Titers. *Pediatrics* **2021**, doi:10.1542/peds.2021-052173.

121. Dowell, A.C.; Butler, M.S.; Jinks, E.; Tut, G.; Lancaster, T.; Sylla, P.; Begum, J.; Pearce, H.; Taylor, G.S.; Syrimi, E.; et al. Children Develop Strong and Sustained Cross-Reactive Immune Responses against Spike Protein Following SARS-CoV-2 Infection. *medRxiv* **2021**, 2021.04.12.21255275, doi:10.1101/2021.04.12.21255275.

122. Karron, R.A.; Quesada, M.G.; Schappell, E.A.; Schmidt, S.D.; Knoll, M.D.; Hetrich, M.K.; Veguilla, V.; Doria-Rose, N.; Dawood, F.S.; Team, Searc.S. *Binding and Neutralizing Antibody Responses to SARS-CoV-2 in Infants and Young Children Exceed Those in Adults*; 2021; p. 2021.12.20.21268034;

123. Riepler, L.; Rössler, A.; Falch, A.; Volland, A.; Borena, W.; von Laer, D.; Kimpel, J. Comparison of Four SARS-CoV-2 Neutralization Assays. *Vaccines* **2021**, *9*, 13, doi:10.3390/vaccines9010013.

124. Dingens, A.S.; Crawford, K.H.D.; Adler, A.; Steele, S.L.; Lacombe, K.; Eguia, R.; Amanat, F.; Walls, A.C.; Wolf, C.R.; Murphy, M.; et al. Serological Identification of SARS-CoV-2 Infections among Children Visiting a Hospital during the Initial Seattle Outbreak. *Nature Communications* **2020**, *11*, 4378, doi:10.1038/s41467-020-18178-1.

125. Greaney, A.J.; Starr, T.N.; Barnes, C.O.; Weisblum, Y.; Schmidt, F.; Caskey, M.; Gaebler, C.; Cho, A.; Agudelo, M.; Finkin, S.; et al. Mapping Mutations to the SARS-CoV-2 RBD That Escape Binding by Different Classes of Antibodies. *Nat Commun* **2021**, *12*, 4196, doi:10.1038/s41467-021-24435-8.

126. Gerhard, W.; Webster, R.G. Antigenic Drift in Influenza A Viruses. I. Selection and Characterization of Antigenic Variants of A/PR/8/34 (HON1) Influenza Virus with Monoclonal Antibodies. *J. Exp. Med.* **1978**, *148*, 383–392, doi:10.1084/jem.148.2.383.

127. Laver, W.G.; Air, G.M.; Webster, R.G. Mechanism of Antigenic Drift in Influenza Virus: Amino Acid Sequence Changes in an Antigenically Active Region of Hong Kong (H3N2) Influenza Virus Hemagglutinin. *Journal of Molecular Biology* **1981**, *145*, 339–361, doi:10.1016/0022-2836(81)90209-6.

128. Dowdle, W.R.; Coleman, M.T.; Gregg, M.B. Natural History of Influenza Type A in the United States, 1957-1972. *Prog Med Virol* **1974**, *17*, 91–135.

129. Harvey, W.T.; Benton, D.J.; Gregory, V.; Hall, J.P.J.; Daniels, R.S.; Bedford, T.; Haydon, D.T.; Hay, A.J.; McCauley, J.W.; Reeve, R. Identification of Low- and High-Impact Hemagglutinin Amino Acid Substitutions That Drive Antigenic Drift of Influenza A(H1N1) Viruses. *PLoS Pathogens* **2016**, *12*, 1–23, doi:10.1371/journal.ppat.1005526.

130. Caton, A.J.; Brownlee, G.G.; Yewdell, J.W.; Gerhard, W. The Antigenic Structure of the Influenza Virus A/PR/8/34 Hemagglutinin (H1 Subtype). *Cell* **1982**, *31*, 417–427, doi:10.1016/0092-8674(82)90135-0.

131. Air, G.M.; Els, M.C.; Brown, L.E.; Laver, W.G.; Webster, R.G. Location of Antigenic Sites on the Three-Dimensional Structure of the Influenza N2 Virus Neuraminidase. *Virology* **1985**, *145*, 237–248, doi:10.1016/0042-6822(85)90157-6.

132. Pica, N.; Palese, P. Toward a Universal Influenza Virus Vaccine: Prospects and Challenges. *Annu Rev Med* **2013**, *64*, 189–202, doi:10.1146/annurev-med-120611-145115.

133. Ellebedy, A.H.; Krammer, F.; Li, G.-M.; Miller, M.S.; Chiu, C.; Wrammert, J.; Chang, C.Y.; Davis, C.W.; McCausland, M.; Elbein, R.; et al. Induction of Broadly Cross-Reactive Antibody Responses to the Influenza HA Stem Region Following H5N1 Vaccination in Humans. *Proc Natl Acad Sci U S A* **2014**, *111*, 13133–13138, doi:10.1073/pnas.1414070111.

134. Whittle, J.R.R.; Wheatley, A.K.; Wu, L.; Lingwood, D.; Kanekiyo, M.; Ma, S.S.; Narpala, S.R.; Yassine, H.M.; Frank, G.M.; Yewdell, J.W.; et al. Flow Cytometry Reveals That H5N1 Vaccination

Elicits Cross-Reactive Stem-Directed Antibodies from Multiple Ig Heavy-Chain Lineages. *Journal of Virology* **2014**, *88*, 4047–4057, doi:10.1128/JVI.03422-13.

135. Andrews, S.F.; Joyce, M.G.; Chambers, M.J.; Gillespie, R.A.; Kanekiyo, M.; Leung, K.; Yang, E.S.; Tsybovsky, Y.; Wheatley, A.K.; Crank, M.C.; et al. Preferential Induction of Cross-Group Influenza A Hemagglutinin Stem–Specific Memory B Cells after H7N9 Immunization in Humans. *Science Immunology* **2017**, *2*, doi:10.1126/sciimmunol.aan2676.

136. Chai, N.; Swem, L.R.; Reichelt, M.; Chen-Harris, H.; Luis, E.; Park, S.; Fouts, A.; Lupardus, P.; Wu, T.D.; Li, O.; et al. Two Escape Mechanisms of Influenza A Virus to a Broadly Neutralizing Stalk-Binding Antibody. *PLoS Pathogens* **2016**, *12*, 1–29, doi:10.1371/journal.ppat.1005702.

137. Hadfield, J.; Megill, C.; Bell, S.M.; Huddleston, J.; Potter, B.; Callender, C.; Sagulenko, P.; Bedford, T.; Neher, R.A. Nextstrain: Real-Time Tracking of Pathogen Evolution. *Bioinformatics* **2018**, *34*, 4121–4123, doi:10.1093/bioinformatics/bty407.

138. Sagulenko, P.; Puller, V.; Neher, R.A. TreeTime: Maximum-Likelihood Phylodynamic Analysis. *Virus Evol* **2018**, *4*, doi:10.1093/ve/vex042.

139. Krammer, F.; Pica, N.; Hai, R.; Margine, I. Chimeric Hemagglutinin Influenza Virus Vaccine Constructs Elicit Broadly Protective Stalk-Specific Antibodies. **2013**, *87*, 6542–6550, doi:10.1128/JVI.00641-13.

140. Knight, M.; Changrob, S.; Li, L.; Wilson, P.C. Imprinting, Immunodominance, and Other Impediments to Generating Broad Influenza Immunity. *Immunological Reviews n/a*, doi:10.1111/imr.12900.

141. Ranjeva, S.; Subramanian, R.; Fang, V.J.; Leung, G.M.; Ip, D.K.M.; Perera, R.A.P.M.; Peiris, J.S.M.; Cowling, B.J.; Cobey, S. Age-Specific Differences in the Dynamics of Protective Immunity to Influenza. *Nature Communications* **2019**, *10*, doi:10.1038/s41467-019-09652-6.

142. Dugan, H.L.; Guthmiller, J.J.; Arevalo, P.; Huang, M.; Chen, Y.-Q.; Neu, K.E.; Henry, C.; Zheng, N.-Y.; Lan, L.Y.-L.; Tepora, M.E.; et al. Preexisting Immunity Shapes Distinct Antibody Landscapes after Influenza Virus Infection and Vaccination in Humans. *Sci. Transl. Med.* **2020**, *12*, eabd3601, doi:10.1126/scitranslmed.abd3601.

143. Jiang, L.; Fantoni, G.; Couzens, L.; Gao, J.; Plant, E.; Ye, Z.; Eichelberger, M.C.; Wan, H. Comparative Efficacy of Monoclonal Antibodies That Bind to Different Epitopes of the 2009 Pandemic H1N1 Influenza Virus Neuraminidase. *Journal of Virology* **2015**, *90*, 117–128, doi:10.1128/JVI.01756-15.

144. Lin, Y.P.; Gregory, V.; Collins, P.; Kloess, J.; Wharton, S.; Cattle, N.; Lackenby, A.; Daniels, R.; Hay, A. Neuraminidase Receptor Binding Variants of Human Influenza A(H3N2) Viruses Resulting from Substitution of Aspartic Acid 151 in the Catalytic Site: A Role in Virus Attachment? *Journal of Virology* **2010**, *84*, 6769–6781, doi:10.1128/JVI.00458-10.

145. Tamura, D.; Sugaya, N.; Ozawa, M.; Takano, R.; Ichikawa, M.; Yamazaki, M.; Kawakami, C.; Shimizu, H.; Uehara, R.; Kiso, M.; et al. Frequency of Drug-Resistant Viruses and Virus Shedding in Pediatric Influenza Patients Treated With Neuraminidase Inhibitors. *Clin Infect Dis* **2011**, *52*, 432–437, doi:10.1093/cid/ciq183.

146. Lee, H.K.; Tang, J.W.-T.; Kong, D.H.-L.; Loh, T.P.; Chiang, D.K.-L.; Lam, T.T.-Y.; Koay, E.S.-C. Comparison of Mutation Patterns in Full-Genome A/H3N2 Influenza Sequences Obtained Directly from Clinical Samples and the Same Samples after a Single MDCK Passage. *PLOS ONE* **2013**, *8*, e79252, doi:10.1371/journal.pone.0079252.

147. Chambers, B.S.; Li, Y.; Hodinka, R.L.; Hensley, S.E. Recent H3N2 Influenza Virus Clinical Isolates Rapidly Acquire Hemagglutinin or Neuraminidase Mutations When Propagated for Antigenic Analyses. *Journal of Virology* **2014**, *88*, 10986–10989, doi:10.1128/JVI.01077-14.

148. Mishin, V.P.; Sleeman, K.; Levine, M.; Carney, P.J.; Stevens, J.; Gubareva, L.V. The Effect of the MDCK Cell Selected Neuraminidase D151G Mutation on the Drug Susceptibility Assessment of Influenza A(H3N2) Viruses. *Antiviral Research* **2014**, *101*, 93–96, doi:10.1016/j.antiviral.2013.11.001.

149. Mohr, P.G.; Deng, Y.-M.; McKimm-Breschkin, J.L. The Neuraminidases of MDCK Grown Human Influenza A(H3N2) Viruses Isolated since 1994 Can Demonstrate Receptor Binding. *Virol J* **2015**, *12*, doi:10.1186/s12985-015-0295-3.

150. Zhu, X.; McBride, R.; Nycholat, C.M.; Yu, W.; Paulson, J.C.; Wilson, I.A. Influenza Virus Neuraminidases with Reduced Enzymatic Activity That Avidly Bind Sialic Acid Receptors. *Journal of Virology* **2012**, *86*, 13371–13383, doi:10.1128/JVI.01426-12.

151. Xue, K.S.; Hooper, K.A.; Ollodart, A.R.; Dingens, A.S.; Bloom, J.D. Cooperation between Distinct Viral Variants Promotes Growth of H3N2 Influenza in Cell Culture. *eLife* **2016**, *5*, e13974, doi:10.7554/eLife.13974.

152. Xue, K.S.; Greninger, A.L.; Pérez-Osorio, A.; Bloom, J.D. Cooperating H3N2 Influenza Virus Variants Are Not Detectable in Primary Clinical Samples. *mSphere* **2018**, *3*, doi:10.1128/mSphereDirect.00552-17.

153. Hoffmann, E.; Neumann, G.; Kawaoka, Y.; Hobom, G.; Webster, R.G. A DNA Transfection System for Generation of Influenza A Virus from Eight Plasmids. *PNAS* **2000**, *97*, 6108–6113, doi:10.1073/pnas.100133697.

154. Wan, H.; Gao, J.; Xu, K.; Chen, H.; Couzens, L.K.; Rivers, K.H.; Easterbrook, J.D.; Yang, K.; Zhong, L.; Rajabi, M.; et al. Molecular Basis for Broad Neuraminidase Immunity: Conserved Epitopes in Seasonal and Pandemic H1N1 as Well as H5N1 Influenza Viruses. *Journal of Virology* **2013**, *87*, 9290–9300, doi:10.1128/JVI.01203-13.

155. Wan, H.; Yang, H.; Shore, D.A.; Garten, R.J.; Couzens, L.; Gao, J.; Jiang, L.; Carney, P.J.; Villanueva, J.; Stevens, J.; et al. Structural Characterization of a Protective Epitope Spanning A(H1N1)Pdm09 Influenza Virus Neuraminidase Monomers. *Nature Communications* **2015**, *6*, 1–10, doi:10.1038/ncomms7114.

156. Lee, J.M.; Eguia, R.; Zost, S.J.; Choudhary, S.; Wilson, P.C.; Bedford, T.; Stevens-Ayers, T.; Boeckh, M.; Hurt, A.C.; Lakdawala, S.S.; et al. Mapping Person-to-Person Variation in Viral Mutations That Escape Polyclonal Serum Targeting Influenza Hemagglutinin. *eLife* **2019**, *8*, e49324, doi:10.7554/eLife.49324.

157. Hoffmann, E.; Stech, J.; Guan, Y.; Webster, R.G.; Perez, D.R. Universal Primer Set for the Full-Length Amplification of All Influenza A Viruses. *Archives of Virology* **2001**, *146*, 2275–2289, doi:10.1007/s007050170002.

158. Martín, J.; Wharton, S.A.; Lin, Y.P.; Takemoto, D.K.; Skehel, J.J.; Wiley, D.C.; Steinhauer, D.A. Studies of the Binding Properties of Influenza Hemagglutinin Receptor-Site Mutants. *Virology* **1998**, *241*, 101–111, doi:10.1006/viro.1997.8958.

159. Yang, H.; Chen, L.-M.; Carney, P.J.; Donis, R.O.; Stevens, J. Structures of Receptor Complexes of a North American H7N2 Influenza Hemagglutinin with a Loop Deletion in the Receptor Binding Site. *PLoS Pathog* **2010**, *6*, e1001081, doi:10.1371/journal.ppat.1001081.

160. Das, S.R.; Hensley, S.E.; David, A.; Schmidt, L.; Gibbs, J.S.; Puigbo, P.; Ince, W.L.; Bennink, J.R.; Yewdell, J.W. Fitness Costs Limit Influenza A Virus Hemagglutinin Glycosylation as an Immune Evasion Strategy. *PNAS* **2011**, *108*, E1417–E1422, doi:10.1073/pnas.1108754108.

161. Meisner, J.; Szretter, K.J.; Bradley, K.C.; Langley, W.A.; Li, Z.-N.; Lee, B.-J.; Thoennes, S.; Martin, J.; Skehel, J.J.; Russell, R.J.; et al. Infectivity Studies of Influenza Virus Hemagglutinin Receptor Binding Site Mutants in Mice. *Journal of Virology* **2008**, *82*, 5079–5083, doi:10.1128/JVI.01958-07.

162. Klenk, H.-D.; Rott, R.; Orlich, M.; Blödorn, J. Activation of Influenza A Viruses by Trypsin Treatment. *Virology* **1975**, *68*, 426–439, doi:10.1016/0042-6822(75)90284-6.

163. Yewdell, J.W.; Webster, R.G.; Gerhard, W.U. Antigenic Variation in Three Distinct Determinants of an Influenza Type A Haemagglutinin Molecule. *Nature* **1979**, *279*, 246–248, doi:10.1038/279246a0.

164. Hensley, S.E.; Das, S.R.; Bailey, A.L.; Schmidt, L.M.; Hickman, H.D.; Jayaraman, A.; Viswanathan, K.; Raman, R.; Sasisekharan, R.; Bennink, J.R.; et al. Hemagglutinin Receptor Binding Avidity Drives Influenza A Virus Antigenic Drift. *Science* **2009**, *326*, 734–736, doi:10.1126/science.1178258.

165. Compans, R.W.; Dimmock, N.J.; Meier-Ewert, H. Effect of Antibody to Neuraminidase on the Maturation and Hemagglutinating Activity of an Influenza A2 Virus. *J. Virol.* **1969**, *4*, 528–534.

166. Lubeck, M.D.; Gerhard, W. Topological Mapping Antigenic Sites on the Influenza A/PR/8/34 Virus Hemagglutinin Using Monoclonal Antibodies. *Virology* **1981**, *113*, 64–72, doi:10.1016/0042-6822(81)90136-7.

167. Webster, R.G.; Hinshaw, V.S.; Laver, W.G. Selection and Analysis of Antigenic Variants of the Neuraminidase of N2 Influenza Viruses with Monoclonal Antibodies. *Virology* **1982**, *117*, 93–104, doi:10.1016/0042-6822(82)90510-4.

168. Shrock, E.; Fujimura, E.; Kula, T.; Timms, R.T.; Lee, I.-H.; Leng, Y.; Robinson, M.L.; Sie, B.M.; Li, M.Z.; Chen, Y.; et al. Viral Epitope Profiling of COVID-19 Patients Reveals Cross-Reactivity and Correlates of Severity. *Science* **2020**, *370*, doi:10.1126/science.abd4250.

169. Chandrashekar, A.; Liu, J.; Martinot, A.J.; McMahan, K.; Mercado, N.B.; Peter, L.; Tostanoski, L.H.; Yu, J.; Maliga, Z.; Nekorchuk, M.; et al. SARS-CoV-2 Infection Protects against Rechallenge in Rhesus Macaques. *Science* **2020**, *369*, 812–817, doi:10.1126/science.abc4776.

170. Deng, W.; Bao, L.; Liu, J.; Xiao, C.; Liu, J.; Xue, J.; Lv, Q.; Qi, F.; Gao, H.; Yu, P.; et al. Primary Exposure to SARS-CoV-2 Protects against Reinfection in Rhesus Macaques. *Science* **2020**, *369*, 818–823, doi:10.1126/science.abc5343.

171. Bergwerk, M.; Gonen, T.; Lustig, Y.; Amit, S.; Lipsitch, M.; Cohen, C.; Mandelboim, M.; Levin, E.G.; Rubin, C.; Indenbaum, V.; et al. Covid-19 Breakthrough Infections in Vaccinated Health Care Workers. *New England Journal of Medicine* **2021**, *385*, 1474–1484, doi:10.1056/NEJMoa2109072.

172. Chung, E.; Chow, E.J.; Wilcox, N.C.; Burstein, R.; Brandstetter, E.; Han, P.D.; Fay, K.; Pfau, B.; Adler, A.; Lacombe, K.; et al. Comparison of Symptoms and RNA Levels in Children and Adults With SARS-CoV-2 Infection in the Community Setting. *JAMA Pediatr* **2021**, doi:10.1001/jamapediatrics.2021.2025.

173. Li, B.; Zhang, S.; Zhang, R.; Chen, X.; Wang, Y.; Zhu, C. Epidemiological and Clinical Characteristics of COVID-19 in Children: A Systematic Review and Meta-Analysis. *Front Pediatr* **2020**, *8*, 591132, doi:10.3389/fped.2020.591132.

174. Harris, P.A.; Taylor, R.; Thielke, R.; Payne, J.; Gonzalez, N.; Conde, J.G. Research Electronic Data Capture (REDCap)--a Metadata-Driven Methodology and Workflow Process for Providing Translational Research Informatics Support. *J Biomed Inform* **2009**, *42*, 377–381, doi:10.1016/j.jbi.2008.08.010.

175. Chu, H.Y.; Englund, J.A.; Starita, L.M.; Famulare, M.; Brandstetter, E.; Nickerson, D.A.; Rieder, M.J.; Adler, A.; Lacombe, K.; Kim, A.E.; et al. Early Detection of Covid-19 through a Citywide Pandemic Surveillance Platform. *N Engl J Med* **2020**, *383*, 185–187, doi:10.1056/NEJMc2008646.

176. Garrett, M.E.; Galloway, J.; Chu, H.Y.; Itell, H.L.; Stoddard, C.I.; Wolf, C.R.; Logue, J.K.; McDonald, D.; Weight, H.; Matsen, F.A.; et al. High-Resolution Profiling of Pathways of Escape for SARS-CoV-2 Spike-Binding Antibodies. *Cell* **2021**, *184*, 2927-2938.e11, doi:10.1016/j.cell.2021.04.045.

177. Case, J.B.; Rothlauf, P.W.; Chen, R.E.; Liu, Z.; Zhao, H.; Kim, A.S.; Bloyet, L.-M.; Zeng, Q.; Tahan, S.; Droit, L.; et al. Neutralizing Antibody and Soluble ACE2 Inhibition of a Replication-Competent VSV-SARS-CoV-2 and a Clinical Isolate of SARS-CoV-2. *Cell Host Microbe* **2020**, *28*, 475-485.e5, doi:10.1016/j.chom.2020.06.021.

178. Dieterle, M.E.; Haslwanter, D.; Bortz, R.H.; Wirchnianski, A.S.; Lasso, G.; Vergnolle, O.; Abbasi, S.A.; Fels, J.M.; Laudermilch, E.; Florez, C.; et al. A Replication-Competent Vesicular Stomatitis Virus for Studies of SARS-CoV-2 Spike-Mediated Cell Entry and Its Inhibition. *Cell Host Microbe* **2020**, *28*, 486-496.e6, doi:10.1016/j.chom.2020.06.020.

179. Johnson, M.C.; Lyddon, T.D.; Suarez, R.; Salcedo, B.; LePique, M.; Graham, M.; Ricana, C.; Robinson, C.; Ritter, D.G. Optimized Pseudotyping Conditions for the SARS-COV-2 Spike Glycoprotein. *J Virol* **2020**, *94*, e01062-20, doi:10.1128/JVI.01062-20.

180. Ou, X.; Liu, Y.; Lei, X.; Li, P.; Mi, D.; Ren, L.; Guo, L.; Guo, R.; Chen, T.; Hu, J.; et al. Characterization of Spike Glycoprotein of SARS-CoV-2 on Virus Entry and Its Immune Cross-Reactivity with SARS-CoV. *Nat Commun* **2020**, *11*, 1620, doi:10.1038/s41467-020-15562-9.

181. Rogers, T.F.; Zhao, F.; Huang, D.; Beutler, N.; Burns, A.; He, W.-T.; Limbo, O.; Smith, C.; Song, G.; Woehl, J.; et al. Isolation of Potent SARS-CoV-2 Neutralizing Antibodies and Protection from Disease in a Small Animal Model. *Science* **2020**, *369*, 956–963, doi:10.1126/science.abc7520.

182. Schmidt, F.; Weisblum, Y.; Muecksch, F.; Hoffmann, H.-H.; Michailidis, E.; Lorenzi, J.C.C.; Mendoza, P.; Rutkowska, M.; Bednarski, E.; Gaebler, C.; et al. Measuring SARS-CoV-2 Neutralizing Antibody Activity Using Pseudotyped and Chimeric Viruses. *J Exp Med* **2020**, *217*, e20201181, doi:10.1084/jem.20201181.

183. Korber, B.; Fischer, W.M.; Gnanakaran, S.; Yoon, H.; Theiler, J.; Abfalterer, W.; Hengartner, N.; Giorgi, E.E.; Bhattacharya, T.; Foley, B.; et al. Tracking Changes in SARS-CoV-2 Spike: Evidence That D614G Increases Infectivity of the COVID-19 Virus. *Cell* **2020**, *182*, 812-827.e19, doi:10.1016/j.cell.2020.06.043.

184. Bryan, A.; Pepper, G.; Wener, M.H.; Fink, S.L.; Morishima, C.; Chaudhary, A.; Jerome, K.R.; Mathias, P.C.; Greninger, A.L. Performance Characteristics of the Abbott Architect SARS-CoV-2 IgG Assay and Seroprevalence in Boise, Idaho. *J Clin Microbiol* **2020**, *58*, e00941-20, doi:10.1128/JCM.00941-20.

185. Padoan, A.; Bonfante, F.; Pagliari, M.; Bortolami, A.; Negrini, D.; Zuin, S.; Bozzato, D.; Cosma, C.; Sciacovelli, L.; Plebani, M. Analytical and Clinical Performances of Five Immunoassays for the Detection of SARS-CoV-2 Antibodies in Comparison with Neutralization Activity. *EBioMedicine* **2020**, *62*, 103101, doi:10.1016/j.ebiom.2020.103101.

186. Bond, K.A.; Williams, E.; Nicholson, S.; Lim, S.; Johnson, D.; Cox, B.; Putland, M.; Gardiner, E.; Tippett, E.; Graham, M.; et al. Longitudinal Evaluation of Laboratory-Based Serological Assays for SARS-CoV-2 Antibody Detection. *Pathology* **2021**, *53*, 773–779, doi:10.1016/j.pathol.2021.05.093.

187. Favresse, J.; Eucher, C.; Elsen, M.; Gillot, C.; Van Eeckhoudt, S.; Dogné, J.-M.; Douxfils, J. Persistence of Anti-SARS-CoV-2 Antibodies Depends on the Analytical Kit: A Report for Up to 10 Months after Infection. *Microorganisms* **2021**, *9*, 556, doi:10.3390/microorganisms9030556.

188. Theel, E.S.; Johnson, P.W.; Kunze, K.L.; Wu, L.; Gorsh, A.P.; Granger, D.; Roforth, M.M.; Jerde, C.R.; Lasho, M.; Andersen, K.J.; et al. SARS-CoV-2 Serologic Assays Dependent on Dual-Antigen Binding Demonstrate Diverging Kinetics Relative to Other Antibody Detection Methods. *J Clin Microbiol* **2021**, *59*, e0123121, doi:10.1128/JCM.01231-21.

189. Lau, E.H.Y.; Tsang, O.T.Y.; Hui, D.S.C.; Kwan, M.Y.W.; Chan, W.-H.; Chiu, S.S.; Ko, R.L.W.; Chan, K.H.; Cheng, S.M.S.; Perera, R.A.P.M.; et al. Neutralizing Antibody Titres in SARS-CoV-2 Infections. *Nat Commun* **2021**, *12*, 63, doi:10.1038/s41467-020-20247-4.

190. Sun, J.; Tang, X.; Bai, R.; Liang, C.; Zeng, L.; Lin, H.; Yuan, R.; Zhou, P.; Huang, X.; Xiong, Q.; et al. The Kinetics of Viral Load and Antibodies to SARS-CoV-2. *Clin Microbiol Infect* **2020**, *26*, 1690.e1-1690.e4, doi:10.1016/j.cmi.2020.08.043.

191. Wu, Z.; McGoogan, J.M. Characteristics of and Important Lessons From the Coronavirus Disease 2019 (COVID-19) Outbreak in China: Summary of a Report of 72 314 Cases From the Chinese Center for Disease Control and Prevention. *JAMA* **2020**, *323*, 1239–1242, doi:10.1001/jama.2020.2648.

192. Lu, X.; Zhang, L.; Du, H.; Zhang, J.; Li, Y.Y.; Qu, J.; Zhang, W.; Wang, Y.; Bao, S.; Li, Y.; et al. SARS-CoV-2 Infection in Children. *New England Journal of Medicine* **2020**, *382*, 1663–1665, doi:10.1056/NEJMc2005073.

193. Bhopal, S.S.; Bagaria, J.; Olabi, B.; Bhopal, R. Children and Young People Remain at Low Risk of COVID-19 Mortality. *The Lancet Child & Adolescent Health* **2021**, *5*, e12–e13, doi:10.1016/S2352-4642(21)00066-3.

194. Onder, G.; Rezza, G.; Brusaferro, S. Case-Fatality Rate and Characteristics of Patients Dying in Relation to COVID-19 in Italy. *JAMA* **2020**, *323*, 1775–1776, doi:10.1001/jama.2020.4683.

195. Dong, Y.; Mo, X.; Hu, Y.; Qi, X.; Jiang, F.; Jiang, Z.; Tong, S. Epidemiology of COVID-19 Among Children in China. *Pediatrics* **2020**, *145*, doi:10.1542/peds.2020-0702.

196. Kudesia, P.; Salimarouny, B.; Stanley, M.; Fortin, M.; Stewart, M.; Terry, A.; Ryan, B.L. The Incidence of Multimorbidity and Patterns in Accumulation of Chronic Conditions: A Systematic Review. *J Comorb* **2021**, *11*, 26335565211032880, doi:10.1177/26335565211032880.

197. Franceschi, C.; Bonafè, M.; Valensin, S.; Olivieri, F.; De Luca, M.; Ottaviani, E.; De Benedictis, G. Inflamm-Aging. An Evolutionary Perspective on Immunosenescence. *Ann N Y Acad Sci* **2000**, *908*, 244–254, doi:10.1111/j.1749-6632.2000.tb06651.x.

198. Palmer, D.B. The Effect of Age on Thymic Function. *Front Immunol* **2013**, *4*, 316, doi:10.3389/fimmu.2013.00316.

199. Salam, N.; Rane, S.; Das, R.; Faulkner, M.; Gund, R.; Kandpal, U.; Lewis, V.; Mattoo, H.; Prabhu, S.; Ranganathan, V.; et al. T Cell Ageing: Effects of Age on Development, Survival & Function. *Indian J Med Res* **2013**, *138*, 595–608.

200. Dugan, H.L.; Henry, C.; Wilson, P.C. Aging and Influenza Vaccine-Induced Immunity. *Cell. Immunol.* **2020**, *348*, 103998, doi:10.1016/j.cellimm.2019.103998.

201. Wolff, J.L.; Starfield, B.; Anderson, G. Prevalence, Expenditures, and Complications of Multiple Chronic Conditions in the Elderly. *Archives of Internal Medicine* **2002**, *162*, 2269–2276, doi:10.1001/archinte.162.20.2269.

202. Mueller, A.L.; McNamara, M.S.; Sinclair, D.A. Why Does COVID-19 Disproportionately Affect Older People? *Aging (Albany NY)* **2020**, *12*, 9959–9981, doi:10.18632/aging.103344.

203. Ahmed, M.S.; Jacques, L.C.; Mahallawi, W.; Ferrara, F.; Temperton, N.; Upile, N.; Vaughan, C.; Sharma, R.; Beer, H.; Hoschler, K.; et al. Cross-Reactive Immunity against Influenza Viruses in Children and Adults Following 2009 Pandemic H1N1 Infection. *Antiviral Res* **2015**, *114*, 106–112, doi:10.1016/j.antiviral.2014.12.008.

204. Isho, B.; Abe, K.T.; Zuo, M.; Jamal, A.J.; Rathod, B.; Wang, J.H.; Li, Z.; Chao, G.; Rojas, O.L.; Bang, Y.M.; et al. Persistence of Serum and Saliva Antibody Responses to SARS-CoV-2 Spike Antigens in Patients with COVID-19. *Science Immunology* **2020**, *5*, doi:10.1126/sciimmunol.abe5511.

205. Ripperger, T.J.; Uhrlaub, J.L.; Watanabe, M.; Wong, R.; Castaneda, Y.; Pizzato, H.A.; Thompson, M.R.; Bradshaw, C.; Weinkauf, C.C.; Bime, C.; et al. Orthogonal SARS-CoV-2 Serological Assays Enable Surveillance of Low-Prevalence Communities and Reveal Durable Humoral Immunity. *Immunity* **2020**, *53*, 925-933.e4, doi:10.1016/j.immuni.2020.10.004.

206. Chia, W.N.; Zhu, F.; Ong, S.W.X.; Young, B.E.; Fong, S.-W.; Bert, N.L.; Tan, C.W.; Tiu, C.; Zhang, J.; Tan, S.Y.; et al. Dynamics of SARS-CoV-2 Neutralising Antibody Responses and Duration of Immunity: A Longitudinal Study. *The Lancet Microbe* **2021**, *2*, e240–e249, doi:10.1016/S2666-5247(21)00025-2.

207. Brockman, M.A.; Mwimanzi, F.; Lapointe, H.R.; Sang, Y.; Agafitei, O.; Cheung, P.; Ennis, S.; Ng, K.; Basra, S.; Lim, L.Y.; et al. *Reduced Magnitude and Durability of Humoral Immune Responses by COVID-19 MRNA Vaccines among Older Adults*; 2021; p. 2021.09.06.21263149;

208. Pierce, C.A.; Preston-Hurlburt, P.; Dai, Y.; Aschner, C.B.; Cheshenko, N.; Galen, B.; Garforth, S.J.; Herrera, N.G.; Jangra, R.K.; Morano, N.C.; et al. Immune Responses to SARS-CoV-2 Infection in Hospitalized Pediatric and Adult Patients. *Science Translational Medicine* **2020**, *12*, eabd5487, doi:10.1126/scitranslmed.abd5487.

209. Jung, J.; Mundle, S.T.; Ustyugova, I.V.; Horton, A.P.; Boutz, D.R.; Pougatcheva, S.; Prabakaran, P.; McDaniel, J.R.; King, G.R.; Park, D.; et al. Influenza Vaccination in the Elderly Boosts Antibodies against Conserved Viral Proteins and Egg-Produced Glycans. *J Clin Invest* **2021**, *131*, doi:10.1172/JCI148763.

210. Chen, Y.-Q.; Lan, L.Y.-L.; Huang, M.; Henry, C.; Wilson, P.C. Hemagglutinin Stalk-Reactive Antibodies Interfere with Influenza Virus Neuraminidase Activity by Steric Hindrance. *Journal of Virology* **2018**, doi:10.1128/JVI.01526-18.

211. Kosik, I.; Angeletti, D.; Gibbs, J.S.; Angel, M.; Takeda, K.; Kosikova, M.; Nair, V.; Hickman, H.D.; Xie, H.; Brooke, C.B.; et al. Neuraminidase Inhibition Contributes to Influenza A Virus Neutralization by Anti-Hemagglutinin Stem Antibodies. *J. Exp. Med.* **2019**, jem.20181624, doi:10.1084/jem.20181624.

212. Liu, L.; Iketani, S.; Guo, Y.; Chan, J.F.-W.; Wang, M.; Liu, L.; Luo, Y.; Chu, H.; Huang, Y.; Nair, M.S.; et al. *Striking Antibody Evasion Manifested by the Omicron Variant of SARS-CoV-2*; 2021; p. 2021.12.14.472719;

213. VanBlargan, L.A.; Errico, J.M.; Halfmann, P.J.; Zost, S.J.; Crowe, J.E.; Purcell, L.A.; Kawaoka, Y.; Corti, D.; Fremont, D.H.; Diamond, M.S. *An Infectious SARS-CoV-2 B.1.1.529 Omicron Virus Escapes Neutralization by Several Therapeutic Monoclonal Antibodies*; 2021; p. 2021.12.15.472828;

214. Schmidt, F.; Muecksch, F.; Weisblum, Y.; Da Silva, J.; Bednarski, E.; Cho, A.; Wang, Z.; Gaebler, C.; Caskey, M.; Nussenzweig, M.C.; et al. Plasma Neutralization of the SARS-CoV-2 Omicron Variant. *New England Journal of Medicine* **2021**, *0*, null, doi:10.1056/NEJMc2119641.

215. Lewnard, J.A.; Cobey, S. Immune History and Influenza Vaccine Effectiveness. *Vaccines (Basel)* **2018**, *6*, doi:10.3390/vaccines6020028.

216. Lv, H.; So, R.T.Y.; Yuan, M.; Liu, H.; Lee, C.-C.D.; Yip, G.K.; Ng, W.W.; Wilson, I.A.; Peiris, M.; Wu, N.C.; et al. *Evidence of Antigenic Imprinting in Sequential Sarbecovirus Immunization*; Immunology, 2020;

217. Wheatley, A.K.; Fox, A.; Tan, H.-X.; Juno, J.A.; Davenport, M.P.; Subbarao, K.; Kent, S.J. Immune Imprinting and SARS-CoV-2 Vaccine Design. *Trends in Immunology* **2021**, *42*, 956–959, doi:10.1016/j.it.2021.09.001.

218. Amanat, F.; Thapa, M.; Lei, T.; Ahmed, S.M.S.; Adelsberg, D.C.; Carreno, J.M.; Strohmeier, S.; Schmitz, A.J.; Zafar, S.; Zhou, J.Q.; et al. The Plasmablast Response to SARS-CoV-2 MRNA Vaccination Is Dominated by Non-Neutralizing Antibodies and Targets Both the NTD and the RBD. *medRxiv* **2021**, 2021.03.07.21253098, doi:10.1101/2021.03.07.21253098.

219. Anderson, E.M.; Goodwin, E.C.; Verma, A.; Arevalo, C.P.; Bolton, M.J.; Weirick, M.E.; Gouma, S.; McAllister, C.M.; Christensen, S.R.; Weaver, J.; et al. Seasonal Human Coronavirus Antibodies Are Boosted upon SARS-CoV-2 Infection but Not Associated with Protection. *Cell* **2021**, *184*, 1858-1864.e10, doi:10.1016/j.cell.2021.02.010.